POLITECNICO DI TORINO

Master Degree Thesis in Automotive Engineering

# Design and validation of a numerical vehicle model for hybrid architectures

**Supervisor**
Prof. Andrea Tonoli

**Co-Supervisors**
Prof. Angelo Bonfitto
Prof. Nicola Amati
PhD Candidate Stefano Favelli
PhD Candidate Eugenio Tramacere

**Candidate**
Luca Nicosia

ACADEMIC YEAR 2022-2023

# Acknowledgements

In questa sezione vorrei dedicare giusto due parole a tutte le persone che mi sono state vicino durante tutto il percorso accademico e che in parte hanno contribuito al raggiungimento di questo importante traguardo. Il primo pensiero va ai miei genitori che mi hanno dato la possibilità di seguire i miei sogni andando a studiare in una nuova città non facendomi mai mancare nulla. Non potrò mai smettere di ringraziarli. Per continuare con il quadro familiare, ringrazio mia sorella Donella per essere la mia spalla dandomi sempre il consiglio giusto al momento giusto. Non posso non citare la mia ragazza Nicoletta che è sicuramente una tra le persone che più di tutte mi ha dato manforte, aiutandomi nei momenti più complicati e che ha saputo consigliarmi saggiamente quando ne avevo bisogno. C'è sempre stata quando dovevo confidarmi sui miei mille cambi di idea e per questo merita un posto speciale in questa sezione.

Iniziando con gli amici, ringrazio Antonio e Andrea, i quali vivendo assieme, mi hanno supportato e sopportato specialmente nei momenti di maggior stress e con cui mi confronto su qualsiasi argomento. Proseguo citando Andò con cui ho condiviso in maniera continuativa il percorso accademico e di vita dal secondo anno in poi, andando a lezione assieme (quando mi andava) e persino nello stesso luogo per svolgere la tesi. Angelo e Giulio sono altre due persone che meritano di essere citate in quanto condivido con loro le stesse passioni e per questo sono contento di trascorrere del tempo con loro. Cito pure i Pasmauro con cui condiviso gran parte del mio tempo libero, specialmente al tempio, confrontadomi e aprendomi con loro. Il duo siculo più amato da tutti composto da Ettore e Giovanni ha reso sicuramente la permanenza lontano da casa meno pesante e più piacevole. Per continuare con gli amici, Stefano Onesto e Gianmarco meritano anche loro un ringraziamento per esserci stati durante il percorso accademico e non. Il mitico Ruggio e Riccardo sono due personaggi che non potevo non scrivere, in quanto con le loro perle riescono sempre a risollevarmi il morale. Voglio un bene dell'anima a tutte le persone sopra citate e spero che possiamo continuare a crescere assieme e a condividere sia le gioie che i momenti difficili con voi tutti! Infine, ma non per importanza, un grazie va anche alle persone che mi hanno aiutato a portare avanti questo lavoro di tesi, tra cui Giulia, Stefano, Eugenio e sicuramente il professore Tonoli, Amati e Bonfitto. Sicuramente ho scordato a citare qualcuno, non me ne vogliate rimedierò in presenza senza dubbio.

Non essendo bravo in questo, mi limito a scrivere queste poche parole per ringrare tutti, spero che riesca a trasmettere meglio dal vivo tutta la mia gratidudine nei vostri confronti.

# Abstract

In the last decades the automotive industry has undergone sweeping changes driven on one hand by the worsening of the environmental conditions and on the other by the rate of innovation of many technologies applied to vehicles. As a matter of fact, governments all around the world are directing their energies to modify the current dramatic scenario that seems to be already defined. The most widespread decision is to decarbonize the transport sector, that is accounting for 14% of the global $CO_2$ emissions, by pointing towards an electrified and automated car sector. At this regard this thesis, tries to be part of this change by analysing different ways in which it is possible to reduce fuel consumption and pollutant emissions of a conventional light duty commercial vehicle, through the introduction of both electrification and automation. In order to assess any possible improvements, it is necessary to have a reliable and validated numerical model of the vehicle, that must represent with high fidelity what happens in the real world scenario. In fact, the starting point of this work is the validation of a complete vehicle model on experimental data related to WLTC and Real Driving Emission (RDE) driving cycles, with a pure thermal configuration of the powertrain. At this regard, the validation phase has covered different aspects related to the pure Internal Combustion Engine (ICE) architecture, going through the extrapolation of the gear shifting logic from experimental data, the usage of the coast down method, as well as the simulation of the engine transient phases to validate the digital twin of the available vehicle. Once an ICE-only baseline is defined, the focus is shifted on the electrification of the powertrain, where a 48V hybrid architecture with a 20 kW electric motor in position P1 is chosen to assess the potential advantages in terms of fuel consumption and $CO_2$ emissions reduction. The Energy Management Strategy (EMS) chosen to control the hybrid configuration is the well-known Equivalent Consumption Minimization Strategy (ECMS), which allows the operation of the battery in Charge Sustaining (CS) mode. The thesis covers also the optimization of the hybrid architecture design in terms of power management strategy, gear shifting logic and 48V battery sizing. Finally, the validated numerical vehicle model coupled with the simulation of hardware and software typical of on Adaptive Cruise Control (ACC), is used to demonstrate the potential benefits of Advanced Driver Assistance Systems (ADAS) on fuel consumption and pollutant emissions reduction in addition to enhanced safety and driving comfort.

# Contents

# List of Figures

# List of Tables

# Chapter 1

# Introduction

## 1.1 Electrification and automation

In the latest years, the automotive sector has undergone radical changes driven principally by the worsening of the environmental conditions and at the same time by the advancements in technology, changing consumer preferences, and new regulatory requirements. As a matter of fact, the automotive field has been a major contributor to environmental degradation, primarily due to the emission of greenhouse gases (GHGs) and other pollutants from gasoline and diesel-powered vehicles. According to the Intergovernmental Panel on Climate Change (IPCC), transportation is responsible for 14% of global greenhouse gas (GHG) emissions, with the majority of these emissions coming from passenger cars and light-duty vehicles [1]. Additionally, vehicles are responsible of the emission of other air pollutants, including nitrogen oxides (NOx), which contribute to the formation of ground-level ozone and particulate matter, both of which have harmful impacts on human health and the environment. Reducing vehicle emissions is therefore a critical component of efforts to address the challenges of climate change and improve air quality.
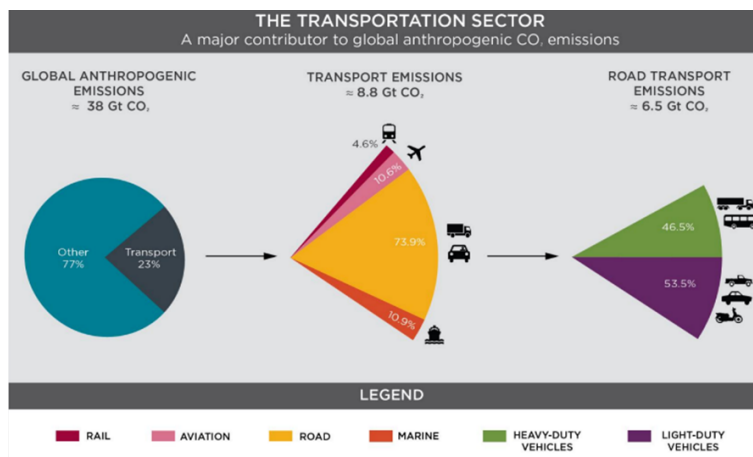
Figure 1.1: Global impact of transport sector on CO2 emisionis

As can be seen from the Figure 1.1, the automotive field (including passenger cars, motorcycles and both light and heavy duty vehicles) weights a significant high part in the transport sector and to address this issue, the industry has been undergoing a transformation towards more sustainable and environment-friendly technologies. This shift is being driven by several factors, including not only increasing concerns over climate change as well as improvements in battery and charging technology, and government regulations. As a consequence of the growing emphasis on sustainability and the need to reduce emissions, electrification and automation are two of the most significant changes that are shaping the future of the automotive industry. The term electrification refers to the increasing use of electric power in vehicles, either in the form of pure electric vehicles (EVs) or hybrid electric vehicles (HEVs), where the difference between the two depends on which type of power and from which propeller is used for the motion. Moreover, although electric vehicles can appear to be a discovery of the last decade thanks to the gaining momentum they are experiencing, already in the late 19th and early 20th centuries, EVs were widely used, but the discovery of oil reserves and the mass production of affordable internal combustion engines led to a decline in their popularity.

Later in the 1960s and 1970s, the energy crisis and growing concern over air pollution led to a renewed interest in EVs, but the technology was still limited and the vehicles were expensive. Whereas today, EVs are becoming more widely accepted and affordable, and the trend towards electrification in the automotive sector shows no signs of slowing down. With increasing concern over climate change, the demand for EVs is expected to continue to rise, and the technology is likely to continue to improve, making EVs an increasingly attractive option for consumers. The electrification of the automotive industry is a critical step towards a more sustainable future, and it is a key part of the transition to a low-carbon economy. In fact, EVs emit significantly less GHGs compared to gasoline and diesel vehicles, as they produce no tailpipe emissions and can be powered by clean energy sources such as wind and solar. In addition, improvements in battery technology have led to longer driving ranges, faster charging times, and lower costs, making EVs more accessible to consumers. Governments around the world are also incentivizing the transition to EVs by offering tax credits, rebates, and other financial incentives[2].

On the other hand, automation refers to the increasing use of technology in vehicles to automate various functions, such as accelerating, braking, and steering. Automation technologies range from simple driver-assistance systems, such as lane departure warning and adaptive cruise control, to more advanced systems like semi-autonomous driving and eventually full autonomous driving. These self-driving cars have many potential benefits, where the most notable ones are increased safety and reduced emissions. For what concerns the former, exploiting advanced sensors, cameras installed on-board and algorithms, autonomous vehicles can process and analyse large amounts of data in real-time to make informed decisions and respond to various driving scenarios. This can result in a significant reduction in the number of accidents caused by human error, such as drunk driving, distracted driving, or speeding. In addition, autonomous vehicles have the potential to prevent accidents caused by fatigue, which can be a major issue for long-distance drivers. Furthermore, autonomous vehicles can also help to optimize traffic flow, reducing congestion, and improving overall road safety.

In terms of emissions reduction, autonomous vehicles have a significant advantage over traditional vehicles thanks to the ability to operate more efficiently by adjusting the vehicle pace based on the information of the vehicle in front and of the road signals, thus having the possibility to reduce fuel consumption and emissions, improving air quality too. Additionally, the improved driving styles of autonomous vehicles can result in reduced wear and tear on vehicles, reducing the need for repairs and maintenance and further reducing emissions, since human decisions will count always less the higher the complexity of the autonomous system. Another benefit of autonomous vehicles is the potential to reduce the cost of transportation. With reduced maintenance costs, improved fuel efficiency, and reduced congestion, autonomous vehicles can make transportation more affordable for individuals and businesses. Additionally, autonomous vehicles can also improve accessibility for individuals who cannot drive, such as the elderly or disabled, giving them greater freedom and independence. Furthermore, autonomous vehicles have the potential to reduce the need for parking spaces, freeing up valuable land for other uses.

Another improvement concerns the possibility of exploiting the Internet of Things (IoT) and the use of smartphones to allow the share of information between vehicles about traffic signals, road congestions and even the information related to the relative speed and distance of a vehicle with respect to another one. The increasing trend towards connected vehicles is shaping the future of the automotive sector by offering new opportunities for innovation and growth. The outcome is that the widespread use of autonomous and connected vehicles could also reduce the need for personal car ownership, reducing GHG emissions and improving air quality, thus helping to create a more sustainable, efficient, and convenient transportation system for the future. It is possible to state that autonomous vehicles have the potential to bring many benefits to society, including increased safety, reduced emissions, and reduced costs. With continued development and investment in this technology, it is likely that we will see widespread adoption of autonomous vehicles in the coming years. However, there are still many challenges that need to be overcome, such as ensuring the reliability and security of autonomous vehicles, ensuring compatibility with existing infrastructure, and addressing concerns about job displacement. Nevertheless, the potential benefits of autonomous vehicles make it an exciting and promising area of development that has the potential to revolutionize the way we travel.

In a nutshell, the trend towards electrification and automation in the automotive sector is having a major impact on the industry. Car manufacturers are investing heavily in developing new technologies and retooling their production lines to accommodate the production of EVs and vehicles with advanced automation systems. The growth of the electric vehicle market is also creating new opportunities for suppliers of components such as batteries, charging systems, and power electronics. In conclusion, these innovations are helping to reduce GHG emissions, improve fuel efficiency, and create a more sustainable transportation system. The industry will continue to play an important role in shaping the future of sustainable mobility and addressing the challenges of climate change.

### 1.1.1 Hardware and software improvements

Once the path to proceed with has been defined, it is necessary to see practically what it requires and how it can be physically implemented in vehicles. In order to meet the common target of reducing tailpipe emissions to be compliant with the always more strict rules the research in the automotive industry seems to be pointing towards two parallel ways: improvements at hardware and software level.

For what concerns the first point, engine downsizing or the use of a more sophisticated transmission allow the powertrain to work in a more efficient manner, thus reducing fuel consumption and pollutant emissions simultaneously. In a similar way, it seems obvious how using lightweight materials for the body in white, such as aluminium or carbon fibre, can reach the same target. However, whenever are required some drastic changes in a sector that has already reached a certain level of maturity and complexity it is fundamental to consider also the economic aspect both from the car manufacturer and customer point of view. In fact, the improvement from one side has to enhance the powertrain efficiency without worsening the performance and above all in the other must be economically sustainable. For this reason, the research is now polarized in improving powertrain efficiency using hybrid and electric propellers. In both cases the dependence on fossil fuels decreases but right now with the current battery technology the former group offers almost the same degrees of freedom of thermal vehicles (in terms of autonomy and charging speed). Moreover, does not require the presence of dedicated infrastructure system designed for recharging the big batteries, but can rely on the home grid. Having said that, hybrid architectures have also some drawbacks related to the additional weight of electric components and for this reason greater maintenance due to the higher number of components present.

This opens the door to software improvements that enhance the working mode and the efficiency of the installed hardware and that can be divided into two families: causal logics and non-causal logics. The former focus on the relationships between events and the causes and effects that result from them. In this type of algorithm, data is processed and analysed to determine the causal relationships between events, such as the relationship between vehicle speed and fuel consumption. Based on this analysis, the algorithm can make real-time adjustments to the engine and transmission control to optimize fuel efficiency. The most representative example of this category are the Advanced Driver Assistance Systems (ADAS) that can adjust the car pace based on the traffic information so that can detect and react to road hazards, implementing actions like lane departure or collision warnings. Even the Equivalent Consumption Minimization Strategy (ECMS) algorithm falls within the causal logic family: it determines the relationship between engine inputs and fuel consumption and then makes real-time adjustments to minimize fuel consumption while maintaining engine performance.

Non-causal logics, on the other hand, are algorithms that do not focus on the causal relationships between events but rather use statistical and mathematical models to make predictions based on data. For example, a non-causal algorithm may use historical data on driving patterns to predict the most efficient operating conditions for the engine and

transmission. These predictions are then used to make real-time adjustments to the vehicle control systems to improve fuel efficiency [3]. Machine learning and image processing algorithms are part of the non-causal logics and are used to analyse vast amounts of driving data coming from the installed camera, as an example, to make predictions and improve vehicle performance and safety.

## 1.2 Thesis project

This thesis work belongs and contributes to the progress of "AutoEco" project, that is part of the "Pi.Te.F" tender (that stands for "Piattaforma Tecnologica di Filiera") funded by Piedmont region that aims at reducing the fuel consumption and pollutant emissions of a light-duty vehicle by means of its hybridization and subsequent automation. This is for sure in line with the current evolution in the automotive sector and to reach the set target different entities are joining forces together, like: Politecnico di Torino, Dayco Europe S.r.l, Podium Engineering S.r.l and other companies. More in detail, the performed activities can be listed as follows:

- Experimental model validation considering the data related to two driving cycles, to create a baseline configuration from which the improvements can be performed;

- Hybridization of the vehicle through the installation of an electric motor in position P1 to exploit and quantify the advantages this solution brings;

- Automation phase by the implementation of a high-level logic to exploits the information coming from the installed ADAS sensors, in particular of an ACC, to reduce fuel consumption and CO2 emissions;

As can be deducted from the above mentioned description, this project is entirely in line with the evolution and changes the automotive sector is requiring, since it is embracing both the electrification and automation topics.

## 1.3 Thesis outline

The thesis work just described is divided into six chapters:

The first one aims to be an introduction to the changes the automotive sector is having, in terms of electrification and automation, in order to contextualize the thesis project, highlighting also the expected outcomes that are in line with the wished ones.

The second one, is dedicated to the pure thermal configuration analysis where is provided an overview about the different vehicle models present in the literature and the one used in this thesis work. The description proceeds with the focus on the software in the loop and the corresponding components present in the Simulink environment. After that, it is present an overview about the validation process, highlighting the methodology used and the initial available data about the two homologation driving cycles, WLTC and RDE. Finally, are analysed more in detail the aspects related to the validation process: the coast

down maneuver as well as the gear shifting strategy extrapolation from experimental data and the transient correction factor implementation to increase the simulation accuracy.

The third one concerns the hybrid configuration of the powertrain that begins with an examination of the current classification present inside this vehicle sector, followed by a description of what an HEV brings in terms of new components to a more classical pure ICE architecture. The analysis comprehends both hardware and software implementations, where in the latter falls the ECMS control logic, necessary to manage in the most efficient way the torque requested to the two propellers. At the end, are described some improvements done in terms of power management of the electric storage in parallel with a study to understand which battery fits the best to the current application. In addition, an optimal gear shifting strategy is highlighted, that allows the engine to work in a more efficient region, thus aiming at reducing fuel consumption and CO2 emissions.

The fourth chapter is related to the ACC installation, where at the beginning is shown the state of the art of this system as well as the classification about the autonomous vehicles. Moreover, it is described how this ADAS system is implemented in the vehicle model and how it is tested, especially in terms of scenario the ego vehicle has to follow. At this regard, the control strategy used is depicted and it is shown the correlated tuning phase to make the system work fine. In conclusion, it is considered just a part of the WLTC driving cycle where a sensitivity analysis is performed in order to assess how the behaviour of the vehicle changes with different parameters.

The fifth chapter is dedicated to the discussion of the results of the validation process for what concerns the two homologation cycles, WLTC and RDE. For what regards the former the analysis is related to the pure ICE configuration of the powertrain and the match with experimental data concerns the principal vehicle characteristics, going from the internal combustion engine revolution speed to the requested torque to the vehicle actual speed. While for the latter, the comparison was related to the fuel consumption and CO2 emissions. To conclude, the simulation was extended also to the hybrid architecture highlighting the advantages this configuration brings.

In conclusion, the last chapter sums up the work conducted in this thesis highlighting the obtained results in correlation with the purpose of this work and a description of possible evolutions and developments to the project.

# Chapter 2

# Pure ICE configuration

This chapter represents the starting point of this thesis work and id dedicated to the review of the pure thermal propeller configuration of the powertrain that represents also the baseline of the vehicle model. At the beginning there is a more theoretical description of how a vehicle can be modelled in the literature, followed by a more practical description of the implementation of the latter in Simulink environment. This modelling phase is functional for the validation part, where is described not only the methodology used as well as some test conducted to increase the accuracy of the match between experimental and numerical data.

## 2.1 Vehicle model

The creation of a virtual vehicle model, as an example using software like MATLAB-Simulink, is a crucial step in the automotive sector since enables to simulate and test several design scenarios for different components of the vehicle. In fact, this virtual representation of the vehicle allows to evaluate the behaviour of the different subsystems that portray a car. Moreover, by changing the parameters of the model it is possible to study the effects of the different variables on vehicle performance and make decisions accordingly. As a confirmation of what just written, in this section will be highlighted the Simulink model of the vehicle, with particular attention on the pure ICE configuration, used in the initial part of this work for the validation phase and during the simulation process. Moreover, the model gathers all the components and technologies that will be discussed during this chapter.

### 2.1.1 Typologies comparison

In the literature the description and modelling of a vehicle in terms of analyzing the energy usage can be realized in two main different ways: using a backward and forward model. In this section the differences between the two strategies will be highlighted putting more attention on the one used in this work [4].

**Backward vehicle model**

In the backward vehicle model, the main feature is that the input is represented by the driving cycle and is assumed to be followed perfectly, therefore the speed is not considered as a dynamic variable and the driver model is useless. Furthermore, the previous mentioned input is usually defined as a function of time or distance, thus the knowledge of all the derivative values is also known. An important point to be highlighted is the absence of any feedback with the driving cycle since the actual vehicle speed is considered to be identical to the reference one. As a consequence, the entire system can be solved using simple algebraic methods, since also the derivatives are known.

However, the backward model has some limitations and technical problems. One of these is represented by the fact that sometimes the power required to keep a certain defined speed can be higher than the power the engine can deliver. When this happens the are no solutions to the mathematical problem and the backward simulation stops. Related to this first issue, the backward model does not reproduce the physical properties of the vehicle. It is assumed that the vehicle will respond to the driver's inputs in a predictable and consistent way, regardless of the vehicle's weight, dimensions, or mechanical properties. This can lead to inaccuracies in the model's predictions, particularly when the vehicle is under stress or operating outside of its normal operating range. On the other hand, one of the primary advantages of the backward vehicle model is its simplicity and ease of use, thanks to the absence of driver model. It requires less data and computational resources than more complex models, such as the forward model. It is also more flexible, allowing to evaluate different control algorithms and scenarios.
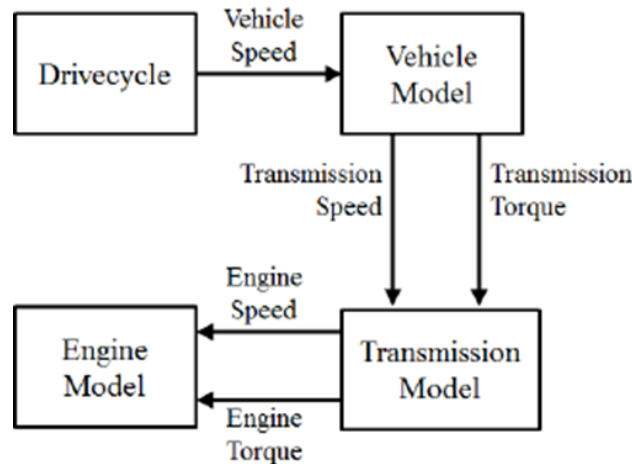


Figure 2.1: Backward vehicle model

To sum up, it is possible to state that in case of steady state or quasi steady state problems the backward vehicle model works fine. This statement does not hold anymore when the system complexity arises (when dynamic variables are present or when power-train components are modelled with high level of detail) and there can be no solutions to the mathematical problem. For what concerns the vehicle behaviour, the backward model assumes that there is a perfect match between the input reference speed and the

actual one, being the propeller able to deliver the corresponding necessary power. This aspect in particular, is the reason why this solution has not been implemented for this thesis work.

**Forward vehicle model**

The discussion about forward vehicle model is exactly the opposite as the previous one. In fact, is counts for a driver model that controls the accelerator and brake pedals, thus providing a torque demand to the powertrain, to meet the target speed coming from the driving cycle. More in detail, the driver model, that will be discussed soon after, can be represented by a PID controller that uses the speed error to adjust the internal combustion engine traction and brake torque. This is possible thanks to the presence of a feedback that goes both to the driver (actual vehicle speed) and to the driving cycle (in terms of vehicle position). It can be stated that, the forward vehicle model is based on differential equations, being the speed a dynamic state in this case. As a matter of fact, fluctuations in vehicle speed are a characteristic of this vehicle model due to the fact that the driver tries to control vehicle performance in correlation with the changing driving scenario.

Like for the backward case, the forward vehicle model has also some criticisms. One of the most obvious is the higher complexity and computational requirements since it requires a significant amount of data and computational resources to create and refine the model. Another weak point is represented by the limited flexibility that this strategy can offer. Having said that, the forward vehicle model suits well for complex system where the components are modelled with high level of detail. In addition, the driver model presence introduces for sure more degrees of freedom to the system and parameters to be tuned but allows also to simulate different driving styles and their effects on vehicle behaviour. As a result of this, the level of reality that a forward vehicle model can offer is for sure higher than the backward one, since even the most extreme conditions can be simulated without big issues. For the reasons just depicted, this vehicle model has been implemented in this thesis work.
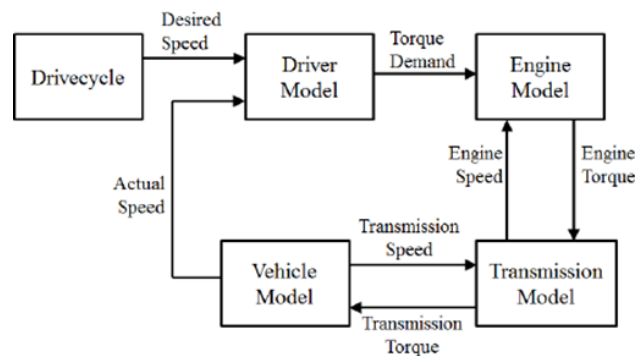


Figure 2.2: Forward vehicle model

### 2.1.2 Vehicle configuration and parameters

Before going in detail with the description of the virtual model it is worth noticing reviewing the real vehicle configuration from which all the work is based on. As stated in the introduction the vehicle under study is a light duty commercial vehicle and is represented by the IVECO Daily, in version 35S14A8V. The main characteristics related to both powertrain and dimensions are listed in the table below:

| Version: 35S14A8V Main Features | |
|:---:|:---:|
| Engine | F1A 2.3 Eu6d |
| Max Power | 136 Cv / 3250 rpm |
| Max Torque | 350 Nm / 1500 rpm |
| Gearbox | Hi-Matic (ZF AT8) |
| Length | 6087 mm |
| Width | 2010 mm |
| Wheelbase | 3250 mm |
| Height | 2660 mm |
| Mass (empty) | 2610 kg |
| Carrying Capacity | 1250 kg |
| Tire size | 225/75R16 (Rr= 0.361 m) |

Table 2.1: Main vehicle characteristics

Nevertheless, to better understand the listed variables, a more representative characteristic is the so-called brake specific fuel consumption (BSFC), that is going to be discussed soon.

**BSFC**

Regarding the thermal part, one of the most indicative manner of characterizing an engine is the brake specific fuel consumption (BSFC), that measures the efficiency of an internal combustion engine in converting fuel into power. It represents the amount of fuel consumed per unit of power produced, usually expressed in units of grams per kilowatt-hour (g/kWh). To compute the BSFC of a vehicle, the amount of fuel consumed by the engine is measured over a period of time, and the power output is calculated using a dynamometer. The BSFC can be mathematically represented as follows:

$$BSFC = \frac{\dot{m}_f}{T_{ICE} \cdot \omega_{ICE}} \tag{2.1}$$

Where the numerator represents the fuel mass flow rate expressed in (kg/s), while the denominator is the effective engine power expressed in (W). It is generally reported graphically in terms of engine torque as a function of engine speed, to which are correlated specific values of fuel economy that can be later translated into efficiency values. In other words, the chart shows the specific points where the engine operates most efficiently, as indicated by the lowest BSFC values. These points are important for determining the

optimal operating conditions for the engine and can help to maximize fuel economy and minimize emissions.
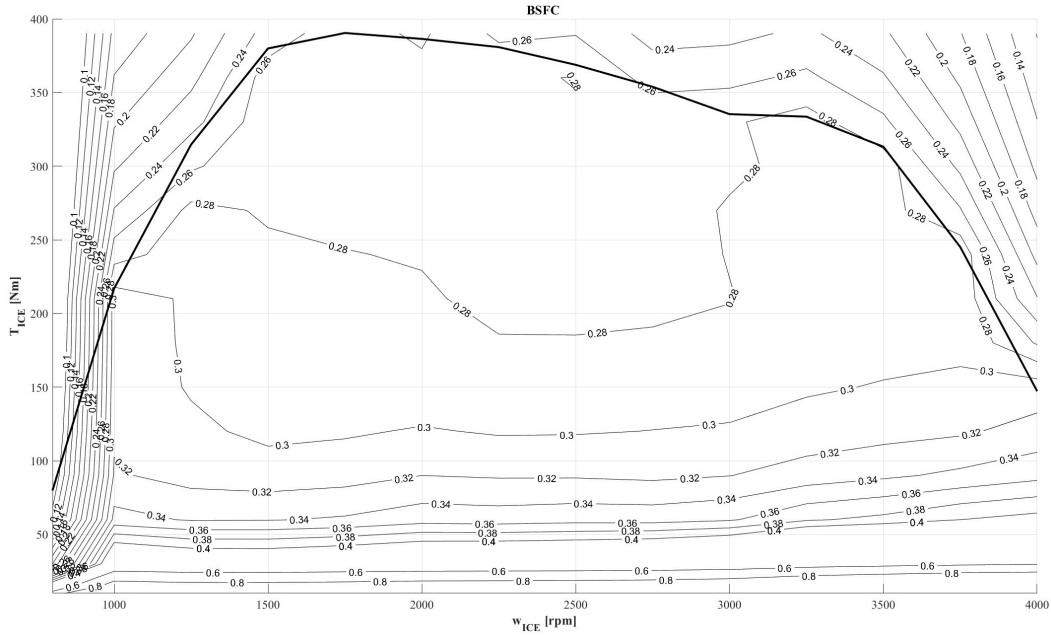


Figure 2.3: Brake specific fuel consumption

## 2.2  Simulation interface

Within this section the description of the different parts defining the vehicle model in Simulink will be carried out. The focus for the moment is not considering the presence of system for the autonomous driving that will be introduced in the dedicated chapter.
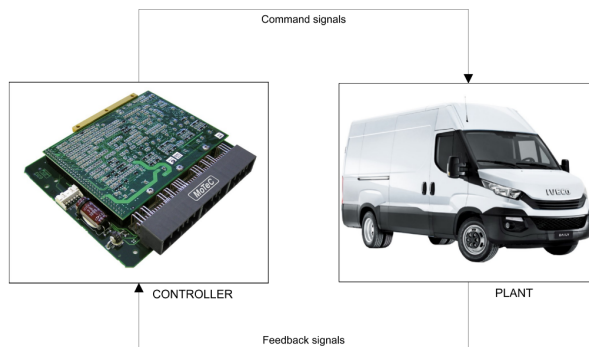


Figure 2.4: Simulink vehicle model

11

As can be seen from Figure 2.4, there complete vehicle model is counting for two macro groups:

- Plant, where are present the principal mechanical components including the powertrain, the driveline and the vehicle longitudinal dynamics;

- Controller, which gathers inside the control logics related to the different vehicle variables based on the feedback coming from the Plant part. This holds for the two modes in which the vehicle model is tested: pure thermal and hybrid.

### 2.2.1 Plant

In the first of the two subsystems is present the heart of the vehicle in terms of hardware and so mechanical components. As a matter of fact, inside the Plant are present: the model of longitudinal dynamics, a more practical part addressed at computing the power delivered by the powertrain (in this section just the pure thermal configuration is analysed, the additional electric components will be discussed in a dedicated chapter). In a nutshell, there is a more "external" description of the vehicle dynamics and then a more "internal" one where the powertrain components are modelled, as shown below:
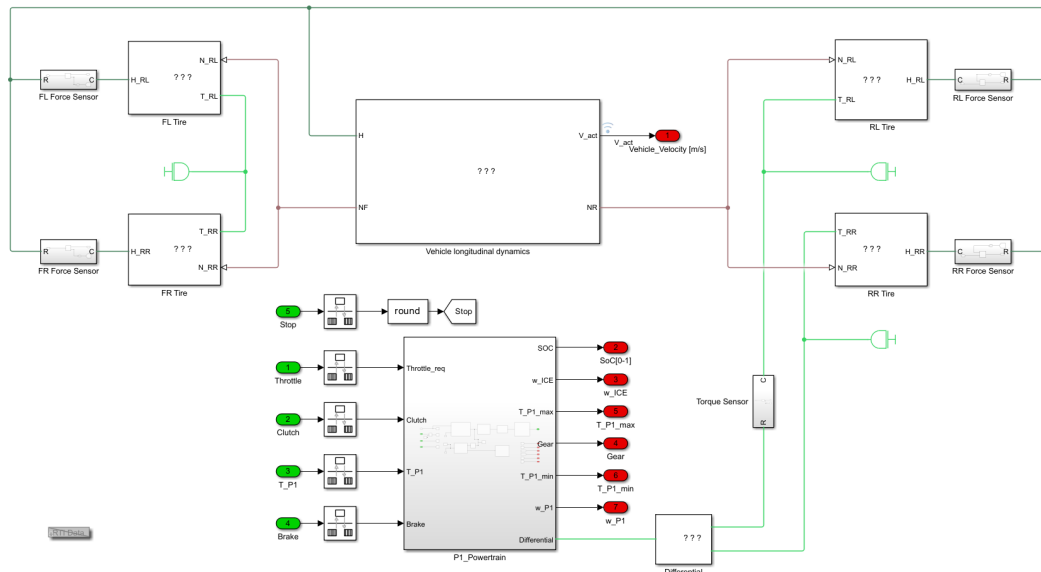


Figure 2.5: Plant model

Going more in detail, each component is modelled using Simulink and Simscape blocks and for what concerns the first element previously mentioned, the vehicle longitudinal dynamics block, it includes:

- The "vehicle body" block;

- Four wheel and disc brake models;

For what concerns the pure ICE powertrain, the main components are:

- The internal combustion engine model;

- The driveline, in terms of clutch, gearbox, transmission and differential;

A more detailed review of the previous mentioned subgroups will be delivered in section 2.3.

## 2.2.2 Controller

Associated with the plant there is the controller side that can be thought as its complementary part since governs the main vehicle requests and in turn, the characteristic variables that enter as a feedback in the plant. In fact, the variables will be updated based on the modifications that the controller acts. In order to fulfill this important task, there are seven inputs entering in the controller:

- actual vehicle speed;

- ICE angular speed;

- Gear engaged;

- EM angular speed;

- Motor torque;

- Generator torque;

- Battery state of charge.

Before describing the different control policies present inside the controller, it is worth noting to depict the presence of a driver model, typical of a forward vehicle model, whose aim is the one of following with high fidelity possible the imposed driving cycle. In order to do so a proportional-integrative block is implemented. The reason behind the use of this system, in addition to its simplicity is that the parameters of the PI function represent the reaction rate of the driver towards present and past errors. In fact, it is possible to underline that:

- The proportional parameter accounts for the present and its command aims at reducing the tracking error;

- The integral parameter considers the past actions and allows precise tracking error for constant or slowly-varying references.

For what concerns the control strategies, these are operated based on which powertrain configuration the simulation is run, that are mainly pure ICE and hybrid mode. There is a huge gap in terms of control between the two configurations. In fact, in the pure thermal mode the controller manages the requested torque that will be supplied entirely from
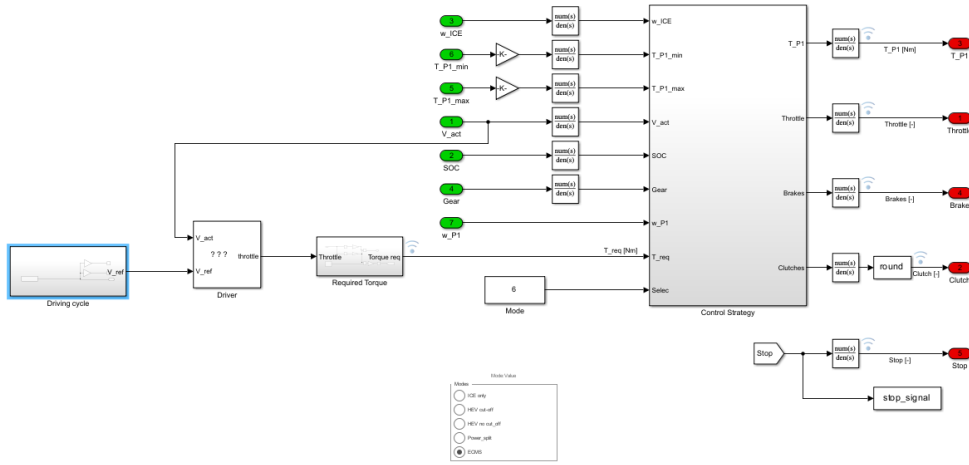
Figure 2.6: Controller model
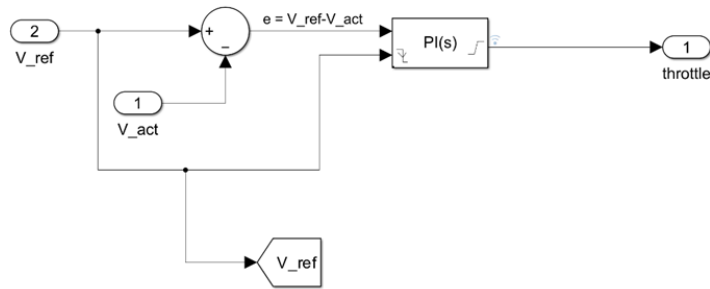


Figure 2.7: Driver model

the internal combustion engine, taking into account as the only constraint the maximum value of torque that the engine can deliver. Concerning the hybrid configuration, the strategy adopted is aimed at enhancing the vehicle performance in terms of reduction fuel and emissions over the two driving cycles, by optimizing the use of the two power sources, thermal and electric. This can be achieved, by using a control logic that based on the requested torque and on the driving action (traction or braking) is able to let the ICE and EM work in synergy, obtaining the lowest consumption. An example of what just described and used in this thesis work is the equivalent consumption minimization strategy (ECMS), that will be better discussed in chapter 3.

## 2.3    Plant components description

Within this section a more detailed description of the components present inside the plant and more in general in a pure thermal powertrain system will be carried out.

### 2.3.1    Longitudinal vehicle dynamics

Inside the Simulink model, as introduced in section 2.2.1, one of the three main subgroups is represented by the longitudinal vehicle dynamics block, fundamental for the correction functioning and representation of the model. Going more in depth are present: the vehicle body block and the wheel models. Taking into account the former it represents a two-axle vehicle body where are inserted the vehicle characteristics in terms of body mass, aerodynamic drag coefficient, road inclination and weight distribution between axles due to acceleration and road profile. Moreover, are present three external output connections: one for the vehicle velocity and the others for front and rear normal wheel forces, respectively. Whereas, inside each wheel model is represented not only the tire but the brake system. Concerning the former, the behaviour is analysed according to the Pacejka magic formula [5]. The connection present are for the tire slip and normal forces that enters in the disc brake block. At this regard, this last model is arranged as a cylinder applying pressure to one or more pads that can contact the shaft rotor, creating friction torque.

Widening the point of view, considering also a more theoretical approach, it is possible to state that the longitudinal vehicle model consists of mainly to main parts: vehicle dynamics and powertrain dynamics [6]. In the former are present longitudinal tire forces, aerodynamic forces, rolling resistance and the contribution related to the slope of the road (that are the input parameters of the "vehicle body" block. Whereas the latter comprises of the internal combustion engine, the gearbox, the transmission, the torque converter and the wheels, that will be object of discussion in the following sections. To better understand the longitudinal dynamics, considering a vehicle moving on a road with a certain slope, the external forces present are the one described above, so the aerodynamic force, rolling resistance force, longitudinal forces of the tire and the gravitational forces. With the knowledge of these forces it is possible to account for the equilibrium along the longitudinal vehicle axis.

$$R = F_{aer} + F_{rr} + F_{grade} \tag{2.2}$$

Where R represents the overall resistance to motion, while on the right side is present the summation of the three contributions. In the paragraph below is carried out a deeper analysis of the three main contributions of the longitudinal dynamics.

**Aerodynamic drag contribution**

Concerning the aerodynamic contribution, both in terms of forces and moments, have a relevant impact not only on vehicle longitudinal dynamics as well as on its handling and comfort. This contribution it is primarily due to the viscous friction of the air that impact onto the vehicle surface, but also to the pressure difference, between the front and rear
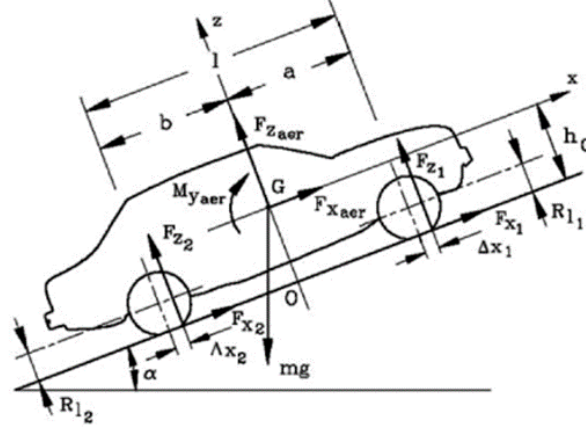
Figure 2.8: Longitudinal vehicle dynamics representation

part of the vehicle (wake region), caused by the air flow separation. This contribution can be expressed as follows:

$$F_{aer} = \frac{1}{2}\rho C_d A_f v^2 \tag{2.3}$$

Where $\rho$ is the air density in standard conditions (temperature of 15°C and pressure of 101.32 KPa), Cd is the drag coefficient (evaluated through a CFD analysis in a wind tunnel environment), A is the vehicle frontal area and V is the longitudinal vehicle speed. As can be seen from the previous equation, especially with the quadratic dependence on vehicle speed, the aerodynamic effect becomes more important with the increase in velocity and are almost negligible for lower values. It can be stated that the impact starts to be more important at around 60-70 km/h and becomes dominating for values higher than 120-140 km/h. However, this ranges have to be considered just as a reference since the aerodynamic effect is mainly dependent on the ratio between the frontal area and the vehicle weight. At this regard, generally for a vehicle, the body surface causes approximately 65% of the aerodynamic losses, while the remaining contribution comes from the wheel housings (20%), another 10% is due to the external mirrors, window housings, antennas and all the other bodies exposed to the air stream flow and the engine ventilation counts for 5% [7].

**Rolling resistance contribution**

The other source of loss is represented by the Rolling Friction forces that is due to the deformation of road and wheel in the area of contact. As a matter of fact, the wheel motion implies that new material undergoes a deformation when in contact with the road. This is not permanent in fact once the wheel is no longer in contact with the tarmac the initial shape will be restored. Of course, this deformation implies that some energy is spent that however will not be completely recovered, thus causing a loss and this represents the rolling resistance that can be expressed as follows:

$$F_{rr} = \mu_r mg cos(\alpha) \tag{2.4}$$

where m is the mass of the vehicle, g the gravity acceleration, the term $cos(\alpha)$ is referred to a an inclined road and finally $\mu_r$ is the rolling resistance coefficient. This last depends on many variables where the most relevant ones are: tire pressure, vehicle speed and road surface conditions. For what concerns the former, it is proportional to $\frac{1}{\sqrt{p}}$ and the coefficient can increase by 20% if the road friction decreases as in wet roads. More in detail, the rolling resistance contribution is caused by the fact that the pressure distribution in the area of contact with the ground is asymmetrical. As a consequence of this the resultant force Fz to be shifted forward generating a torque $My = -Fz\Delta x$ with respect to the wheel rotation axis.
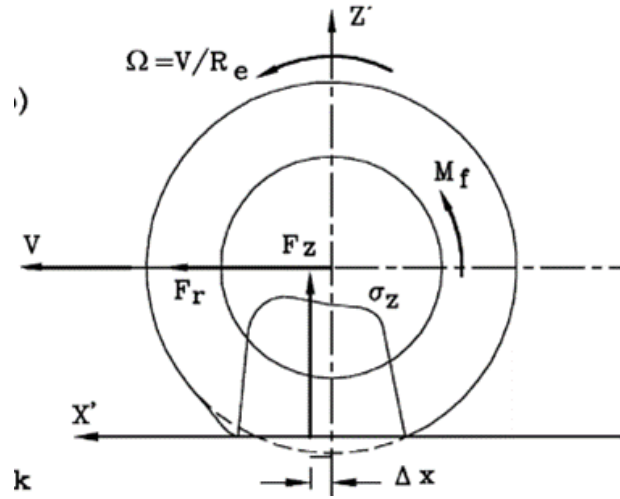


Figure 2.9: Vertical force contribution

The vehicle speed has a small influence at lower values, but its influence increases for higher values when it reaches a critical value. The equation representing the influence of the speed can be expressed using two terms:

$$\mu = \mu_0 + Kv^2 \tag{2.5}$$

where the former term $\mu_0$ and the coefficient K are specific for each tire type. The speed value corresponding to the knee of the diagram is the so-called critical speed, at which the resonance phenomena starts and the tire stops functioning in a normal manner. In fact, once this limit condition is reached waves propagate all along the tire circumference and the tread band vibrates in its plane and in the wheel axis direction as well. Moreover, the rolling resistance increases with the propagated waves and the reason behind that is related to the fact that the wavelength of these last is similar to the length of the contact zone. This happens because there is a decrease of pressure on

17

the trailing part of the wheel and consequently an increase in the leading one that causes the resultant force Fz to move forward.

It is clear that the critical speed value should not be exceeded also because strong thermal phenomena arises at high speed value that could even lead to tire destruction.

The longitudinal tire forces can be considered as the friction forces from the ground that act on the tires that depend on three main factors: slip ratio, friction coefficient between tire and ground and tire normal load. In particular the latter arises from part of vehicle weight and it is influenced by the position of the center of gravity and all the other resistive forces.

**Road grade contribution**

This last contribution related to the inclination of the road is not always present, but plays an important role in the equilibrium equation presented before. In fact, when the road is not flat, there is a weight contribution parallel to the speed that must be considered and that is expressed as follows:

$$F_{grade} = mgcos(\alpha) \tag{2.6}$$

Despite the aerodynamic contribution, this gravitational force becomes very affecting even at low value of road slope [8]. Moreover, the presence of this term implies that the equation (2.2) has to be re-written since the weight contribution is no more just one but is now divided along two directions: parallel and perpendicular to the road. So that the total resistance to motion becomes:

$$R = (mgcos(\alpha) - \frac{1}{2}\rho v^2 S C_z)(\mu_0 + K v^2) + \frac{1}{2}\rho S C_x v^2 + mgsin(\alpha) \tag{2.7}$$

### 2.3.2 Engine model

In the literature there are several ways in which it is possible to model the internal combustion engine and the most used one are:

- static map approach;

- static map and lumped parameter model;

- mean value model;

- one-dimensional fluid dynamic model;

- three-dimensional fluid dynamic model.

For what concerns the last two categories, they are seldomly used for representing and analysing engine subsystems [9]. Whereas the other approaches are more in line with this thesis work. In fact, are functional for describing the ICE thought as a part of a larger

system, that could be the powertrain or the entire vehicle. The first of the three initial approach considers the engine as an ideal actuator, thus reacting in an instantaneous way to the inputs. The main parameters necessary for the engine modelling phase are the ICE torque and revolution speed, that have to be known a priori. More in detail, the former is considered as control variable, while the latter is a measured input, coming from the interaction of the entire powertrain components. Moreover, thanks to these two variables it is possible to estimate the fuel consumption using a correlated look-up table. Finally, the BSFC map presented in section 2.1.2 is typical of this engine model and it accounts for the ICE torque limitations and verify that this value is never exceeded.

The logic behind this block is that the requested torque coming from the controller side is converted into a throttle signal, that in turn commands the engine functioning. In other words, the ICE will adjust its revolution speed and gear engaged to match the torque request. With the knowledge of the revolution speed and of the maximum torque curve, using a look-up table, the brake engine torque can be obtained. This calculation considers also the resistive negative torque especially when the throttle signal is almost null and when idling. The ICE angular speed and torque are also used in combination with a fuel rate look up table, based on specific engine working points, to estimate the fuel consumption over the entire driving cycle and the emissions too.



Figure 2.10: ICE model

### 2.3.3 Driveline modelling

**Gearbox**

For what concerns the gearbox, the family used and modelled in Simulink belongs to the automatic transmission (AT). The introduction of this category several years ago brought different advantages compared to the classical manual transmission mainly in terms of improved driving comfort to the driver (relieved physical effort of pushing the clutch pedal during start-up phases and gearshifts) and reduced jerk to the passengers. More in general, the classification of automatic transmission can be done according to the following list:

- Automation level,

- Gearshift mode,

- Transmission ratios availability,

- Gear trains type

- Start-up device.

The first group can be further split into three subgroups: full automatic, where the transmission control strategy is responsible for all the principal operations (start-up, gear selection and shifting), semiautomatic where the control strategy acts just on the shifting sequence (heavy duty application) and automated that are designed to reduce the production cost, with respect to the other automated transmission type offering at the same time improved sport performance. The division about the gearshift mode concerns the: powershift and without powershift. The difference is related to the power lost during the gear change, that happens just in the second case due to the need of disengaging the current gear to pass to the next one (as in manual transmission). Regarding the third AT classification there are other two typologies: stepped, characterized by a fixed number of gear ratios and stepless (or CVT), with unlimited choice of transmission ratios. The penultimate group is related to the architecture where the discussion is between fixed rotation axis, solution similar to the manual transmission ones and adopted in the DCT (dual clutch transmissions) and epicycloidal transmissions, that that in combination with multi disc clutches can realize different ratios including reverse speed. Finally, the start-up device classification concerns the use of the more classical friction clutch or the torque converter. The transmission type present in the light-duty vehicle under study and represented by the name HI-MATIC, is a full automatic, powershift, stepped epicycloidal gear train with the application of the torque converter. In the virtual environment, this description is translated into the usage of a "variable ratio transmission" block, whose inputs are the torque coming from the propeller as well as the eight gear ratios, while the output is the gearbox torque that enters directly into the differential.

| Gear ratios | |
|---|---|
| $\tau_1$ | 4.714 |
| $\tau_2$ | 3.314 |
| $\tau_3$ | 2.106 |
| $\tau_4$ | 1.667 |
| $\tau_5$ | 1.285 |
| $\tau_6$ | 1 |
| $\tau_7$ | 0.839 |
| $\tau_8$ | 0.667 |
| $\tau_f$ | 3.33 |

Table 2.2: Gear ratios

Particular attention must be put on the gear shifting control logic implemented in Simulink. As a matter of fact, the previous mentioned logic allows to engage and shift
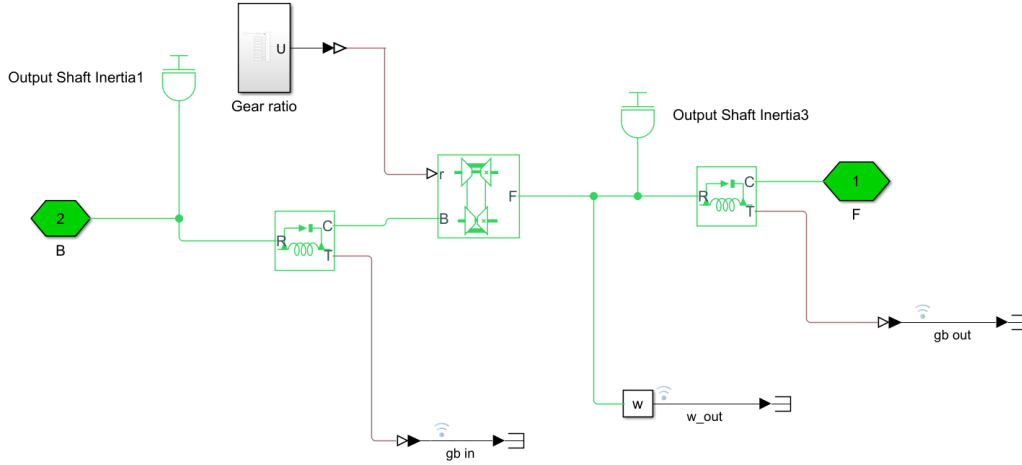
Figure 2.11: Gearbox model

the eight gears based on a simple condition: whether the actual vehicle speed is greater or lower than some predefined thresholds, both for the upshift and downshift case. These values are stored in two different one dimension look-up table and are derived using the beneath formula:

$$v = \frac{n_{ICE}\pi R_{wheel}}{30\tau_i\tau_f} \tag{2.8}$$

Where $R_{wheel}$ is the loaded radius of the wheel and ti and tf are the gear ratio of the eight gears and the final drive gear ratio. For what concerns $n_{ICE}$ is the engine revolution speed at which the gear change must be operated.

A more detailed review of this logic will be held in section 2.4.3. In a more practical way, these decisions are taken using a flow chart block, that computes after 1.1 seconds for the upshift and 1.2 seconds for the downshift the gears that must be engaged based on the previous described input. The intervals used are functional to avoid having a too frequent gear shift, that would lead to a not efficient driving style and uncomfortable driving.

**Torque converter**

This component represents a start-up device for automatic transmission vehicle that connects the ICE to the transmission with a continuously variable transmission ratio. More in detail, it is a fluid coupling system made up of three elements: the turbine (connected to the transmission side), the impeller (connected to the engine side) and the stator (placed in between the two parts). The connection among the components is realized through the transmission fluid [10].

The main aim of the torque converter is the ability to increase the torque coming from the propeller after the idling and complete stop phases, thanks to the stator presence.
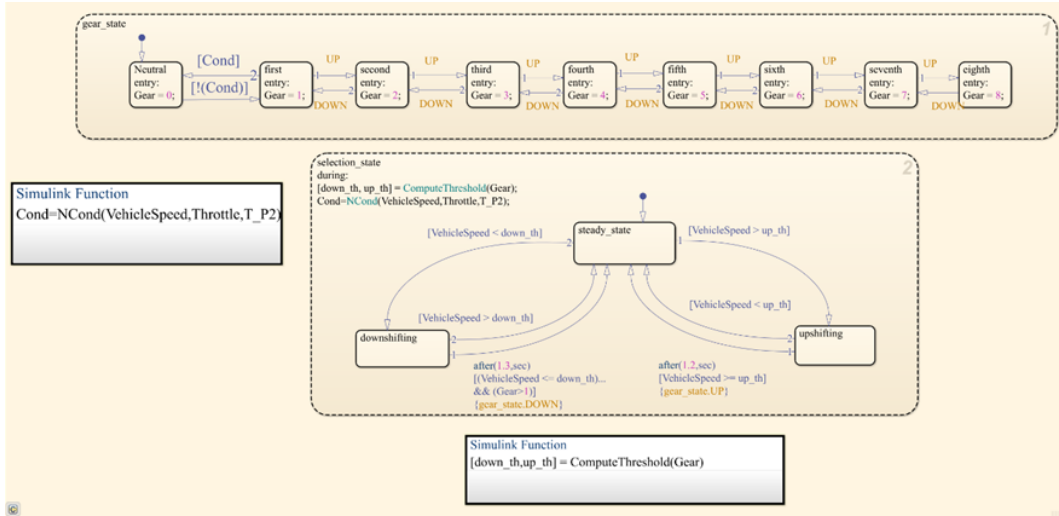
Figure 2.12: Gear shifting logic flow chart

In fact, in more classical fluid coupling system (where there is no stator) the fluid going back from the turbine to the impeller, acts against the impeller rotation, thus leading to large amount of wasted energy. Vice versa, the same fluid is readdressed in a way that helps the impeller rotation, resulting in a larger amount of energy in the input side and higher flow to the turbine side. This is what causes an increase in the output torque. This action can be expressed mathematically with the following formula:

$$T_T = T_S + T_P \tag{2.9}$$

Where $T_T$ is the turbine torque, $T_s$ the stator torque and $T_P$ the impeller torque. As happens more frequently, the turbine torque is greater than the impeller one, implying that the stator torque must have the same direction of the input torque. It is worth noticing that the stator is installed using a one-way clutch that avoids its counter rotation with respect to the impeller when the fluid travels from turbine to impeller. Moreover, the main parameters that characterize the torque converter can be listed as follows:

- Speed ratio $\nu$, defined as the ratio between output and input speed;

- Torque ratio $\mu$, defined as the ratio between output and input torque;

- Performance coefficient $\lambda$.

The latter can be derived from the following equation:

$$M_1 = \lambda \rho \omega_1^2 D^5 \tag{2.10}$$

Where D is the outer diameter of the largest wheel, $\rho$ is the fluid mass density, while $\omega_1$ and $M_1$ are the corresponding input rotational speed and torque. Thanks to the

knowledge of the previous described features it is possible to obtain the characteristic curve of the torque converter.
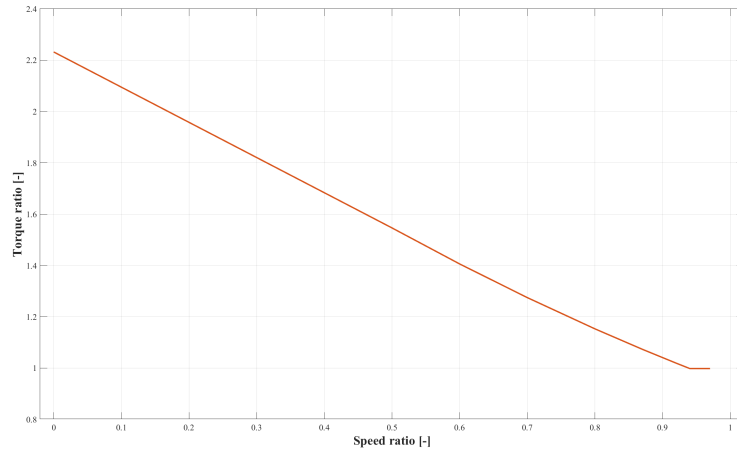


Figure 2.13: Torque converter diagram

For what concerns the modelling and implementation of this component in Simulink environment the elements used, in addition to the torque convert block itself, are the clutch, two torque sensors and two inertias. The first of the last three, allows the impeller and the turbine to couple one each other after a stalling or idling phase; the second ones are used to measure the torque values going in and out of the torque converter and finally, the last ones are necessary to have a more accurate representation of the system.
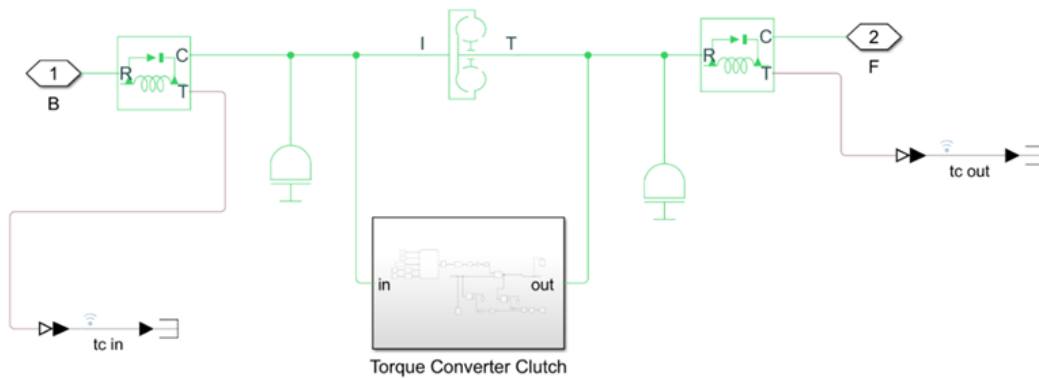


Figure 2.14: Torque converter model

**Differential**

The last component of the driveline is represented by the differential. This device allows the torque coming from the input shaft to be split into the two output shafts. The

most frequent solution is when the torque exiting from the final drive (that is a gear train designed to further reduce the speed of the gearbox) is divided in equal parts acting on the traction wheels of the same axle. The virtual model shown below is representing an ideal differential, so without any friction losses. It is used a planetary gear set (PGS) to model this driveline component thanks to which the ordinary transmission ratio, with 1 degree of freedom and carrier locked can be derived:

$$r = -\frac{z_1}{z_2} \tag{2.11}$$

Where $z_1$ and $z_2$ are the sun and ring gear numbers, while the minus sign is due to the fact that the sun and ring rotate in the opposite direction [11].
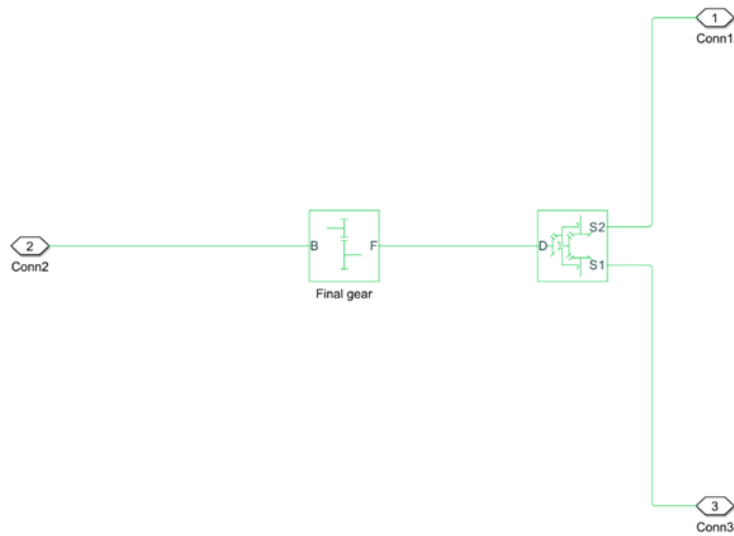


Figure 2.15: Differential model

## 2.4   Validation phase

This section represents the heart of the second chapter where at the beginning the validation phase is introduced in terms of methodology and importance related to the automotive sector, with particular focus on the tool used for acquiring data. In a later stage, with the knowledge of the modelled powertrain components, are performed proper practical validation procedures, related to two homologation driving cycles, WLTC and RDE and then to specific operations related to the gear shift and coast down. At the end it is introduced the so-called TCF to enhance the measurement accuracy.

**Model validation**

Validation of an experimental model in the automotive sector, is a fundamental step and consists in verifying and validating the accuracy of mathematical models that are used

to simulate the behavior of various systems and components present in a vehicle. This includes powertrains, chassis systems, and other subsystems, such as suspension, steering, and braking. The objective of this validation is to ensure that the model accurately predicts the behavior of the system under various operating conditions and loads. The validation process typically involves collecting data from physical testing of the actual system and comparing the results with the predictions from the model. The collected data is then used to fine-tune the parameters of the model to increase its accuracy. Moreover, in the automotive sector more than in other realities, model validation is critical for the development of new vehicles and for the improvement of existing ones. This helps to identify any design or manufacturing issues early in the development process, reducing the risk of problems and increasing the likelihood of a successful launch, improving at the same time the reliability and performance. Another positive aspect is the possibility of seeking for improvement after the model has been validated. This allows the manufacturer to reduce the cost of physical testing and have simultaneously reduction in fuel consumption and emissions as well as improved safety.

Furthermore, models can be validated using several techniques used in specific phases of modelling and simulation procedure, all of which have common aspects to software validation so much that the same methods can be used for model validation. The several techniques present are a mirror of the diverse requirements and levels of validity along the process. Before going in detail with the methods used it is worth saying that model validation is closely correlated with model verification, thus the definition of one is impossible without considering the other. To have a clearer thought about model validation, relying on what Balci states, is possible to declare that: "Model Validation is substantiating that the model, within its domain of applicability, behaves with satisfactory accuracy consistent with the model and simulation objectives" [12]. According to what comes out from the previous lines, the concept of validation is analyzing a model within a specific domain, related to the target that the model and the system have to fulfill. In other words, the validation process concentrates on solving the right problem and satisfying the user requirements. This definition in also in accordance with the IEEE 102 standard [13]: "The validation process provides evidence whether the software and its associated products and processes satisfy system requirements allocated to software at the end of each life cycle activity. Solve the right problem and satisfy intended use and user needs" [13]. It is clear how from both the above-mentioned definitions is sharp that the concept of validation is different from the verification, although the two are closely related. As a matter of fact, the latter is "substantiating that the model is transformed from one form into another, as intended, with sufficient accuracy. Model verification deals with building the model right" [13]. In a nutshell, verification is aimed at looking for the correct transformation from one form to another focusing on the relation between the model itself and the desired properties of the model.

Having said this, in the literature there is not a deep separation between the two definitions. The reason behind this misunderstanding can be related on one side to the improper use of the verb with the meaning or checking or testing something. To confirm this, there is a contrast between what IEEE standards and ISO 9001 [14] declare. For the latter the discrepancy among verification and validation is based on the application time

during the software development. In this case, the validation is related to the analysis of the software product at the end of each phase, whereas the validation consists in checking the products once the development is finished. Another important field of investigation is the one related to the methods used. In fact, the verification phase can be performed by mathematical proofs, while the same cannot be said for the validation phase since they would require expressing the context of application. All these discrepancies show how both validation and verification are complex multi-facetted processed that in parallel represent a fundamental and robust part in the automotive industry.

| Aims/Requirements | Experimental Validation = Dynamic Verification/Validation = Dynamic Testing = Empirical Verification | | | | | Non-Experimental Validation (sometimes Static Validation) | Verification = Static Verification /Validation |
|---|---|---|---|---|---|---|---|
| | Configuration | Evaluation | Simulation | Observation | Testing | | |
| -model comparison -degenerative tests -historical data -predictive data -extreme conditions -Turing-test -event validity -visual analytics | -factorial designs -randomized block designs -covariance designs -hybrid designs -sensitivity analysis -internal validity | -metrics | -engine -event queues -RNG | -black-box -gray-box -white -box -simulation traces | -statistical test -simulation-based model-checking | -code inspection -design inspection -visualization of model structure -walkthrough | -model-checking -formal code analysis -cause-effect graphing -control analysis -data analysis -fault/failure analysis -symbolic evaluation |

Figure 2.16: Validation methodologies

### Levels of validity and similarity with software testing

In the literature different levels of validity have been defined. Just to name one, for Zeigler there are three levels of validity [15]:

- replicative validity (or historical validity), where the model under study is able to reproduce the behavior of the real system;

- predictive validity, where the model reproduces data in advance before the real system is observed;

- structural validity, in which the model reproduces the real system in terms of structural relations.

The former of the three is what is used in this thesis work, where the real system data is the one where the vehicle has performed the two driving cycles, WLTC and RDE. In addition, to the classification about the different levels of validity, model validation, but more in general the modeling phase, defined as a detailed description of a model using formal language, has many common aspects with software testing. In fact, the same strategies used for software testing can be used for the model validation too.

According to Myers [16] there are two main families of strategies for software testing: static testing and dynamic testing. The former comprises of inspections, walkthroughs, and reviews that are addressed for non-experimental validation. Whereas the latter is related to the usage of a software and as a consequence is strictly related to experimental validation. As a result of this, the tool used to perform the simulation affects the final

outcome of the validation by simulation, that is way more challenging than the modeling step. At this regard, Zeigler considers the experimental frame [15] that is made up of three elements: a generator, representing the model itself, an acceptor and a transducer. The previous mentioned frame accounts to not only the modeling layer but also the simulation layer that refers to the conditions of observation and experimentation of the model.

### 2.4.1   Chassis dynamometer test

During the development of a new vehicle model, it is essential to test and validate the performance and functionality of the various components and systems that make up the vehicle. One common tool used for this purpose is a chassis dynamometer test bench, that is a piece of equipment that simulates the conditions of real-world driving in a controlled environment, allowing to evaluate and optimize the performance of the vehicle before it is released for production.

One of the primary benefits of using a chassis dynamometer test bench is that it provides a controlled and repeatable environment for testing. With a dynamometer, it is possible to simulate a wide range of driving conditions, including acceleration, braking, and cruising at different speeds and loads. This allows for a more comprehensive evaluation of the vehicle's performance and can help identify any issues or areas for improvement. The controlled environment also makes it easier to compare the performance of different vehicle models or configurations and to make objective assessments of their strengths and weaknesses. Another advantage of using a chassis dynamometer test bench is that it allows the real-time collection and analysis of data. In fact, during a test run, sensors placed on various parts of the vehicle can measure a wide range of parameters, such as engine speed, torque, and fuel consumption. This data can then be analyzed to identify patterns and trends, which can provide insights into the performance of the vehicle and the effectiveness of any modifications or improvements that have been made. Additionally, the real-time data can be used to identify any potential issues or malfunctions before they become more significant problems.

The use of a chassis dynamometer test bench is beneficial also to evaluate the durability and reliability of the vehicle's components and systems. By simulating real-world driving conditions, the vehicle can be subjected to a wide range of stresses and strains, including high speeds, hard braking, and rough terrain. This can help identify any weaknesses or areas of the design that may need to be reinforced or improved to ensure that the vehicle can withstand the rigors of regular use. At the same time a crucial aspect is the possibility to measure vehicle emissions and environmental impact. This data can then be used to assess the vehicle's compliance with emissions regulations and to identify any areas of the design that may need to be modified to reduce emissions further. Finally, the use of a chassis dynamometer test bench can help streamline the development and validation process, reducing costs and time to market. By identifying and addressing any performance or reliability issues early in the development process, the risk of costly delays or recalls once the vehicle is in production is reduced. Additionally, by using a controlled environment to test the vehicle's performance, it is lowered the need for expensive and time-consuming field testing, which can further reduce costs and time to market.

### 2.4.2 Homologation driving cycles

Homologation driving cycles, such as the Worldwide Harmonized Light Vehicles Test Cycle (WLTC) and the Real Driving Emissions (RDE) test, are used in the automotive sector to assess the fuel efficiency and emissions of vehicles. These driving cycles are designed to replicate real-world driving conditions, including different driving styles, speeds, and road types, to provide a more accurate representation of a vehicle's actual performance.

**WLTC**

In the latest years the attention towards the environment is increasing exponentially and with it the legislations to keep pollution under control and reduce it as well. As a matter of fact, it is possible to gather together the main targets in three bullet points: lower the greenhouse gases (GHG), reduce the dependance on petroleum-based fuels and improve local air quality. To achieve these quite challenging goals a legislative framework must be taken in consideration in all those sectors harmful for the environment. At this regard, concerning the transport one the focus on air quality has been object of study since the 60s especially in three parts of the world where the progress was increasing steeply: North America, Europe and Japan. In these countries pollutants such us CO, $CO_2$ and $NO_2$ reached critical levels such that procedures aimed at determining pollutant emissions started to be thought. The creation of the previous mentioned test involved the cooperation of industries and environment authorities with the common target of defining an harmonized test procedure. Since vehicle emissions are correlated to the working pointes of the engine, there is the need for a differentiation based on the type of internal combustion engine. Nowadays the classification concerns: light duty vehicles, heavy duty vehicles, motorcycles and engine not used for road applications. In order to estimate the vehicle emissions and set some corresponding limits, several driving cycles have been implemented towards the years. One of the oldest is the New European Driving Cycle (NEDC) that however is no more used due to mainly two criticisms: the inability to represent real life driving conditions and the so called "cycle beating" by means which car manufacturers falsify the results in terms of pollutant emissions.

To overcome the issues of the previous driving cycle the so called WLTC (World-wide harmonized duty test cycle) is introduced with the aim of represent in a more realistic way the driving conditions. In fact, this newer test last longer (30 minutes instead of the previous 20 minutes), has a higher average speed due to the more dynamic speed profile and has also an higher distance to be covered, 23,336 km. In addition to the characteristics of the driving cycle, specific environment and road conditions have been defined: lower cold start temperature of 14-23°C, that will have a lower impact over the longer cycle compared to the NEDC; a more realistic road load estimation in which the tested vehicle is as close as possible representative of the existing one. In other words, WLTC is a laboratory test, performed in a dynamometer with well-defined and repeatable conditions and can be also used to estimate the fuel consumption for light duty vehicles. There is a criterion thanks to which it is possible differentiate the vehicle type and apply this test. As a confirmation of this there are three WLTC tests that can be performed based on the power to weight ratio (PWr) of the vehicle. This last parameter is defined as

28

the ratio of the rated power over the mass in running order (defined as vehicle mass with the fuel tank at its 90% plus driver mass and the weight of other liquids stored onboard plus the weight of the cabin, bodywork, the couplings and the spare wheel) minus 75 kg. The classification is divided in three levels:

- Class 1: representing low power vehicles with a PWr lower than 22;

- Class 2: in which belongs vehicles with a PWr included between 22 and 34;

- Class 3: for high power vehicles with a PWr over 34;
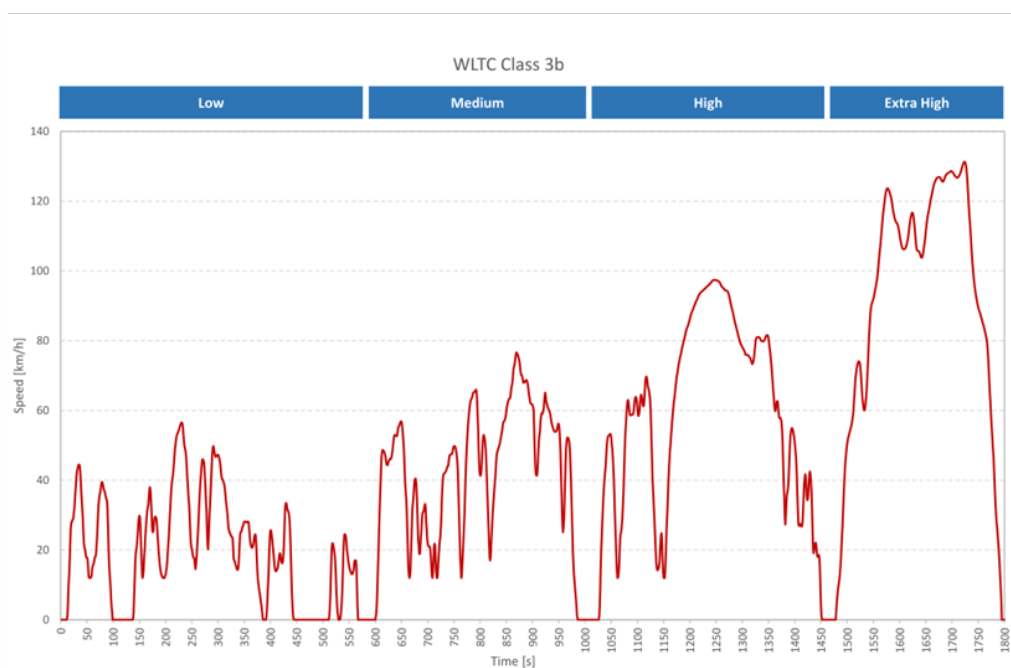


Figure 2.17: WLTC homologation driving cycle

Nowadays, most of the cars driven in Europe and Japan fall in the last group since the average PWr is usually between 40 to 100 W/kg. it could also be possible to make a further differentiation of the third group based on the maximum speed: class 3a for those vehicles with a speed not higher than 120 km/h and class 3b for the others. Is clear that the speed trend for each of the three groups us different whereas the duration does not change. For class 3 the driving cycle is divided into four parts characterized by a maximum speed each. From the picture below it is possible to state that the first part, Low, can reach a speed up to 56.5 km/h, the "Medium" 76.6 km/h, the "high" one 97.4 km/h and finally the "extra high" the speed can go up to 131.3 km/h [17].

**RDE**

| WLTC class 3 test cycle | | | | | |
|---|---|---|---|---|---|
| | Low | Medium | High | Extr High | Total |
| Duration [s] | 589 | 433 | 455 | 323 | 1800 |
| Stop duration [s] | 150 | 49 | 31 | 8 | 235 |
| Distance [m] | 3095 | 4756 | 7162 | 8354 | 23366 |
| Duration [s] | 589 | 433 | 455 | 323 | 1800 |
| Percentage of stops [%] | 26.5 | 11.1 | 6.8 | 2.2 | 13.4 |
| Maximum speed [km/h] | 56.5 | 76.6 | 97.4 | 131.3 | |
| Averge speed withot stops [km/h] | 25.3 | 44.5 | 60.7 | 94.0 | 53.5 |
| Averge speed with stops [km/h] | 18.9 | 39.4 | 56.5 | 91.7 | 46.5 |
| Minimum acceleration $[m/s^2]$ | - 1.5 | - 1.5 | - 1.5 | - 1.44 | |
| Maximum acceleration $[m/s^2]$ | 1.611 | 1.611 | 1.666 | 1.055 | |

Table 2.3: WLTC characteristics

The second driving cycle analyzed is the Real Driving Emission (RDE), that was created to overcome the limitations related to the WLTC. In fact, the move from the previous cycle to the latter described was necessary for the following reasons:

- Limited real-world relevance: The WLTC driving cycle was designed to be more accurate than the previous New European Driving Cycle (NEDC) test, but it still had limited real-world relevance. The test was conducted in a laboratory, and the driving conditions were not representative of real-world driving patterns, leading to discrepancies between the laboratory results and actual on-road performance.

- Manipulation by manufacturers: There were concerns that some manufacturers were manipulating the test results to make their vehicles appear more fuel-efficient and emit fewer pollutants than they actually do in real-world driving conditions. This led to calls for a more stringent test procedure that would be harder to manipulate.

- Stricter emissions regulations: The European Union (EU) introduced stricter emissions regulations, with the aim of reducing air pollution from vehicles. The RDE driving cycle was developed in response to these regulations, as it measures actual emissions under real-world driving conditions and is more representative of on-road performance than the laboratory-based WLTC test.

- Increased public scrutiny: There was growing public awareness of the environmental impact of vehicles, and consumers were demanding more accurate information about a vehicle's actual emissions performance. The RDE driving cycle was seen as a way to provide more reliable and transparent information about a vehicle's real-world emissions.

This new procedure was firstly introduced in March 2016 and it is not meant to replace the laboratory test one but is thought to be use with it. In fact, RDE checks that limits imposed for pollutants are not exceeded during a real situation using a portable emission monitoring system (PEMS). The data acquired from the previous mentioned system have

to be processed in two methods: a CO2 moving average window (EMROAD) and a power binning (CLEAR). Moreover, RDE emission limits are the same as the WLTC, multiplied by a conformity factor. This last considers the error during the instrumentation, since it is not possible to guarantee the same level of accuracy and repeatability of a laboratory test. Furthermore, to be compliant with its definition, this new test is more articulated than the previous one and the vehicle is tested under several conditions (including height, temperatures, slopes, etc) [18].

More in detail, there are three driving scenarios each of which must cover at least 16 km: an urban part, in which the speed is lower than 60 km/h), a rural part, speed lower than 90 km/h and a motorway part for higher speed than 90 km/h. Having said this, RDE did not enter in law immediately but followed three steps. A first monitoring phase, in which the test was introduced without any conformity factor in April 2016. A second phase, for the RDE type approval test where conformity factors for NOx and PN were introduced. For the former it went from 2.1 in 2017 to 1.43 in 2020, whereas for the latter it was set to 1.5. Finally, the last phase including the in-service conformity requirements in which RDE was applied for vehicle designed for people transport and for those designed for the carriage of goods (N1 category) with a maximum weight of 3.5 tons of class I approved after 1 January 2019 and registered after 1 September 2019 and to N1 classes II and III and N2 vehicles based on types approved after 1 September 2019 and registered after 1 September 2020. The previous mentioned classification is based on reference mass RW, that is defined as the mass of the vehicle in running order minus the driver weight of 75 kg and increased by 100 kg.

|  | **Euro1-2** | **Euro 3+** |
|---|---|---|
| Class I | $RW \leq 1250kg$ | $RW \leq 1305kg$ |
| Class II | $1250kg < RW \leq 1700kg$ | $1305kg < RW \leq 1760kg$ |
| Class III | $1700kg < RW$ | $1760kg < RW$ |

Table 2.4: Classification based on reference mass

More in particular, the RDE test performed in this thesis work is a combination of two driving cycles: the so-called TFL (traffic in London) and SIM95. The former, the TFL scenario, is repeated two times, where each part last 8.9 km, so that the overall length of the cycle is 84,1 km including the urban, rural and highway part.

|  | **TFL1** | **TFL2** | **Rural** | **Highway** | **Total** |
|---|---|---|---|---|---|
| Start time [s] | 0 | 2310 | 4620 | 6270 | 0 |
| End time [s] | 2310 | 4620 | 6270 | 7425 | 7425 |
| $\Delta t[s]$ | 2310 | 2310 | 1650 | 1155 | 7425 |
| Distance [km] | 8.9 | 8.9 | 31.3 | 35.0 | 84.1 |
| $v_{max}[km/h]$ | 50.7 | 50.7 | 119.8 | 147.0 | 109.1 |
| $v_{min}[km/h]$ | 13.9 | 13.9 | 68.1 | 109.1 | 40.8 |

Table 2.5: RDE characteristics

**Differences between WLTC and RDE**

It is worth noting highlighting the difference between testing a vehicle in a WLTC versus an RDE driving scenario since they can significantly impact the engine working points and overall behavior. The WLTC test cycle involves a series of standardized driving conditions that are designed to replicate typical driving patterns and speeds in urban, suburban, and highway environments. During the WLTC test, the engine will be operated at a range of different working points, including low speeds and high loads, to evaluate the vehicle fuel efficiency and emissions performance under different driving conditions. As a result, the engine behavior during the WLTC test will be more representative of typical driving conditions.

In contrast, the RDE test involves driving the vehicle on real roads, under various conditions, such as different altitudes and temperatures, to assess the vehicle's emissions performance during actual driving. This test measures the pollutants that the vehicle emits, such as NOx and particulate matter, and how they vary with different driving conditions. As a result, the engine's working points and overall behavior during the RDE test will be less predictable and more dependent on the specific driving conditions encountered during the test. The RDE test, therefore, provides a more accurate assessment of the vehicle's emissions performance during real-world driving conditions but is less suitable for evaluating the engine's fuel efficiency and overall performance.

### 2.4.3 Gear shifting logic extrapolation

As the work went on, it was noticed that the gear shifting strategy had a huge impact on vehicle behavior and performance related to the validation purpose. As a matter of fact, one of the main causes of difference between numerical and experimental data was due to the different gear shifting strategy used. As a confirmation of what just written, the gears change logic directly affects the operating working points of the engine, allowing it or not to work in its optimal speed range. Moreover, all the main powertrain variables are altered, thus leading also to some changes in fuel consumption and components wear. Another fundamental parameter to consider along with the engaged gears is the powertrain output torque, as the gear ratio affects the amount of torque transmitted to the wheels. Proper gear selection can ensure that the vehicle output torque matches the required driving conditions, ensuring optimal performance and fuel efficiency.

For what regards the validation process, the available useful data for this task were the engine revolution speed, the actual vehicle speed and the gear ratios (including the final drive ratio) related to the WLTC. After several attempts in understanding the exact gear engaged for each time step of the driving cycle based on the engine and vehicle acceleration, the right procedure was found. From the experimental data was computed the gear ratio variation corresponding to each ICE and vehicle speed value using equation (2.8) where in this case, the term of the left-hand side was the $\tau_i$. With the knowledge of the latter, through the use of proper thresholds (equal to the eight experimental gear ratios) it was possible to understand the exact shifting sequence. In other words, it has been possible to have the trend of the engaged gears within the overall cycle duration.

Figure 2.18 represents the experimental gears succession that will be used as base

for deriving the numerically one in Simulink environment. In fact, the experimental timeseries of the gears is imported in the virtual model and used as a reference to be matched in a second moment using the flow chart described in section 2.3.3. More in detail, the array of gears is used in open loop as an input in order to identify the ICE revolution speed at which each gear is changed, that are gathered in the tables below.
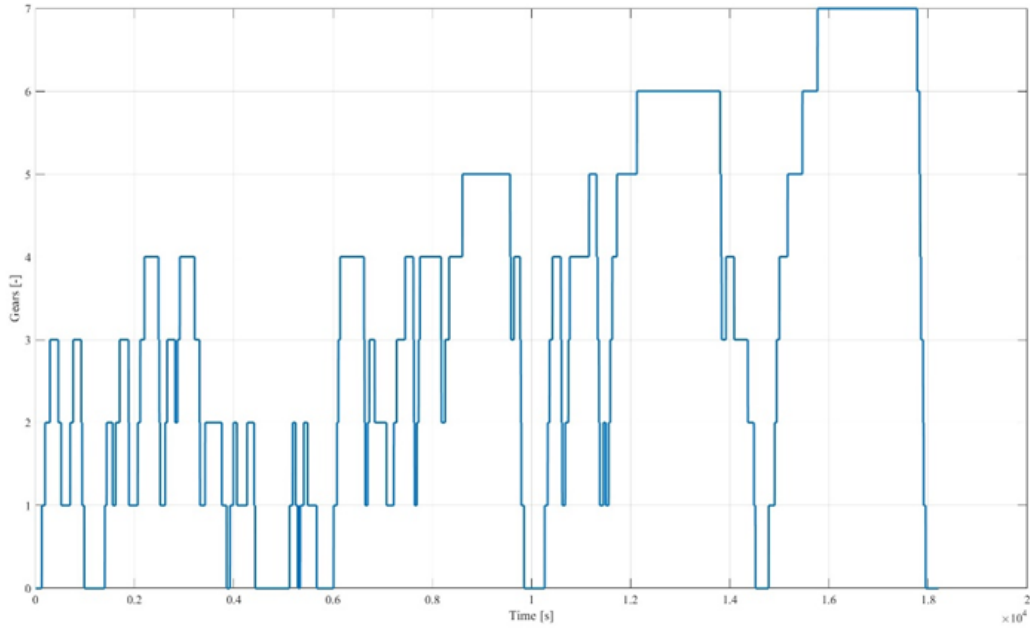


Figure 2.18: Gears sequence

| Upshift | |
|---|---|
| Gears | Engine speed [rpm] |
| $1 \rightarrow 2$ | 2405 |
| $2 \rightarrow 3$ | 2775 |
| $3 \rightarrow 4$ | 2400 |
| $4 \rightarrow 5$ | 2600 |
| $5 \rightarrow 6$ | 2770 |
| $6 \rightarrow 7$ | 2880 |
| $7 \rightarrow 8$ | 3000 |

| Downshift | |
|---|---|
| Gears | Engine speed [rpm] |
| $1 \rightarrow 2$ | 800 |
| $2 \rightarrow 3$ | 800 |
| $3 \rightarrow 4$ | 800 |
| $4 \rightarrow 5$ | 800 |
| $5 \rightarrow 6$ | 800 |
| $6 \rightarrow 7$ | 800 |
| $7 \rightarrow 8$ | 800 |

Table 2.6: Engine speed for upshifts          Table 2.7: Engine speed for downshifts

It is worth noting that the revolution speed during the downshift has been kept constant in order to better delimitate the passage from one gear to another one. After this reverse engineering operation it was possible to use the logic present in the Simulink model and adjust the sequence in terms of fast gear fluctuations by using as markers the thresholds corresponding to each upshift and downshift. As a result, the final gear shifting logic is found in Figure 2.18.

The level of mismatch between experimental and numerical value can be considered good in terms of model validation.
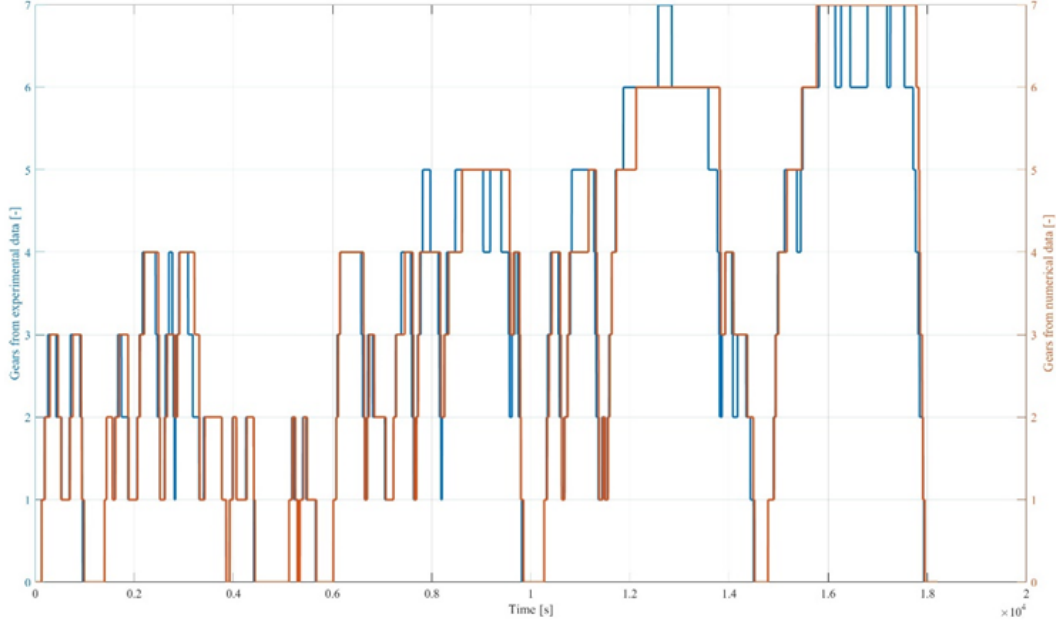


Figure 2.19: Gear comparison

### 2.4.4 Coast down method

Another field to inspect is the power available at 100 [km/h]. This evaluation can be done taking into account the Coast Down method thanks to which is possible to estimate the exact expression of the forces acting on a road vehicle during the so-called coast down maneuver. These last could be also used to estimate the fuel consumption by reproducing the previous mentioned forces in a dynamometer test. More in detail this test is performed in a sufficiently long closed track and with no slope where the vehicle is accelerated at a speed higher than 130 km/h, then the gearbox is placed in neutral position, and the driver let decelerate the vehicle with the clutch engaged and without using the brakes. The previously mentioned forces are resistive forces that act against the vehicle motion due to air and tire rolling resistance (the contribution related to the slope is neglected being the road flat). In addition are also considered the forces computed at the wheels due to driveline downstream the gearbox and due to a possible remaining torque of the braking system.

Furthermore, among the several vehicle tests, coast down is one of the most recurring used to generally acquire information about the vehicle and its interaction with the environment. In this work, this test has been used to estimate, for specific speed values, the expression of resistance forces acting on the vehicle, whose contribution and equations have already been presented in section 2.3.1. In addition, are also considered the forces

computed at the wheels due to driveline downstream the gearbox and due to a possible remaining torque of the braking system:

$$F_{dvl} = T_0 + T_1 v \tag{2.12}$$

$$F_{brk} = 4\frac{T_{brk}}{R} \tag{2.13}$$

Where $T_{brk}$ is the possible remaining braking torque for each wheel, that is usually lower than 5 Nm and R is the tire rolling radius. Finally, the overall resistive forces can be gathered together and represented as the sum of three terms, leading to a two degrees of freedom equation, as follows:

$$F_{cd} = F_0 + F_1 v + F_2 v^2 \tag{2.14}$$

In addition, since speed values during the coast down maneuver are moderate it is possible to perform a linear regression of equation (2.14), so that the rolling resistance coefficient can be thought linearly dependent on vehicle speed, leading to a new equation:

$$F_{cd} = F_0 + F_2 v^2 \tag{2.15}$$

Furthermore, several requirements concerning the vehicle, test track, test speed, atmospheric conditions and measuring equipment must be met when performing the coastdown tests. These requirements differ depending on the type of regulation used and based on the different driving cycle. The WLTC requirements are listed in Table 2.8.

| Measurements requirements | |
|---|---|
| Longitudinal slope [%] | $\pm 1$ |
| Local inclination [%] | $\pm 1$ |
| Cross sectional slope [%] | 1.5 |
| Wind average speed [m/s] | 7 |
| Wind speed [m/s] | 10 |
| Wind cross vector component [m/s] | 4 |
| Air temperature [°C] | 5-40 |
| Vehicle run-in [km] | 3 |
| Tire run-in [km] | 200 |
| Tread depth [%] | 80-100 |
| Frequency [Hz] | 5 |

Table 2.8: Coast down tolerance values

Moreover, the results obtained in accordance with the WLTC requirements are used to determine the type-approval fuel consumption by transferring the vehicle load onto a dynamometer [19,20]. For what concerns the obtained result the discussion is postponed in chapter 5.

### 2.4.5   Transient correction factor

Nowadays car companies are putting lots of effort in developing a vehicle model able to reproduce all its features, but in the majority of cases these models use steady-state maps of the ICE to estimate the fuel consumption. More in detail, the fuel consumption rate values are fitted as a function of engine torque and speed through a look-up table. However, the consumption estimation with these models does not represent the reality. In fact, measured values are always higher compared to the computed ones based on steady-state maps, that are not able to reproduce the engine transient phases. Some experiments have been done to prove confirm the previous statement in which two vehicles, a Chevrolet Silverado and a Ford F-150, were compared [21]. The outcome was that the lack of transient phases brings a difference in the estimation in the range from 2 to 4%. The situation can get worse in more aggressive driving style cases where the relevance of acceleration and deceleration is higher. At the same time the vehicle parameters and engine type are influencing the measurement too. In the literature there are several techniques aimed at considering the transient behavior of the engine under different situations and different operating conditions.

Among the several methods present in the literature, what is particularly interesting is the approach used in [22] where four different cases are studied according to the sign of the derivative of engine speed and torque, that are defined as dynamic variables. To mind the inaccuracy of steady state based models, a correction factor, called transient correction factor (TCF), is multiplied to the computed fuel consumption value. In a nutshell, the use of TCF is addressed at enhancing the calibration of steady-state fuel consumption rate.

**Transient fuel consumption model**

In the literature, used as reference in this work, among the several TCF expressions the most accurate one is the following:

$$TCF = A \cdot \omega_{ice} + B \cdot \frac{d\omega_{ice}}{dt} + C \cdot T_{ice} + D \cdot \frac{dT_{ice}}{dt} + E \qquad (2.16)$$

in which the four coefficients multiplying the derivatives are obtained by a regression analysis. In particular the D coefficient is the most relevant one since it is two orders of magnitude higher than the the others. So, equations (2.16) can be re-written in a more simplified form:

$$TCF = D \cdot \frac{dT_{ice}}{dt} + E \qquad (2.17)$$

From the previous equation it is possible to state that the main responsible for transient fuel consumption is the torque change rate. Concerning the above mentioned coefficients, they are evaluated according to four different scenarios based on the sign of engine speed and torque change rate.

From the above table is clear that numerical data, in terms of dynamic variables, are divided in four cases, according to which the TCF value will be then computed as the ratio of experimental over steady-state fuel consumption. More in deep in this analysis

| Case a | $\frac{d\omega_{ice}}{dt} > 0$ | $\frac{dT_{ice}}{dt} > 0$ |
|--------|-------------------------------|---------------------------|
| Case b | $\frac{d\omega_{ice}}{dt} > 0$ | $\frac{dT_{ice}}{dt} < 0$ |
| Case c | $\frac{d\omega_{ice}}{dt} \leq 0$ | $\frac{dT_{ice}}{dt} > 0$ |
| Case d | $\frac{d\omega_{ice}}{dt} \leq 0$ | $\frac{dT_{ice}}{dt} > 0$ |

Table 2.9: Classification of TCF

the "E" coefficient is imposed equal to one so that there is a correction of fuel consumption just when there is a change of torque.

After the data were correctly subdivided, thanks to the use of the MATLAB application "polyfit curve" it was possible to estimate the D coefficient for the four cases, as depicted in the figures below. The input values were the torque change rate and the corresponding TCF values. The table below gathers the obtaiend coefficients:

| Cases | D coefficients |
|-------|----------------|
| a | 0.002648 |
| b | -0.002271 |
| c | 0.005909 |
| d | -0.00434 |

Table 2.10: D coefficients

With the knowledge of the correction factor the new fuel consumption can be obtained simply multiplying it by the steady state one. The result gives 2,563 liters of fuel consumed over the WLTC driving cycle with respect to the original 2,493 liters, that is a 6.16% higher consumption, in line with the expected range of improvement. The accuracy improvement will be discussed in detail in chapter 5.
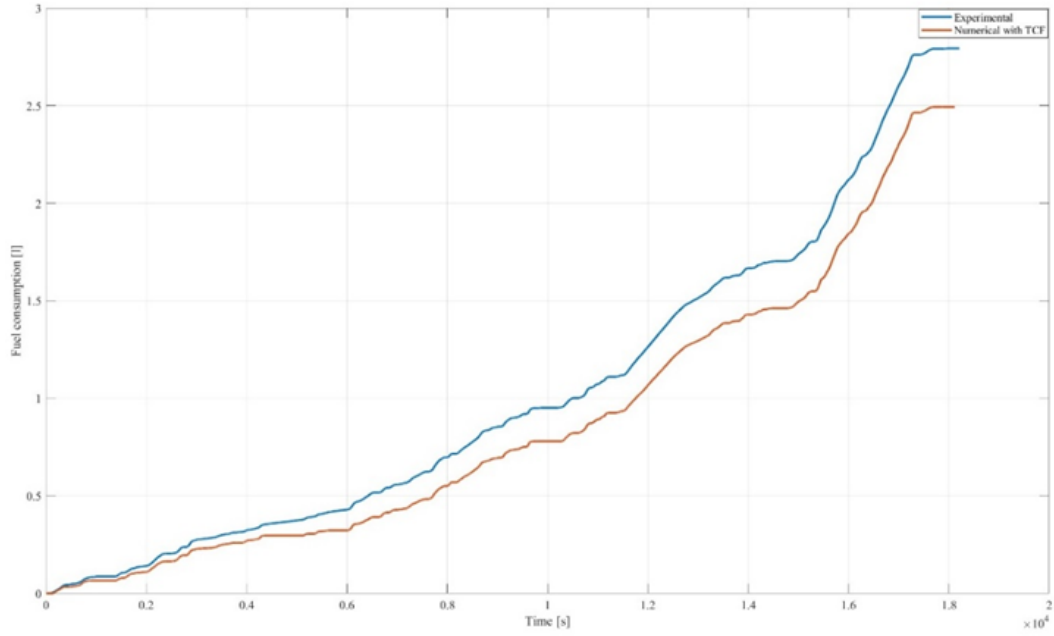
Figure 2.20: Fuel consumption with TCF
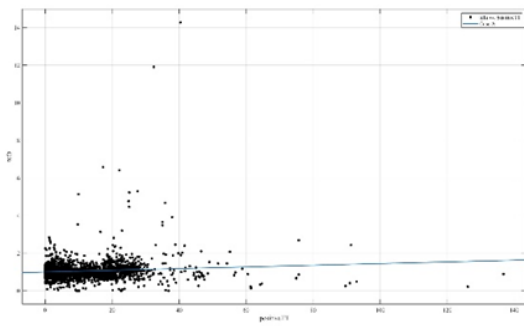


Figure 2.21: D coefficient for case a
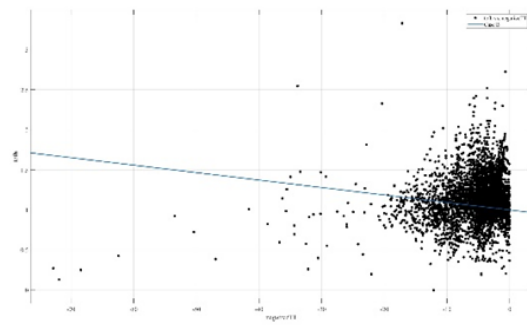


Figure 2.22: D coefficient for case b
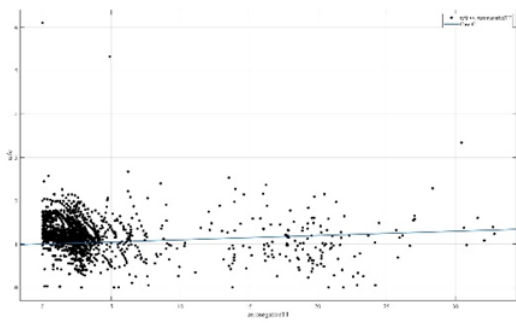
Figure 2.23: D coefficient for case c
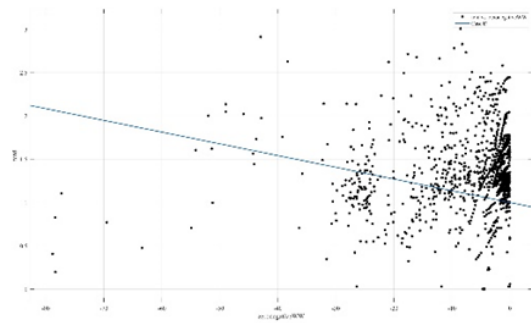


Figure 2.24: D coefficient for case d

# Chapter 3

# Hybrid configuration

In this chapter more focus in put on hybrid electric vehicles highlighting first the classification based on the different architectures present in the market, but also on the level of degrees offered and the position of the electric machine with respect to vehicle body, specifying also the one used in this thesis work. The chapter ends with the review of some improvements done in order to enhance the performance of the hybrid architecture and of the vehicle in general.

## 3.1 Hybrid electric vehicles

Hybrid vehicles are becoming increasingly popular in the current automotive sector due to their improved fuel efficiency and lower emissions compared to conventional vehicles. A hybrid electric vehicle is characterized by the presence of two power sources, where the most common configuration is the one where are present the internal combustion engine and the battery, that is not only aimed at storing energy (working as a generator) but also at providing energy for the motion (working as a motor). As a matter of fact, the electric motor provides extra power during acceleration and captures energy that would otherwise be lost during braking, which is then stored in a battery for later use.

A first classification of this type of vehicles can be based on the architecture used, defined as the connection between the components that define the energy flow routes and control ports. Furthermore, another distinction concerns the level of hybridization, that is the power of the electric propeller with respect to the total power and the capacity of the hybrid system to store electric energy [23].

### 3.1.1 HEV architectures

According to this subgroup three categories are present:

- Series hybrid;

- Parallel hybrid;

- Series-Parallel (or Power-split) hybrid;

**Series HEV**

In the series architecture the only power source is the electric one coming from the battery, reason why this configuration is very close to the pure electric one. As a matter of fact, the thermal energy from the ICE is not sent directly to the wheels, but to the generator to power the electric motor and recharge the battery. The absence of a physical link between the internal combustion engine and the wheels allows to operate the former with higher efficiency and without any constraints about its allocation in the vehicle. Despite these advantages, the main issue of series hybrid is that being the electric machine the main power source for the motion it must be designed to fulfil the power request. As a result, more weight and volume are added to the vehicle making this configuration more complex and as a consequence, more expensive too. In addition, the power from the ICE has to flow through all the driveline, meaning that part of this energy will be lost, making series configuration not so efficient and not widespread in the market.
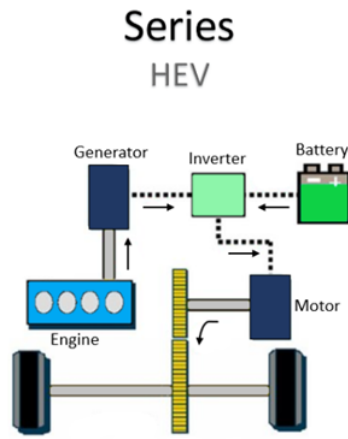


Figure 3.1: Series HEV

**Parallel HEV**

The definition of parallel is due to the fact that both thermal and electric power sources are placed in parallel one with respect to the other and linked through a mechanical hub. In this configuration, the power request can be satisfied by ICE and battery together or even one at a time. In fact, a possible usage of this architecture is the one where the electric motor is used during short distances (low power request), while the ICE for longer distance at high power. Having said this, the main cons are the increase of the system complexity and the ICE is no more operated in higher efficiency zone.

Finally parallel configuration is way more versatile than the series one and offers several configurations based on the position of the EM:
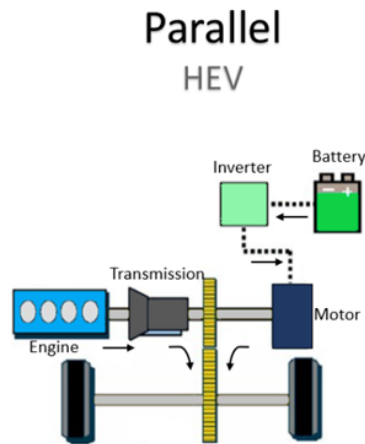
Figure 3.2: Parallel HEV

- In P0 configuration the electric machine is mounted in front of the ICE through a belt and that can deliver a maximum power of 15 kW. The main issue of this architecture is that both power sources cannot be disconnected so the engine friction torque will count as a parasitic loss;

- In P1 configuration the electric machine is connected at the exit of the ICE directly with the crankshaft, also in this case the power delivered is limited but in any case higher than the one of the BSG. Due to the lack of any speed or torque ratio the electric torque demand could be quite demanding,

- The P2 configuration introduces a clutch to disconnect the ICE and EM, that is mounted between the engine and the transmission. It is possible to drive in pure electric mode and regenerate higher amount of energy during the braking phases;

- In P3 configuration the electric machine is connected on the output shaft of the transmission, thanks to which all losses are minimized since EM is dragging just the final part of the transmission. However, on the other side such implementation is more costly than the previous ones;

- in P4 configuration the electric machine is placed in the opposite axle with respect to the driving one, that enables the 4WD capability.

**Series-parallel HEV**

The last architecture is the most complex and sophisticated one, where the engine power is divided along two paths: one goes to the generator to produce electricity and one
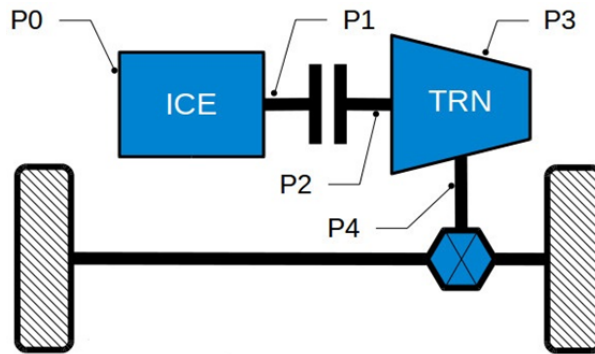
Figure 3.3: EM positions

goes though a planetary gear set system to drive the wheels. This dual presence allows to obtain large amount of fuel savings thanks also to the electric variable transmission (EVT)that the decouples the power setting to the speed the vehicle. Moreover, the power-split system allows to conjugate the benefits of parallel and series configuration with the possibility to switch from the first one to the second one thanks to the EVT system.
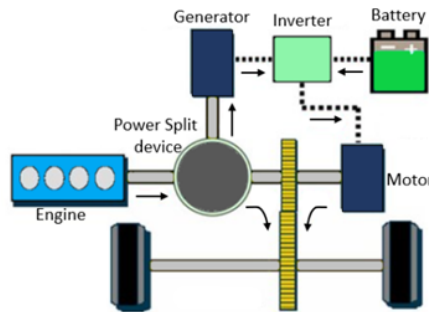


Figure 3.4: Power-split HEV

### 3.1.2 HEV degrees

Another classification concerning hybrid vehicles, as mentioned above, is based on the hybridization, that is related to the power that the electric machine can deliver related also to the capacity of the battery [24]. Moreover, the main capabilities of the EM,

such as regenerative braking, Start&Stop as well as torque assistance are strictly related and are feasible or not depending on which type of group the vehicle is belonging. The distinction concerns four groups:

- Micro hybrid: is the simplest configuration in which is not present a dedicated electric motor aimed at moving the car but there is just an alternator electronically managed in order to produce more currents in case of slowdowns. The two main features are the Start&Stop system and the regenerative breaking. The installed batteries have voltage of 12 Volt and the power of electric motors does not exceed 10 kW.

- Mild Hybrid: is the evolution of the previous configuration characterised by an electric motor that works together with the thermal, one but cannot operate in an autonomous way. There are the same features of micro hybrid configuration plus the possibility to provide extra power assist during the accelerations and generate electric energy during deceleration phases in a more efficient way. The batteries have voltage below 48 Volt. This type of hybrid configuration is relatively simple and cost-effective and is often used in small vehicles such as city cars.

- Full hybrid: vehicles equipped with this system are embedded with an electric motor that works with the internal combustion engine as well as autonomously; this very efficient system allows also to drive in pure electric mode. Installed batteries have voltage higher than 48 Volt. Full hybrids are often used in larger vehicles such as SUVs and sedans;

- Plug-in hybrid: in this case the battery can be completely discharged during the motion. In fact, the presence of the external socket allows to charge back the battery, offering similar features compared to pure electric vehicles. This type of hybrid configuration offers the most flexibility, as the vehicle can be driven on electric power for short trips, and the internal combustion engine can be used for longer trips. However, plug-in hybrids are also the most complex and expensive type of hybrid vehicle.

## 3.2 Components description

Within this section a more detailed description of the additional components present in the hybrid powertrain configuration will be carried out.

### 3.2.1 P1 electric motor

The hybrid architecture is composed in this application principally by two elements: the electric motor and the battery [25]. Before going in detail with both of them, it is necessary to consider the principal features that must be present and considered during the modelling phase to have the correct functioning of the hybrid components:

- Electrical parameters: that include the motor voltage, current, resistance, and inductance.

- Mechanical parameters: these include the motor torque, speed, and inertia.

- Control parameters: where are present the motor control signals, such as PWM signals or analog control signals, as well as any feedback signals, such as speed or position feedback.

- Thermal parameters: this crucial aspect is related to the motor thermal resistance, heat capacity, and thermal time constant.

- Environmental parameters: these include the ambient temperature and air flow rate, as well as any other factors that may affect the motor's performance, such as altitude or humidity.

For what concerns the electric motor, that is attached just after the ICE, in position P1, the last two bullet points are not present since for this thesis work it has been decided to proceed with a simplified model. As depicted in Figure 3.5 the input value of the EM motor model is the request of electric torque coming from the controller, that is converted into electrical power that the battery has to supply. With the knowledge of the EM angular speed, that for this specific configuration coincides with the one of the ICE, two look-up tables are used to estimate the EM efficiency both when working as a motor or as a generator. These are useful to understand the actual power that can be delivered during traction phases and that can be restored during the braking ones. Moreover, two additional look-up tables are necessary to estimate the actual torque value at which the electric machine is working considering the curve of maximum torque in both traction and braking situations.
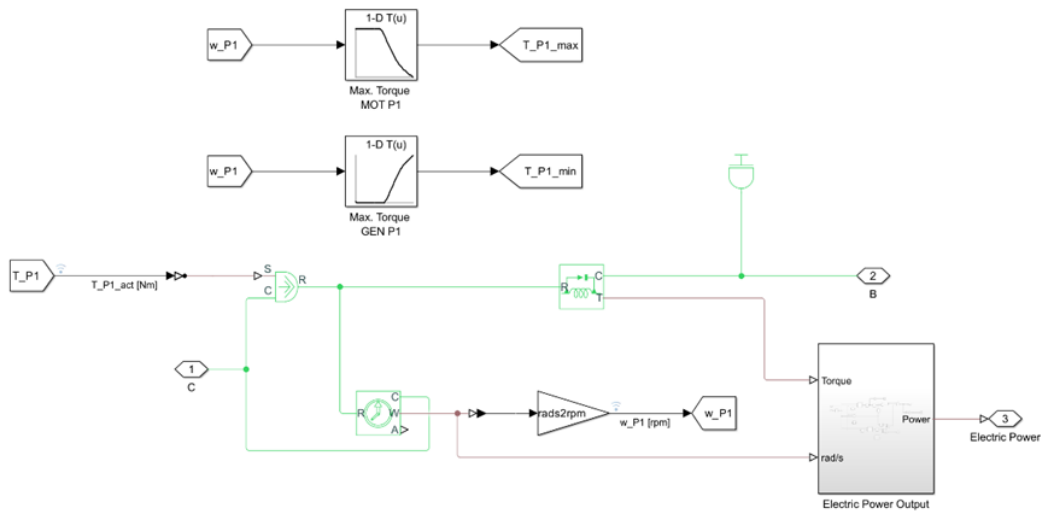


Figure 3.5: P1 electric motor model

The following table gathers all the main features of the P1 EM:

| Electric motor characteristics | |
|---|---|
| $T_{EM,max}[Nm]$ | 200 (from 0 - 2500 rpm) |
| $\omega_{EM,max}[Nm]$ | 4000 rpm |
| $\eta_{EM,max}[Nm]$ | 0.96 |

Table 3.1: Electric motor characteristics

**Electric machine efficiency map**

For an hybrid and electric propeller one of the most representative characteristics is the efficiency map, that as the name suggests is a graphical representation of the efficiency of the machine at various operating points. It shows the relationship between the input power and output power of the EM and how the efficiency changes as the machine operates under different loads and speeds. It typically consists of a series of curves or contour lines representing the efficiency at which the machine operates at different combinations of speed and torque. The highest efficiency point is usually located at a specific operating point, known as the peak efficiency point.

So that it is clear how one application of this diagram is to optimize the performance of the motor and the power electronics to achieve the maximum driving range. Moreover, it is worth noting that the diagram extends also in the negative part since the electric machine can work both as a motor (positive torque) or generator (negative torque) and the EM working points are related to the system efficiency in the two operative modes.
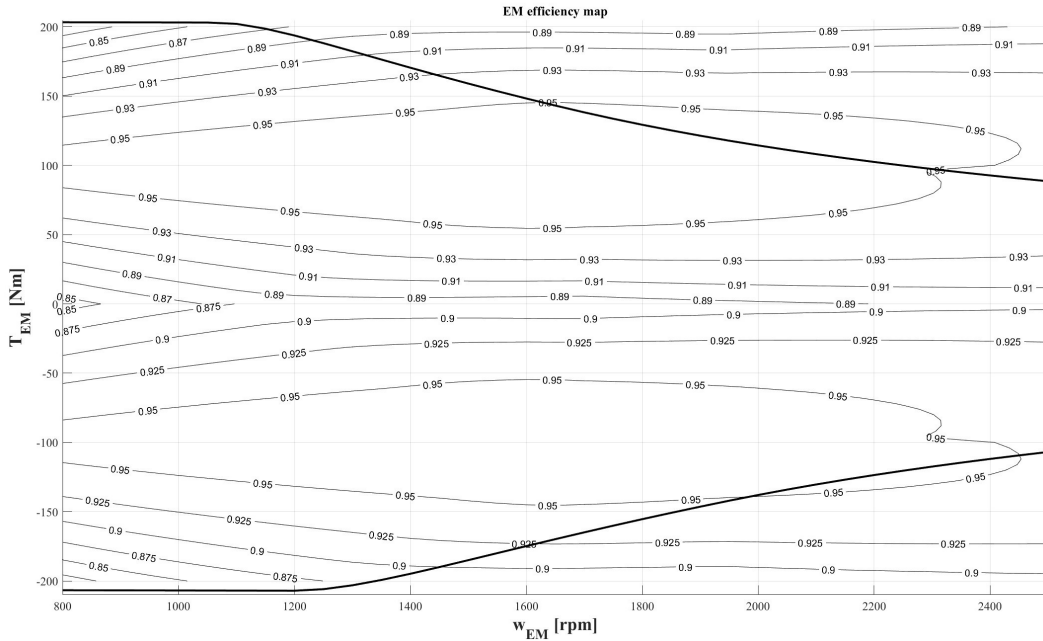


Figure 3.6: Efficiency map

47

### 3.2.2 Battery

As previously mentioned in section 3.2.1, there are some characteristics where is necessary to pay more attention when dealing with hybrid architectures. For the battery case there is an additional consideration that must be done and regards the chemical parameters. In particular the discussion is related to the battery state of charge (SOC), state of health (SOH), and capacity. These parameters are necessary to model the chemical behaviour of the battery, which affects the performance and lifetime [26]. For what concern its modelling phase the discussion can become very complex since enters in action different variables (previous section bullet points list) and control strategies (like to battery management strategy (BMS) just to make an example). However, in this application as holds for the electric motor, it has been decided to proceed with a simplified battery model that does not consider neither any thermal aspect nor any additional control policy, at least at a first glance. The model is realized using Simscape blocks where it is used an equivalent circuit model to represents the behaviour of the battery (where are considered a series of resistors, capacitors, and voltage sources). The model includes parameters such as the battery capacity, internal resistance, and voltage limits, which can be obtained from experimental data.

The logic used to integrate this electric source to the rest of the powertrain considers the electric power that will be converted into current that must be delivered to satisfy the initial request during traction phases. At the same time is capable of storing energy coming during the braking phases, that otherwise would be lost. At the end with the knowledge of the battery capacity, the state of charge can be estimated.
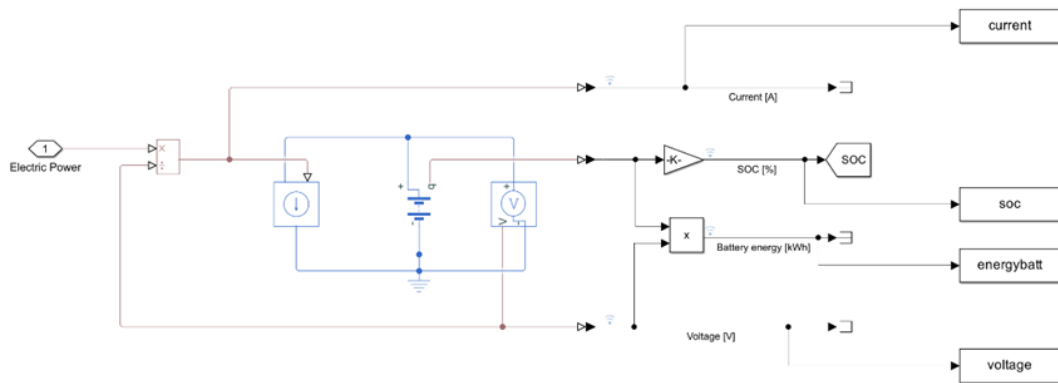


Figure 3.7: Battery model

## 3.3 Hybrid control strategies

The presence of two propellers in hybrid architectures [27], make necessary the implementation of control strategies that merge the thermal and electric part in most efficient and effective way. In the literature exists several strategies and some of them are reported as

follows:

- Rule-Based Control: this strategy uses a set of predetermined rules to manage the power split between the electric and thermal systems. The rules are designed based on the driving conditions and power demand of the vehicle.

- Model Predictive Control (MPC): within this strategy is necessary the presence of a predictive model of the vehicle and its components to optimize the power split between the electric and thermal systems. The model takes into account factors such as battery SOC, engine efficiency, and vehicle speed to determine the optimal power split.

- Adaptive Control: the main aim of this control policy is to adapt to changing driving conditions and optimizes the power split between the electric and thermal systems accordingly. The strategy uses sensors to monitor the vehicle and its components and adjusts the power split in real-time based on the information gathered.

- Dynamic Programming (DP): this strategy uses a mathematical algorithm to determine the optimal power split between the electric and thermal systems. The algorithm takes into account various factors, such as battery SOC, engine efficiency, and vehicle speed, to calculate the optimal power split.

In the list above is missing one of most recurrent and commonly used hybrid control strategy (even in this thesis work), the equivalent consumption minimization strategy (ECMS), whose detailed description is remanded in section 3.3.1.

### 3.3.1 ECMS

In this section a brief description of the ECMS and of the algorithm implemented in this work will be carried out. Nowadays, with the constantly increasing hybridization of the automotive sector, is becoming always more important to let the two power sources work in the maximum efficiency manner, to exploit the benefit of the electrification process. In the literature exist several control strategies that aim at enhancing the power split between ICE and EM, one of this is for sure the equivalent consumption minimization strategy. This is nothing but an energy management strategy with the aim of providing an instantaneous optimization algorithm to reduce a specific cost function, that in the majority of the cases is represented by the fuel consumption. To achieve this target, the ECMS suggests an optimal power split between the two power sources according to the requested torque, defined as input value. At this regard since the cost function is just based on the energy drawn from both fuel tank and battery, this implies the presence of a penalty factor related to electric power from the latter source, known as equivalence factor. This last is playing a fundamental role due to the fact that it counts for how much the battery is stressed to reduce the fuel consumed [28].

Moreover, to determine this factor is necessary the a priori knowledge of the entire driving cycle, that is normally very difficult to be foreseen except the analysis is based on

well-known homologated driving scenarios, like the WLTC. Mathematically this problem can be translated as follows:

$$J = \int min[\dot{m}_{eq}(u,t)]dt \tag{3.1}$$

$$u(t) = argmin(\dot{m}_{eq}(u,t)) \tag{3.2}$$

Where J is the cost function to be minimized and u is the nominal control strategy.

**Actual work**

The input values of the ECMS algorithm used in this work are listed below and sequentially described:

- Minimum and maximum torque that the electric machine can deliver, corresponding to the generator and motor mode;

- Requested torque coming from the throttle signal;

- ICE and EM angular velocity, that coincide being the hybrid solution in position P1;

- SOC boundary limits;

- Maximum ICE torque;

- Equivalence factor s.
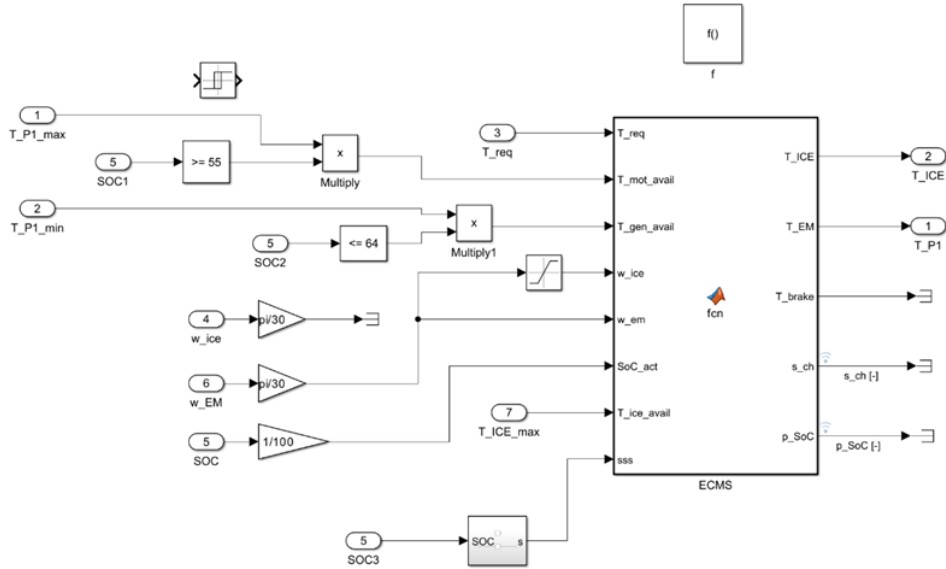


Figure 3.8: ECMS model

The first inputs are the same of the electric machine present in the plant model, so they come from the two look-up tables where, based on the EM angular velocity, the available motor and generator torque are obtained by interpolating the map given by experimental measurements, representing the maximum torque curve. Proceeding with the inputs, the requested torque is nothing but the value of throttle, obtained from the PI driver model, converted into a traction and braking request by multiplying the throttle positive values by the maximum brake engine torque and the negative ones by the maximum braking torque the system can deliver. The angular speed of the two power sources are measured by an ideal angular sensor in the plant model. For what concerns the SOC limits and the equivalence factor, the discussion is quite linked. In fact, the ECMS can provide an optimal fuel economy with the constraint that the state of charge does not reach the upper and lower limits, but oscillates within a predefined working window. For this reason, it has been chosen to let the battery work within a range of values that goes from 55 to 65%. In this way the battery health will be preserved over the years during the charge sustaining working functioning, without reaching the maximum and minimum values that can become critical for repeated operations. Related to this, the equivalence factor must be designed in a way to avoid stressing to much the electric machine and at the same time to do not let the thermal engine supply all the requested power.

**Cost function**

After a brief introduction about how the ECMS works and about what are the variables necessary for its correct functioning, more attention can be put on the algorithm cost function. As previously mentioned, the target is to reduce the equivalent fuel consumption, defined as the sum of two contributions: the first considers the real fuel the engine requires to burn while the other is the virtual fuel consumption due to the use of the electric power from the battery. This concept is enclosed in the following equation:

$$J = \dot{m_{ICE}} + \dot{m_{EM}} \tag{3.3}$$

To go more in deep, the second term can be express as the ratio of the battery power whose equation changes whether the EM is working as a motor or generator, over a virtual weight factor expresses by two terms, that will be discussed soon after. More specifically:

$$\dot{m_{EM}} = \frac{P_{batt}}{Q_{fuel}\eta_{max}} \tag{3.4}$$

Where $P_{batt}$ can be further written in two different manners:

$$P_{batt} = \frac{T_{EM}\omega_{EM}}{\eta_{EM}} \tag{3.5}$$

$$P_{batt} = T_{EM}\omega_{EM}\eta_{EM} \tag{3.6}$$

This mutual behavior has been already explained in section 3.2.1 when the EM efficiency map was introduced. In fact, during the traction phases the electric power the battery is supplying is higher than the one coming from the thermal source, efficiency at the denominator. This is due to the presence of losses in the conversion process. The

discussion is the opposite in case of braking where the electric power than will be stored in the battery is lower with respect to the mechanical one, always due to some losses present in the conversion. Whereas for what concerns the denominator, it is necessary to properly account for the virtual consumption. As a matter of fact, it connects the fuel the internal combustion engine is going to burn in the future to produce the same amount of power delivered from the electric source. The first of the two values $Q_{fuel}$ is the fuel calorific value that is a measure of the amount of heat released during the combustion and expressed in Joule per specific amount of fuel, as an example in kg. The other term is the maximum internal combustion engine efficiency that is a measure of how efficient is the process of transforming chemical energy into mechanical one.

Furthermore, it is clear that electric energy from the EM and fuel energy from the ICE are not directly comparable unless an equivalence factor is used. To consider the equivalence between the two terms, the equivalence factor considers the energy path necessary from the fuel to the storage of electrical energy. In other words, every modification in the battery state of charge will be compensated in the future by the internal combustion engine. So, the equivalent fuel consumption can be re-written as:

$$\dot{m_{eq}} = \dot{m_{ICE}} + s\dot{m_{EM}} \tag{3.7}$$

This multiplicative term is influencing in the ECMS cost function the weight the electric power has based on the actual state of charge value. As a matter of fact, as stated in the introduction paragraph of this algorithm, there is an important trade off to be accounted between the fuel saved using the electric machine for the motion and the behavior and health of the battery. A proper tuning of this parameter is of fundamental importance to let the battery work in an optimal condition, also with the possibility of modifying some characteristics: discharge less the battery whenever the SOC is close to the lower limit, thus avoiding any dangerous phenomena in the future or use more the EM in the opposite case for higher SOC values. In addition, the s coefficient has different values [29] whether the battery is delivering power (discharging) or storing energy (charging). The two values are linked with the following relation:

$$s_{charge} = \eta_{batt}^2 \cdot s_{discharge} \tag{3.8}$$

During the discharge phase the battery provides the power required by the vehicle, represented in the figure below by the thick black path. While the dotted one is the virtual consumption associated with the engine operation, necessary to restore the electric energy left from the battery.

Finally, how much fuel will be used in the future to recharge the battery depends not only on the engine operating point as well as by the energy recovered during braking phases.

In the opposite situation, during the charge phase the EM receives the mechanical energy from the ICE that is converted then into electrical energy so that can be stored in the battery. Here the dotted path represents the electrical energy that in the next phases will be converted into mechanical one, so representing the fuel saving.

In this thesis work the behavior of the equivalence factor is represented in Simulink environment through a relay block, whose output switches between two predefined values
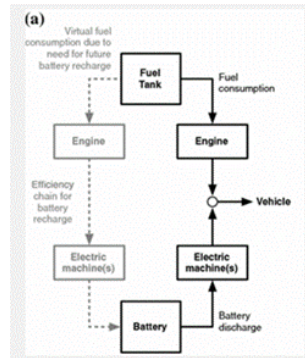
Figure 3.9: S chrage
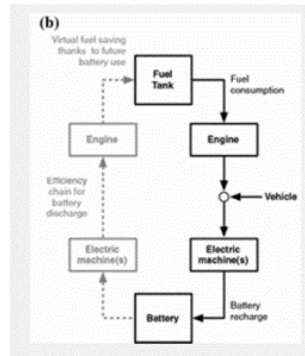


Figure 3.10: S idschrage

according to the actual SOC value. In fact, when the relay it is activated, it stays in this condition up to when the battery charge reaches a threshold value, set as switch off point. In the contrary, it remains deactivated until the SOC overcomes the threshold point, that in this work has been set to 54%. In particular, what is happening is that when the state of charge is lower than the switch value the ECMS promotes the use of the thermal power source to satisfy the torque request, while in the other situation the EM has more priority compared to the ICE.

**ECMS work functioning**

In this section will be examined the logic with which the ECMS works in the model, highlighting the corresponding output that are going to be sent back to the plant. The control strategy is subdivided into two macro scenarios: traction and braking phases, so positive and negative torque request. Analyzing the first of the two, the algorithm responsible for the torque split begins with the creation a vector of one hundred possible level of splits between the two propellers. For the traction case the upper limit of this division represents the maximum percentage of requested torque that the EM can menage.

$$u = min(\frac{T_{mot,avail}}{T_{req}},1) \qquad (3.9)$$

For sure in this traction case, the vector of possible splits is just positive since the electric machine is used as a motor, in the case of braking the situation will be the opposite one including also the load shifting scenario: when the ICE supplies a higher amount of torque with respect to the requested one and the extra is converted into electrical energy by means of the generator. The algorithm then proceeds with the calculation of the engine torque that considers the previously computed levels of split and once $T_{ICE}$ is defined, the remaining torque will be provided by the electrical machine (the definition of the two torque values must consider the maximum available value that the system can deliver).

With the knowledge of the vector of possible splits and the power sources torque, it is possible to estimate for both ICE and EM the corresponding cost functions, taking into consideration some constraints, like avoiding points that are out of the map and some not feasible requests. At the end, is found the level of split that minimizes the fuel consumption so that then ICE and EM torque can be outputted. The same working functioning happens during the braking case with the only exception that the entire torque request is managed by the electric machine.

## 3.4 Hybrid configuration model improvements

This section is dedicated to some improvements done in order to make the electric architecture work better with feasible requests and to improve the vehicle performance in terms of reduced fuel consumption and CO2 emissions. In particular, three actions are taken to obtain some system enhancements: a battery choice suitable for the current application, related to the first point, a power management analysis related to the electric propeller and finally, an optimal gear shifting logic addressed at let the engine work in a more efficient area.

### 3.4.1 Battery sizing

The first model improvement, related to the hybrid architecture, is related to the battery dimensioning analysis, that is the process of determining the appropriate size and capacity of a battery for a specific application, taking into consideration various factors such as power demand, operating conditions, temperature, and safety. This analysis is done to ensure that the battery can meet the performance and safety requirements of the application while optimizing its cost and lifespan [30]. This study is particularly relevant for electric vehicles (EVs) and hybrid electric vehicles (HEVs) as they rely heavily on batteries to power their electric motors. So that, the battery pack in an EV or HEV must be designed in one hand to provide sufficient power required for motion and in the other hand must consider and respect the physical design limitations, thus ensuring a correct and safe behaviour. Concerning this thesis work, the reasons behind this analysis are: choose a battery pack feasible for a light duty application and be compliant with the

design constraints. At the beginning of the work, the original installed battery had the characteristics highlighted in the table 3.2.

| Original battery data | |
|---|---|
| Mass [kg] | 13.75 |
| Capacity [kWh] | 1.1 |
| Capacity [Ah] | 22.916 |
| Specific energy [Wh/kg] | 80 |

Table 3.2: Original battery data

However, the previously described battery was not suitable for the light-duty commercial vehicle under study. As a matter of fact, after several battery configurations in which the main changing parameter was the capacity, it was found the most feasible and realistic battery application, where the principal characteristics are the following ones:

| Optimal battery data | |
|---|---|
| Mass [kg] | 18.75 |
| Capacity [kWh] | 1.5 |
| Capacity [Ah] | 31.25 |
| Specific energy [Wh/kg] | 80 |

Table 3.3: Optimal battery data

The reason behind this battery capacity increment is that the previous configuration was not able to provide the amount of current corresponding to the power request coming from the electric powertrain. In addition, are evaluated both the current and voltage trend during the WLTC driving cycle to verify that the initial request is in line with the battery design features. With the new configuration, this statement is verified and the two variables have reasonable values that oscillates around the design ones.

### 3.4.2 Power management strategy

In parallel to the choice of a proper battery for the current application, thus in terms of light-duty commercial vehicle, it is performed an analysis considering on one side the requests from the vehicle and on the other side what actually the battery can deliver. For this reason, a power management strategy for the battery is performed and this involves balancing the power demands of the electric motor with the available energy the battery can provide. In addition, the strategy must ensure that the battery is used efficiently and does not become depleted prematurely, while also providing sufficient power to meet the vehicle performance requirements.

In the literature there are several strategies [31], one common approach is to use a control algorithm that manages the charging and discharging of the battery to optimize its performance. This strategy takes into account a number of factors, including the current state of charge of the battery, the requested current the system can deliver, the expected vehicle load, and the expected driving conditions. In terms of requested current, the
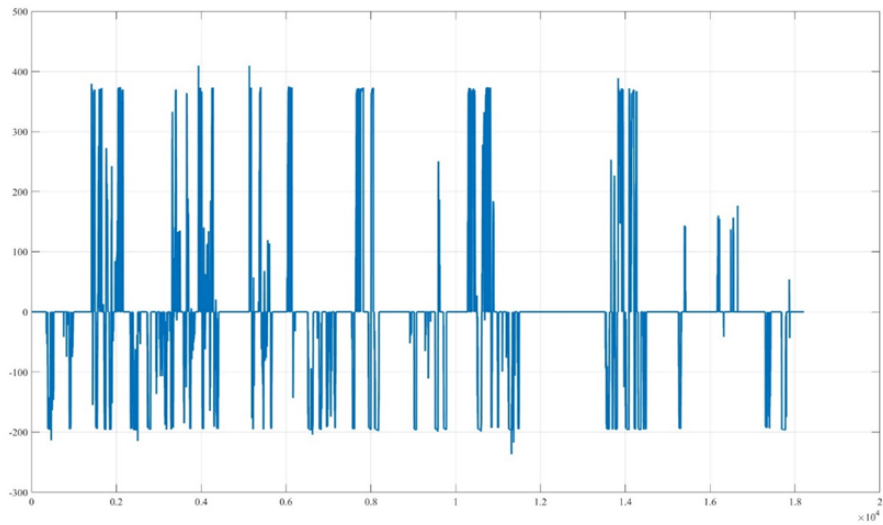
Figure 3.11: Battery current
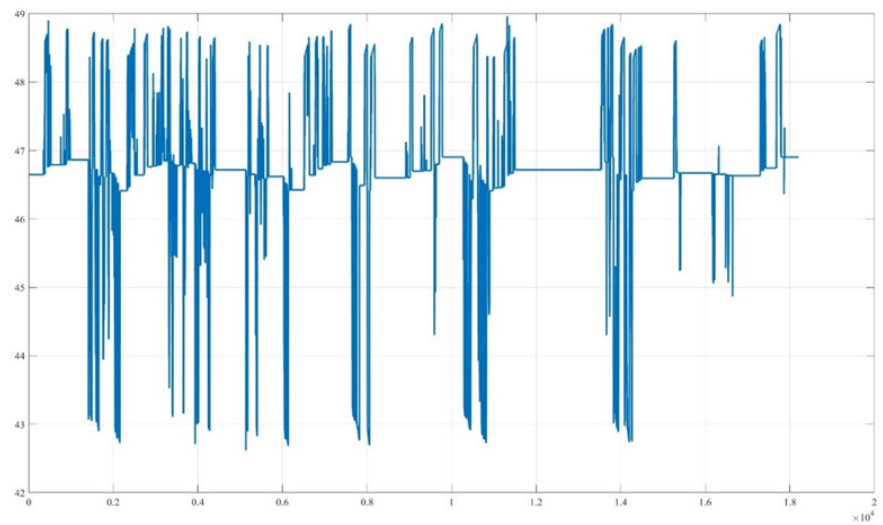
Figure 3.12: Battery voltage

power management strategy may prioritize the use of the battery stored energy for high-power demands, such as acceleration or hill climbing, while using regenerative braking to recharge the battery during lower-power demands, such as cruising or coasting. This allows the battery to maintain a consistent state of charge and avoid being overcharged or undercharged, which can reduce its overall lifespan. Other factors that may influence the power management strategy for a hybrid vehicle battery include the type of battery

56

chemistry used (such as lithium-ion or nickel-metal hydride), the vehicle powertrain configuration, and the desired balance between fuel efficiency and performance. Overall, a well-designed power management strategy can help ensure optimal battery performance and extend the life of the battery in a hybrid vehicle.

The strategy used in this thesis works, attempts to keep the instantaneous battery power within the dynamic charge and discharge limits. In particular, this algorithm checks if the electrical power request is within the two limits: if it is the battery will provide the corresponding request (in terms of current), while in the opposite way the operated strategy changes whether there is a traction or braking manoeuvre. More in detail, to the actual power request is subtracted the upper and lower limit, based on the current condition, after which is computed, dividing by the EM revolution speed, the corresponding torque that the ICE has to supply. In this case, to the battery will arrive a request that is already aware of its power limitations and the "extra" request that the battery cannot supply will be covered by the thermal propeller. In a more practical manner, the control algorithm is implemented in the controller side, so that the output (electric torque) feedbacked to the plant is already updated.
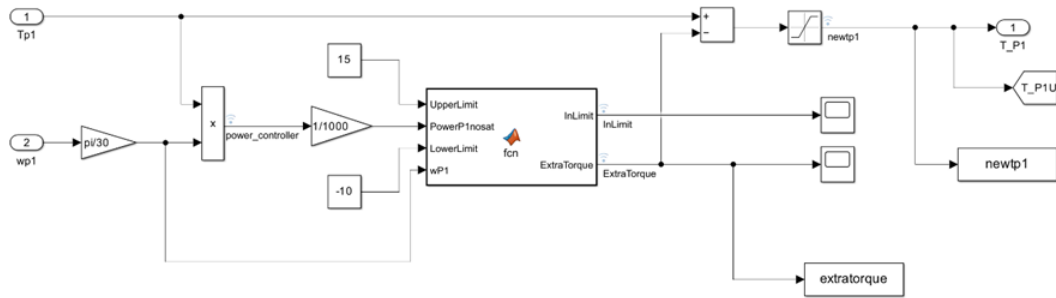


Figure 3.13: Power management strategy

The following figures explains better how the strategy actually works. In particular, in Figure 3.14 is depicted the original power request that does not consider any type of control and where the two constant lines (orange and yellow) represent the battery charge and discharge power limits. Whereas, the remaining two represent the updated torque that the electric motor has to supply and the additional torque the ICE has to deliver.

### 3.4.3 Optimal gearshifting logic

This last improvement is not strictly related to the hybrid architecture working mode, but is oriented in a more general way at enhancing the overall vehicle performance. In fact, the main aim of having an optimal gear shifting strategy is the one of reducing fuel consumption and pollutant emissions just by changing the driving style without any additional components or control policy. As a matter of fact, based on the logic presented in section 2.4.3, through a trial and error approach it was possible to see by changing the ICE revolution speed at which each gear is changed in which part of the map the engine working points were placed. This operation is not considering the last gear, 8th, because
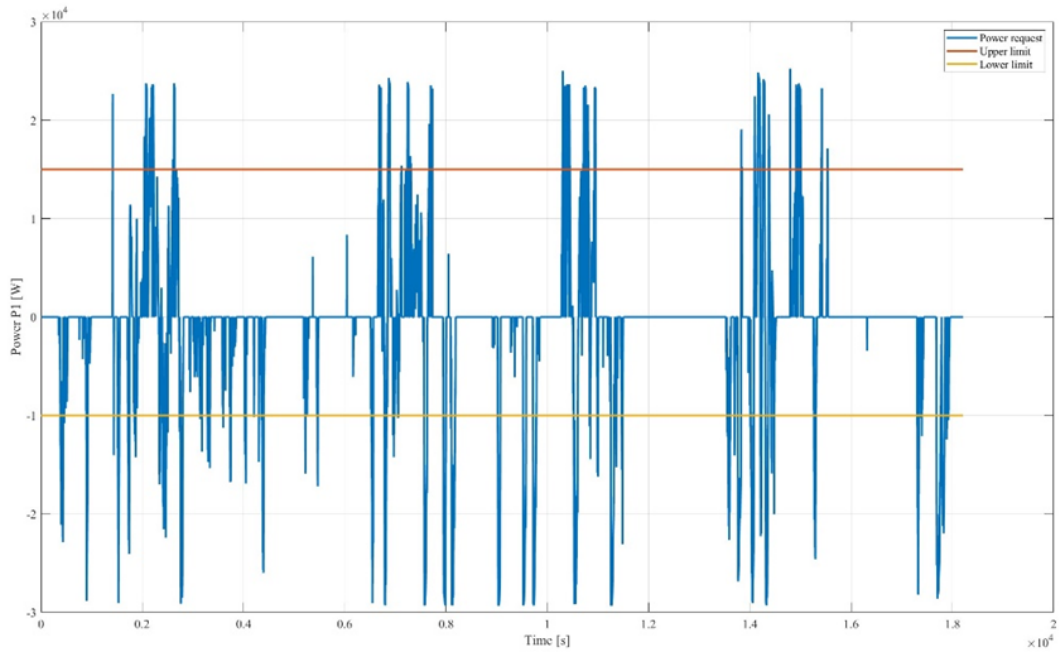
Figure 3.14: Power limits
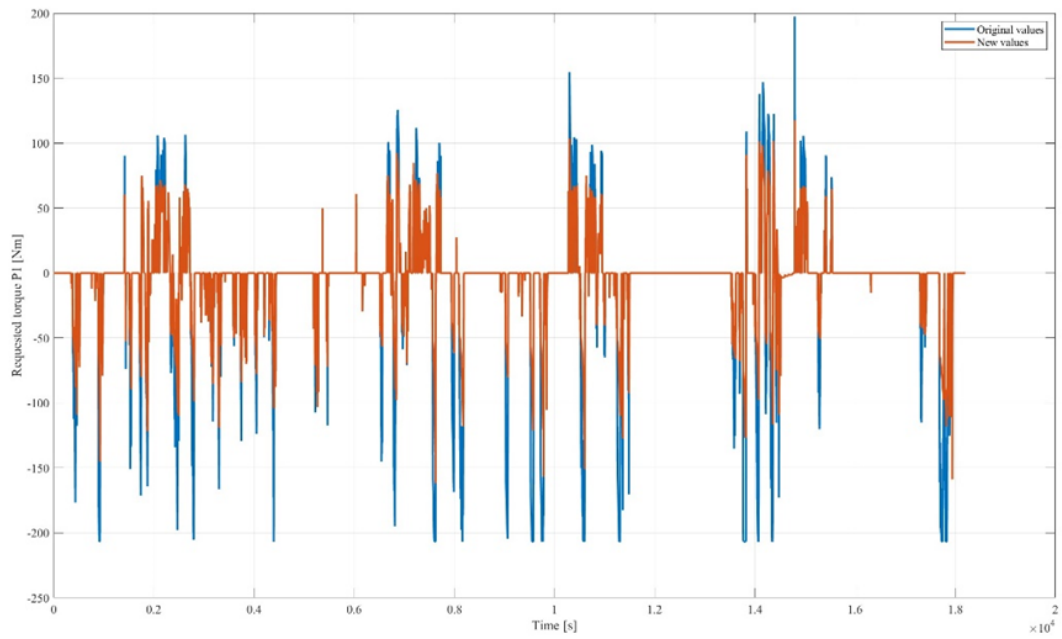


Figure 3.15: New electric motor torque

this causes the engine to work in a worst efficiency zone of the BSFC.
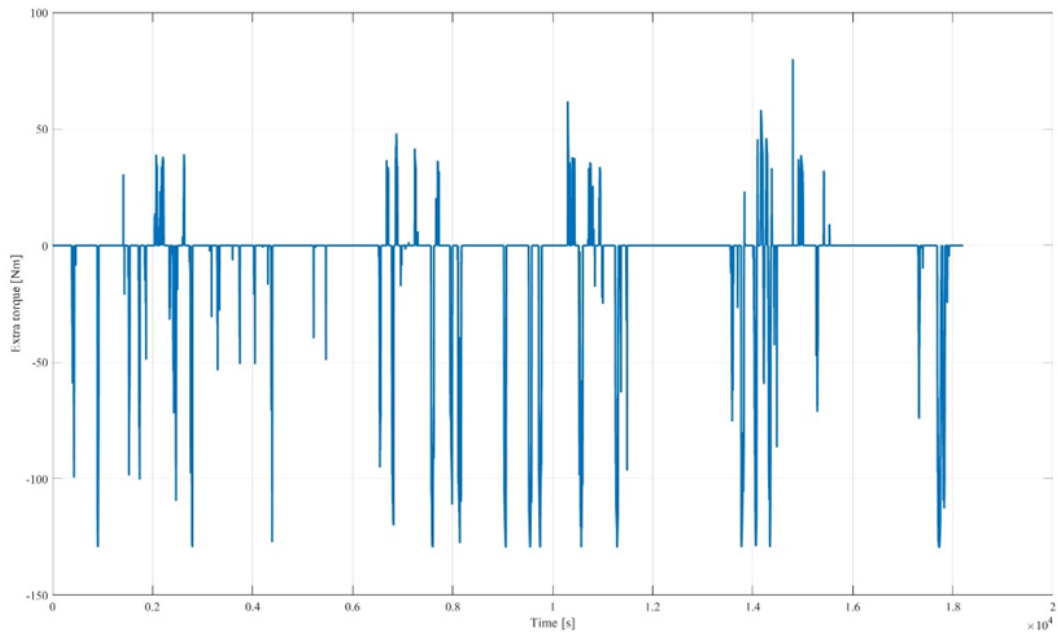
Figure 3.16: Extra torque
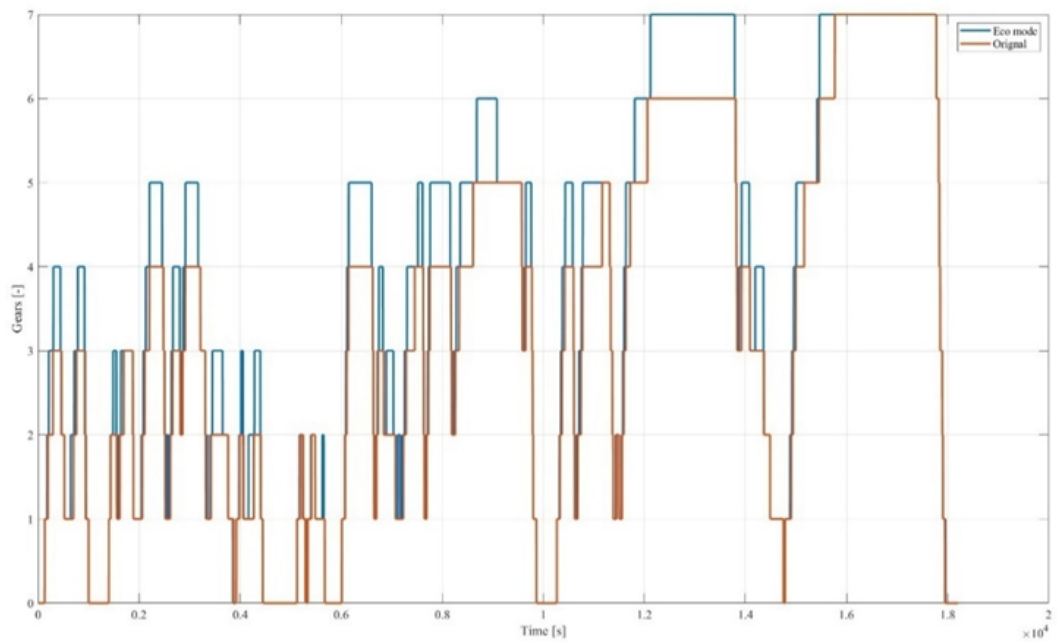


Figure 3.17: Optimal gears choice

The newer internal combustion engine revolution speed related to the upshift thresholds are shown below:

59

| Upshift thresholds ||
|:---:|:---:|
| Gears | Engine speed [rpm] |
| $1 \to 2$ | 1825 |
| $2 \to 3$ | 2050 |
| $3 \to 4$ | 1875 |
| $4 \to 5$ | 1950 |
| $5 \to 6$ | 2300 |
| $6 \to 7$ | 2150 |

Table 3.4: Engine speed for optimal gearshift

It is possible to better appreciate the improvement by looking at the BSFC diagram with and without the control logic. As it is clear, on the left side where there is not the algorithm, the engine working points are spread in a wider region of the map especially in the lower side where the consumption is higher. On the right side, where the logic is implemented, there is like a virtual vertical asymptote at around 2500 rpm and the points are more concentrated in the upper region of the map. In a more practical manner, the use of this control logic allows to have improvements over the WLTC driving cycle of 6.74%, thus this shows how important and effective is the gear shifting strategy in perspective of reducing fuel consumption and pollutant emissions.

| | |
|:---:|:---:|
| Baseline fuel consumption [l] | 2.243 |
| Reduction compared to hybrid mode [%] | 2.85 |
| Reduction compared to ICE only [%] | 6.74 |

Table 3.5: Fuel consumption reduction with optimal gearshifting logic
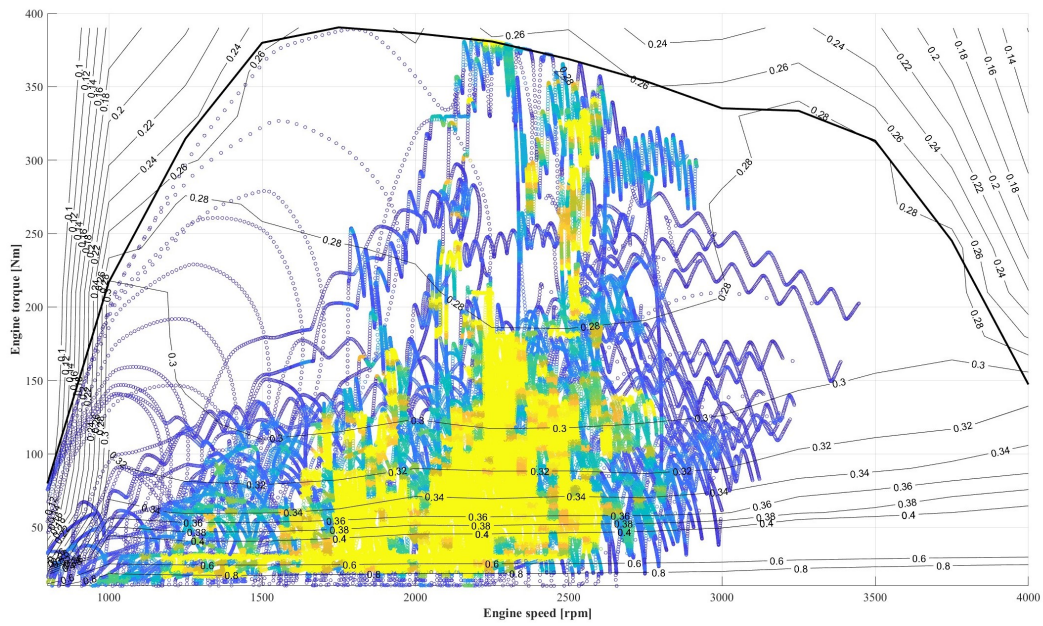
Figure 3.18: Original BSFC
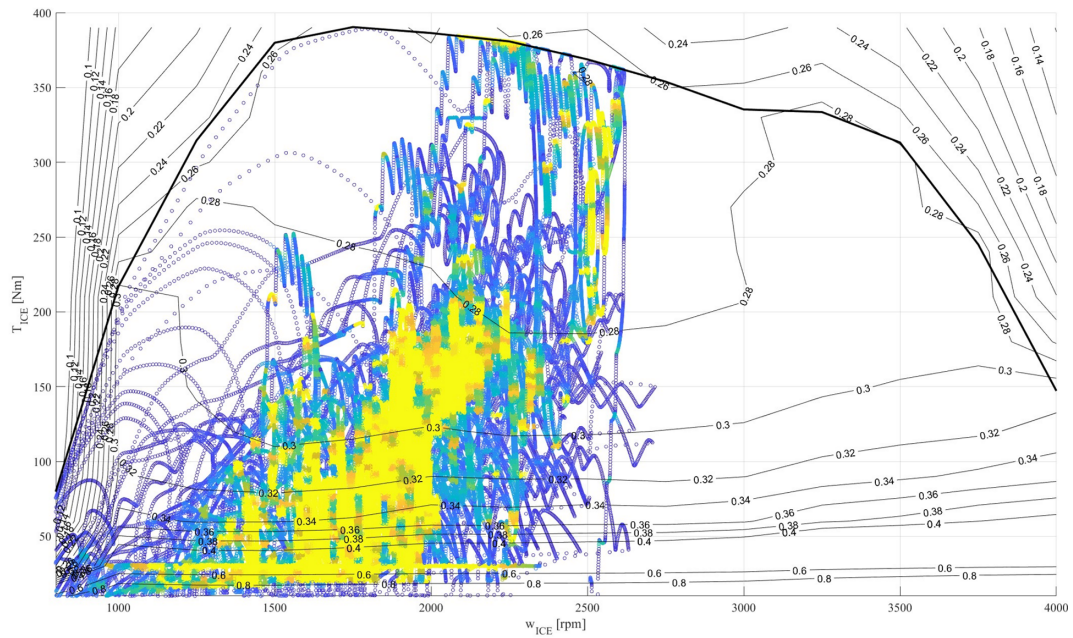


Figure 3.19: Optimal BSFC

61

# Chapter 4

# Vehicle automation

This chapter is dedicated to the description of a possible usage of the validated and properly tuned numerical vehicle model with hybrid configuration. As a matter of fact, it has been decided to go towards the automation direction and implement the hardware and software corresponding to one ADAS sensor, the adaptive cruise control (ACC). The reason behind this choice is to demonstrate that in addition to improved driving comfort and safety it is possible to obtain fuel consumption and pollutant emissions reduction too. Going more in detail, this chapter comprehends a brief introduction about autonomous vehicle, with a consequent description about of ACC working functioning. Finally, in order to assess the previously mentioned improvements, a sensitivity analysis is conducted in order to obtain a proper setting of the main parameters that characterize this system.

## 4.1 ADAS introduction

The evolution of technology in the automotive and computer science field has brought several improvements in terms of transport safety and comfort through the introduction of systems that perceive in a more complete manner the environment around the vehicle with respect to what the driver does. These devices fall under the common name of advanced driver assistance system (ADAS) and are particularly designed to work in un rural and intercity scenarios. As a matter of fact, by exploiting the road information, in terms of distance to the vehicle in front (or even pedestrians and traffic signals) and relative speed, coming from on board sensors they are able to adjust vehicle pace, thus reducing the risk of accidents. In addition, is worth saying that every year there are between 20 to 50 million injuries coming from road accidents. Moreover, ADAS are also designed to enhance passengers comfort, since thanks to their introduction, vehicles are becoming more autonomous and can even substitute the driver in the near future.

At this regard, SAE has introduced a classification in six groups based on the level of autonomy, from the least to the most autonomous [32]:

- Level 0: in this family belongs vehicles without any type of autonomous feature, where the so-called dynamic driving task is addressed entirely to the driver;
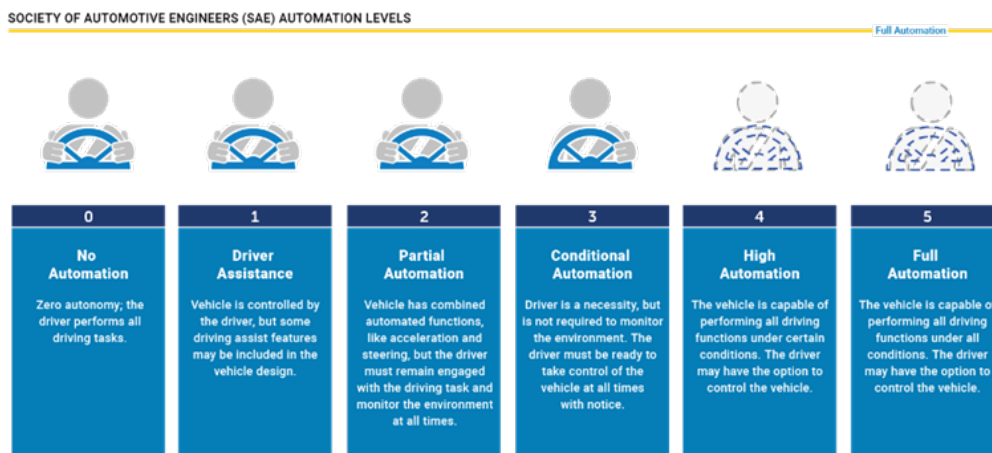
Figure 4.1: Autonomous levels

- Level 1: starting from here some autonomous features are present and can control just one degree of freedom: steering or accelerating. The adaptive cruise control (ACC) is an example.

- Level 2: the system can now control both actions, steering and accelerating and the driver control becomes less necessary, even if he can intervene at any time.

- Level 3: vehicles can decide how to adjust its pace and react thanks to environmental information coming from sensors. Having said this, the driver has to remain always alert.

- Level 4: the human dependency is marginal since vehicle can even intervene in case of system failure. Self-driving mode is possible.

- Level 5: complete absence of human interaction to the vehicle. In fact, neither the steering wheel nor the accelerator pedal are present.

A crucial step in this thesis work is the implementation of an high level control logic using ADAS, in particular of an ACC (adaptive cruise control) in order to evaluate their effectiveness always with the same target of reducing fuel consumption. The hardware used for environment perception consists of a stereo camera and a radar to detect the presence and speed of vehicles in front.

### 4.1.1 ACC state of the art

The adaptive cruise control is the evolution of the well-known cruise control that allows the vehicle, called ego vehicle, to not only follow a desired speed but also to maintain a set distance from the vehicle in front, defined as lead vehicle. In a nutshell, the main advantages of this improved solutions are: improved road safety and comfort, higher

traffic capacity and lower fuel consumption. This control logic can be applied both to a single vehicle or a platoon. In this last case, there are two configurations: centralized and decentralized vehicles. In the first one, there is a unique controller that receives and sends information to all the vehicle to control them in a coordinated way; in the other case there is not a common supervisor, but each vehicle controls itself, using for sure less amount of information [33]. Even if at the beginning the centralized mode could seems to be the best option, the huge amount of information and calculations that have to be done online make this configuration impractical. Another possible differentiation is the one between non-connected and connected vehicles. The main difference is that in the former the actions are taken based on the information coming from solely the on-board sensors, with respect to the latter case where vehicles can exchange information between them (V2V) or with the infrastructure (V2I). In this thesis work, the system used falls in the decentralized non-connected case. For what concerns the operating mode of the ACC, there are two possible scenarios:

- Standard cruise control: whenever there is not a preceding vehicle or the target speed is lower than the actual one;

- Following mode: the control strategy starts to work and adjust the vehicle longitudinal dynamics.

Another difference concerns the architecture that is hierarchical and subdivided into two controllers:

- Upper level controller: whose aim is to obtain the set the desired vehicle acceleration;

- Lower level controller: acts at the throttle/brake level to have the wanted acceleration.

Furthermore, among the different control logics present in the literature about the ACC, the one implemented in the thesis work is based on sensor fusion, to provide a safe and comfortable driving experience. In fact, the ACC system uses a combination of sensors such as radar, lidar, camera, and ultrasonic sensors to gather information about the surrounding environment. This information is then processed by a computer to create a 3D map of the surrounding vehicles, road conditions, and other relevant objects. The sensor fusion algorithm combines and integrates this information, providing the ACC system with a comprehensive understanding of the driving environment. This allows the ACC system to automatically adjust the vehicle's speed to maintain a safe following distance from the vehicle in front, as well as to respond to changing road conditions. the driver's workload. In conclusion, the ACC can be activated by pressing a button on the steering wheel or dashboard, and the driver can select the desired speed and following distance. The system can be deactivated by pressing the brake pedal or the ACC off button. In some vehicles, ACC may also be integrated with other ADAS systems, such as lane departure warning or lane keep assist, to provide a more comprehensive driver assistance package.

**ACC model**

The implementation of the ACC control logic using Simulink environment comprises of two main subgroups, that will be later discussed, where there is just one input coming from the Plant and one output entering in the Controller side. Regarding this last, the control action of the ACC is aimed at changing the vehicle pace to keep a safe distance, so the output is represented by the acceleration command. To have a clear understanding about how the ACC practically works, it is possible to go more in detail highlighting what is present in the model implemented in Simulink. So, if in one hand the output is the acceleration command, whose range goes from 2 to $-3m/s^2$ to limit the jerk during the motion, on the other the input is just the actual vehicle speed.
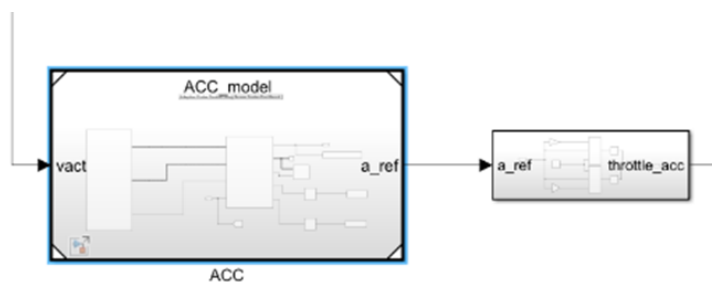


Figure 4.2: ACC model

The block on the right it is used to convert the acceleration command coming from the control logic into a throttle signal. This is done by multiplying the acceleration by $\frac{1}{2}$ and $\frac{1}{3}$, to obtain a signal that goes from 0 to 1, that accounts for both acceleration and deceleration phases. Inside the ACC model block the logic is split into two subgroups, as stated at the beginning: the "vehicle and environment" and "sensor fusion" part. Inside the former, are computed the ego vehicle position and speed in both longitudinal and lateral sense that are used to trace the vehicle path according to the imposed scenario the ego vehicle has to follow, that in this analysis is represented by the WLTC homologation driving cycle. In fact, instant by instant are communicated to the "sensor fusion" block the information coming from the radar and the camera, as well as the prediction time. These data, thanks to sensor fusion logic are used to detect the relative distance and speed between ego and lead vehicle, that will be then used to obtain the desired acceleration command.

## 4.2 Driving scenario simulation

The common idea within the ADAS sensors is that in order to improve the vehicle performance is necessary to exploit the information coming from the infrastructure, road signals, sensors installed on board and from the other vehicles. So in all of these cases the presence of certain environmental conditions is mandatory for the correct functioning of the autonomous driving strategies. Focusing just on the adaptive cruise control the
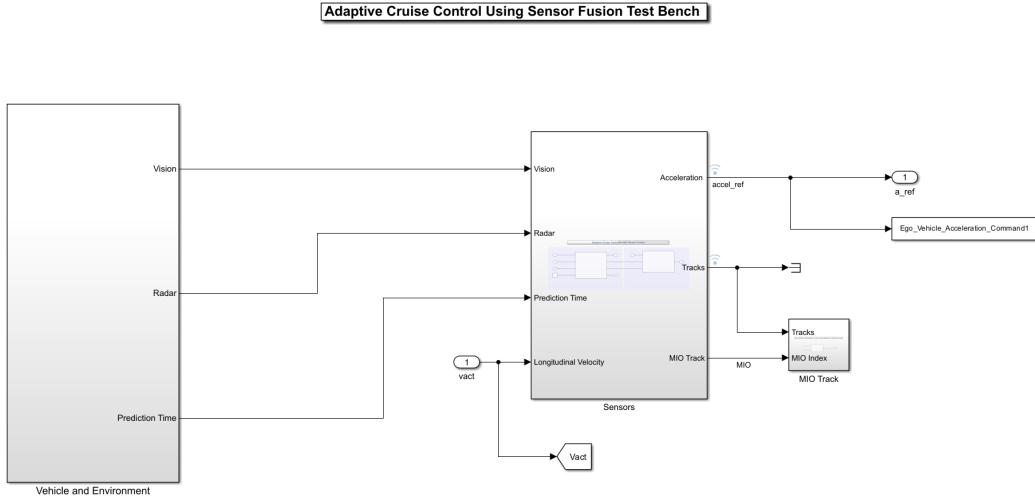
Figure 4.3: Environment and sensor fusion model

only necessary constraint is the presence of a preceding vehicle, the so-called lead vehicle. This last has a crucial relevance for what concerns the control strategy that will be implemented. In fact, the main information acquired from the radar and camera are the relative speed and distance from the lead vehicle and base on that it is possible to adjust the ego vehicle pace. In a nutshell, the improvements that can arise from this system are depending on the driving cycle the lead vehicle is performing. In this thesis work it has been decided to use for this analysis the WLTC homologation cycle. In order to let the lead vehicle follow this precise path, inside the Simulink environment it is present a dedicated block, inside the "vehicle and environment" subgroup, where it is possible to import the information related to the cycle.

Going more in detail, the "Scenario Reader" is requiring the information of vehicle speed and distance travelled both in terms of lead and ego vehicle. These can be obtained using a dedicated Matlab function called "DrivingScenarioDesigner", whose name is self-explicative for its scope. For what concerns the lead vehicle, the speed values are for sure the ones of the WLTC driving cycle, identical to the one discussed in section 2.4.2. The corresponding travelled distance can be easily computed taking into account the following formula:

$$s = s_0 + v_0 \cdot t + \frac{1}{2} \cdot a \cdot t^2 \qquad (4.1)$$

where $s_0$ is the initial distance (in this case is null), $v_0$ is the lead vehicle initial speed (also null) and a is the lead vehicle acceleration, that can be obtained in a straightforward manner from the vehicle speed. In the other hand, related to the ego vehicle, the speed information inserted in the Matlab function are just for critical cases whenever the lead vehicle exits from the radar field of view. As a matter of fact, the actual ego vehicle speed will be computed according to the algorithm that is going to be presented in the
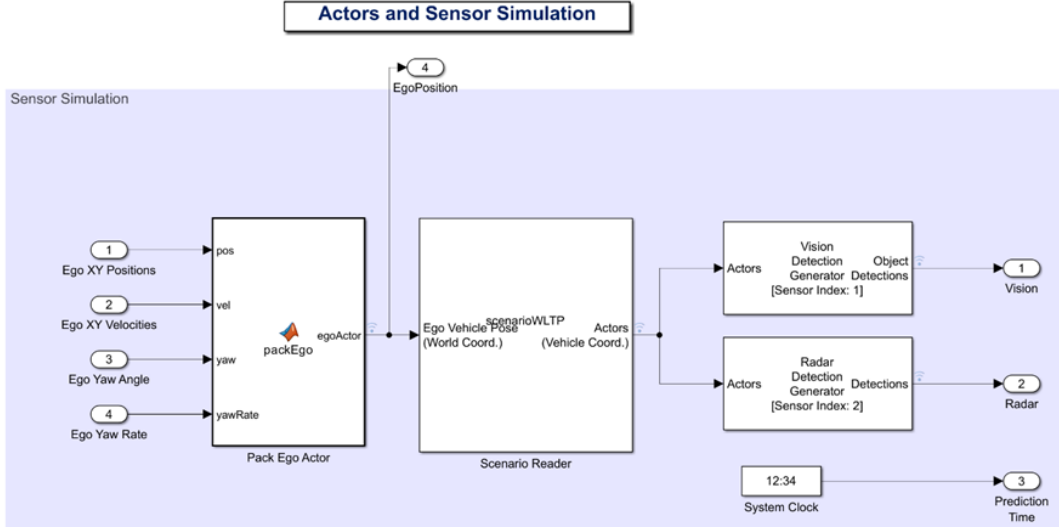
Figure 4.4: Scenario Reader

following section. Moreover, it is necessary to consider the fact that there must be an initial distance between the two vehicles, so that the travelled distance is the one of the lead vehicle minus the initial gap.

## 4.3 Control strategy development

The adaptive cruise control model implemented in the model is the classical default one where the sensor fusion is used to estimate the relative speed and distance to the lead car. The desired distance that the ego vehicle is designed to maintain is defined as follows:

$$D_{safe} = D_{default} + T_{gap} \cdot V_x \tag{4.2}$$

Where the first two variables on the right side are design parameters: $D_{default}$ is nothing but the space in between the two vehicles when the ego vehicle speed is zero, $T_{gap}$ accounts for the distance between lead and ego vehicle in terms of time, while the last term is the actual speed of the ego vehicle. In order to fulfil this requirement, the ACC produces an acceleration command for the ego vehicle based on the three previous described variables. However, sometimes the relative distance can become lower with respect to the desired one and in this case the priority is to decelerate the vehicle to match once again a safe distance. In the opposite case, for example when the lead vehicle exits from the perception field of the ego vehicle, this last is designed to reach a predefined set velocity large enough to encounter the lead vehicle while maintaining the desired space.

In order to improve the performance of the ACC in terms of reactivity and fuel consumption, an important phase is the parameter tuning one. As can be
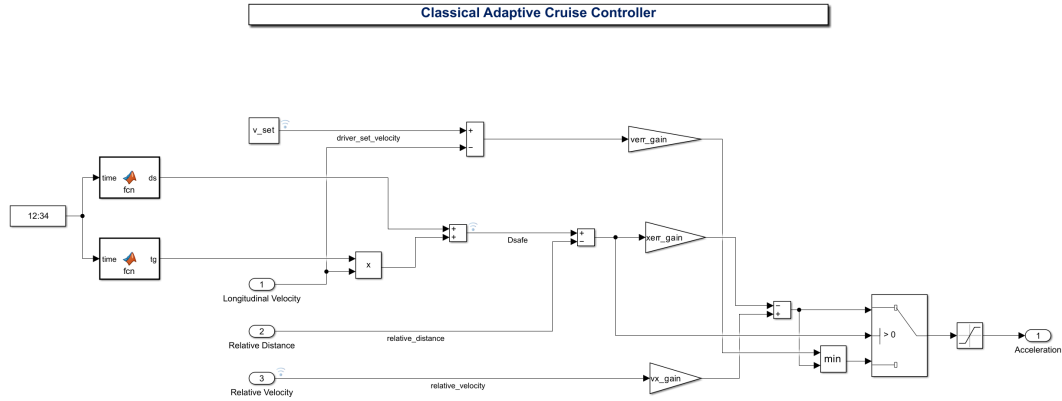
Figure 4.5: Constant Time Gap

seen from the previous image, in addition to the time gap and default spacing already described, are present three gains that affects the system functioning too:

- $V_{err}$, that weights the relative speed,

- $X_{err}$, that weights $D_{safe}$,

- $V_x$, that weights the difference between $V_{set}$ and $V_{act}$

It has been decided to differentiate the tuning phase depending on which part of the driving cycle WLTC the car is travelling because the characteristics in terms of average speed and torque request are very different. Of course, this can be applied on a case study where it is known a priori the driving cycle in terms of speed and distance travelled. At the same time, in the future by exploiting the IOT, the V2I information or even in a simpler way the GPS data of the imposed journey it could be possible to have a real time tuning phase. Going back to the implemented logic, based on the simulation time corresponding to each of the four cycle parts, the time gap and default spacing values (that are the most affecting parameters) are properly tuned. In fact, in the urban part there is a larger value of $T_{gap}$ and $D_{default}$ due to the quite low speed values that allow to have a more relaxed ACC behaviour. As soon as the speed grows both the two parameters start to decrease. This allows to reduce the speed between ego and lead vehicle in order to be able to react in a more responsive manner to sudden acceleration. In the table below are listed the variables used:

As a result of the previous parameter mix, the ego vehicle is not only able to follow the lead vehicle in a good way, as shown in Figure (4.6), but it is also capable of reducing the fuel consumption. this is possible thaks to the additional degree of freedom allowed by the ACC policy. At this regard, the main responsible of this performance improvement is the smoother ego vehicle acceleration that it translated in less peaks and spikes compared to the lead one. In addition, it has been decided to focusjust on a specific driving cycle part to try reduce even more the fuel consumption.

| ACC parameters | Low speed | Medium speed | High speed | Extra high speed |
|:---:|:---:|:---:|:---:|:---:|
| $V_{set}[m/s]$ | 40 | | | |
| $T_{gap}[s]$ | 16 | 12 | 9 | 7 |
| $D_{default}[m]$ | 2.5 | 5 | 8 | 14 |
| $V_{err}[-]$ | 0.5 | | | |
| $X_{err}[-]$ | 0.18 | | | |
| $V_x[-]$ | 0.5 | | | |

Table 4.1: ACC time varying parameters
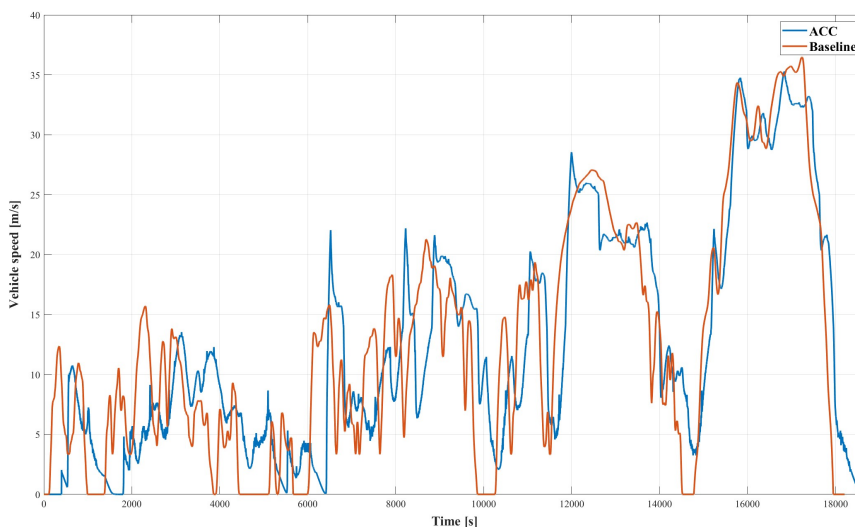


Figure 4.6: Lead and ego vehicle speed comparison

| | |
|:---:|:---:|
| Baseline fuel consumption [l/100km] | 9.88 |
| Fuel consumption with ACC [l/100km] | 8.98 |
| Reduction [%] | 9.10 |

Table 4.2: Fuel consumption reduction with ADAS

## 4.4  Sensitivity analysis

The last section of this chapter is addressed to the description of the sensitivity analysis performed in order to assess further improvements in the vehicle performance. The object of this study is to understand how the main ACC parameters affect the working functioning of the control logic and as a consequence the vehicle behavior. Going more in deep, the two parameters that mostly affect the ACC logic, as stated above, are the time gap and the default spacing and for this reason they are the protagonist of this sensitivity analysis. It has been decided to focus the attention just on a restricted part

70

of the WLTC driving cycle in order to see clearly the results. In particular, the highway part has been chosen, since it represents the most common situation where the adaptive cruise control is usually operated. More in detail, the new cycle is characterized by the repetition of three times the final part of the homologation driving cycle, so that the new length covered is of 6.57 kilometers. After the creation of this new scenario, following the steps reviewed in section 4.2, sixteen simulations have been conducted with different time gap and default spacing values. For each of them the corresponding fuel consumption and average speed value is registered. It has been seen that the best results converge toward a specific direction: for high speed values, lower time gap and large default spacing give lower fuel consumption values. As shown in Figure (4.7) the combination of time gap equals to 7 seconds and default spacing equal to 12 meters leads to a 16.83% reduction in terms fuel consumed over 100 kilometers.

|          | d=6    | d=8    | d=10   | d=12   |
|----------|--------|--------|--------|--------|
| τ=7      | 9.565  | 9.532  | 9.696  | 9.463  |
| τ=8      | 9.663  | 9.700  | 9.668  | 9.770  |
| τ=9      | 10.480 | 10.768 | 10.914 | 10.906 |
| τ=10     | 11.757 | 11.539 | 11.794 | 11.858 |
| *Fuel consumption baseline 11.379 [l/100km]* | | | | |

Figure 4.7: Sensitivity analysis for fuel consumption

Looking at the average speed table, it is possible to state that for equal default spacing and different time gap values the mean velocity is almost identical, this implies that the table must be read by columns and not by rows, moving from left to right. Moreover, looking at the baseline average speed (that is lower) it is possible to state that the improvement is purely related to the way in which the driving cycle is performed.

A confirmation of what just written above can be found in Figure 4.9 where are compared both the best and worst simulations with the baseline one. It is possible to see clearly that the green line (best parameters combination) has a smoother accelerations and this is visible from the slope of the speed profile. Vice versa, the red line (worst parameters combination) shows very steep acceleration and deceleration phases, especially at very high speed and this happens whenever the lead vehicle exits from the field of view of the radar. Furthermore, another field of inspection for this enhancement is the net electric energy, so the spent and recovered one. By comparing these values with and without the use of the ACC it is possible to see, as in table 4.3 that with ADAS sensor the net energy is lower, thus reinforcing the fact that the fuel consumption reduction is all up to the more smooth and calm driving style.

Finally, the last comparison between the baseline hybrid configuration and the one with the best combination of parameters for the ACC concerns the requested torque. As

| | d=6 | d=8 | d=10 | d=12 |
|---|---|---|---|---|
| τ=7 | 65.624 | 65.606 | 65.588 | 65.567 |
| τ=8 | 65.624 | 65.606 | 65.585 | 65.567 |
| τ=9 | 65.624 | 65.603 | 65.585 | 65.563 |
| τ=10 | 65.621 | 65.603 | 65.581 | 65.560 |
| Average speed 64.645[km/h] | | | | |

Figure 4.8: Sensitivity analysis for vehicle speed
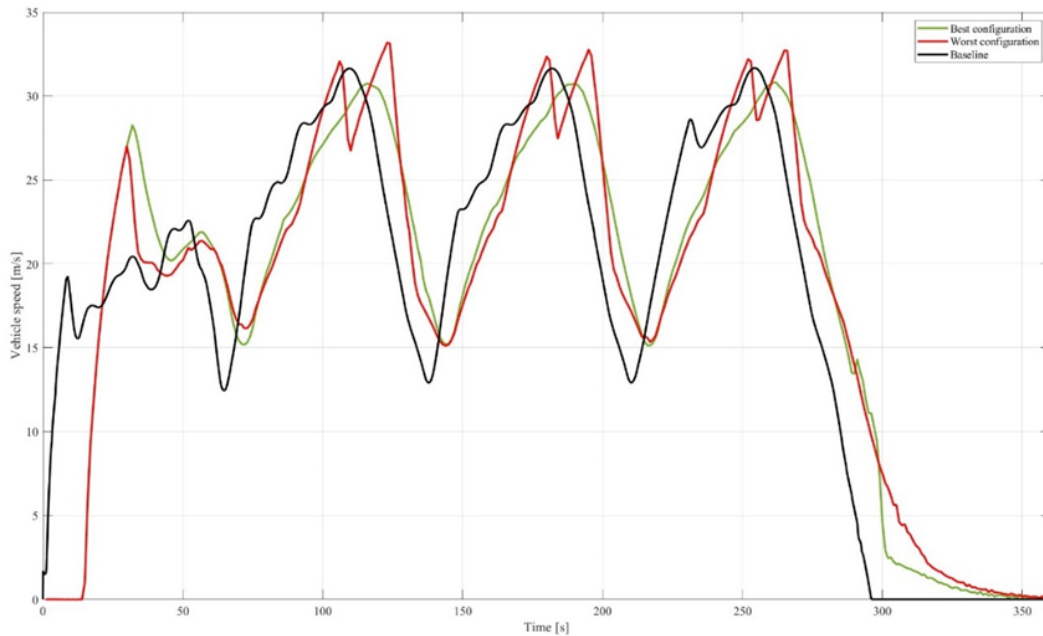


Figure 4.9: Best and worst comparison

a matter of fact, looking at picture 4.11 there is a clear difference that retraces what just said and can be demonstrated by considering the maximum torque requested. In fact, in the baseline configuration there is always an ICE requested torque close to the peak value, while in the ACC case this does not happen and apart from the initial part (where the higher values are necessary to initially catch the lead vehicle) the values are below 300 Nm.

| Energy balance without ACC | |
|---|---|
| Required cycle energy [kWh] | 3.051 |
| EM energy spent [kWh] | 0.238 |
| EM energy recovered [kWh] | - 0.406 |
| EM net energy [kWh] | - 0.168 |

Table 4.3: Energy balance without ACC

| Energy balance with ACC | |
|---|---|
| Required cycle energy [kWh] | 3.143 |
| EM energy spent [kWh] | 0.245 |
| EM energy recovered [kWh] | - 0.392 |
| EM net energy [kWh] | - 0.147 |

Table 4.4: Energy balance with ACC
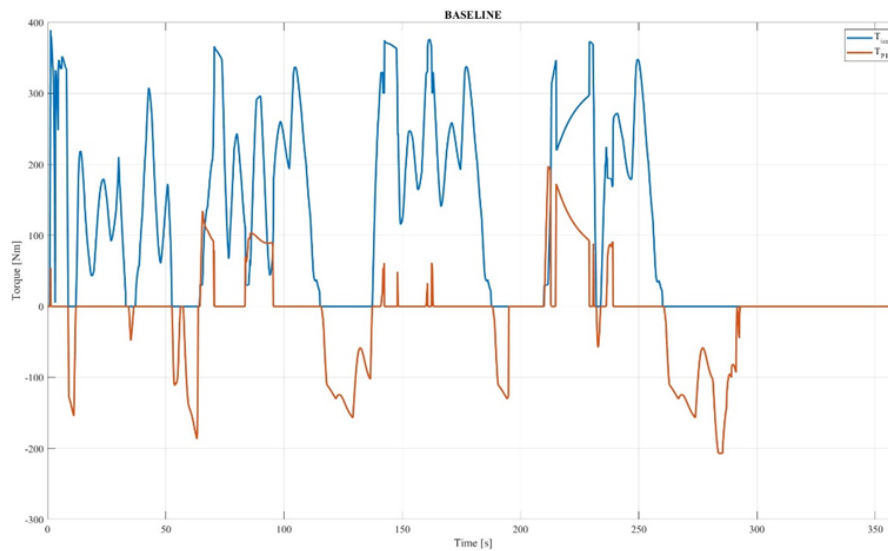


Figure 4.10: Basline requested torque
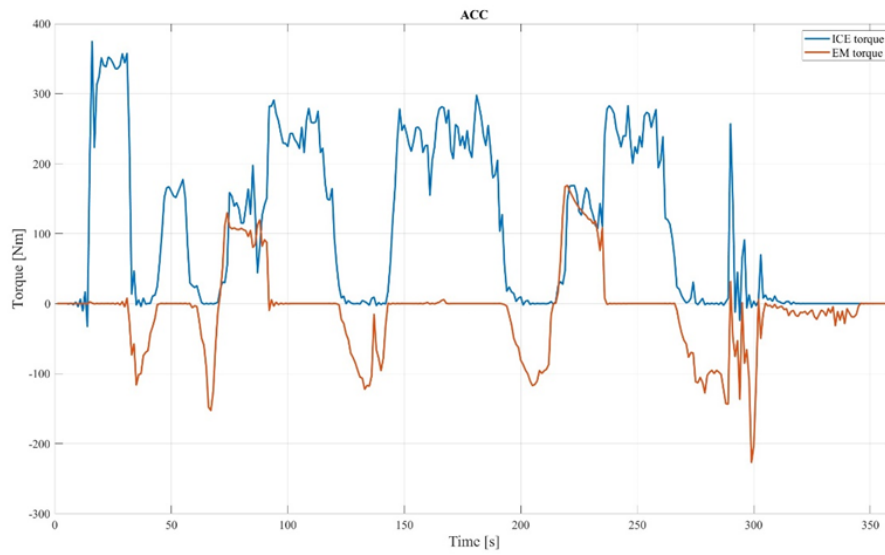
Figure 4.11: ACC requested torque

# Chapter 5

# Results

This chapter is dedicated to the analysis of the results related to validation phase concerning the two driving cycles WLTC and RDE. The discussion is related to the pure thermal configuration in which there is a correspondence in terms of experimental data. The match between this last and numerical results obtained with the model developed and properly tuned in Simulink regards the main vehicle characteristics: going from the vehicle actual speed to the ICE revolution speed to the fuel consumption and CO2 emissions.

## 5.1 Simulation of pure thermal configuration

The first analysis and simulations are related to the pure thermal configuration of the powertrain in which the main components are described in section 2.3. Before analyzing more in deep the obtained results it is worth noting introducing the experimental data available and the procedure conducted. For what concerns the former, FEV has played a fundamental role, since it has provided the data related to two homologation driving cycles, WLTC and RDE. In particular the information was related to the following vehicle characteristics:

- Reference and actual vehicle speed;

- Internal combustion engine revolution speed;

- Torque request;

- Fuel consumption;

- CO2 emissions;

The knowledge of this variables is crucial for validation purposes that will be discussed in the next section. Regarding the procedure used, the discussion can be subdivided between the controller and plant part. In the first of the two, the starting point consists in the proper selection of the driving cycle that it is wanted to be performed (both in the Matlab initialization script and in the corresponding Simulink block addressed ad

importing the right reference speed and time). Moreover, it is necessary to select the right mode in which the entire simulation, thus powertrain architecture, must be run: so pure ICE or with the presence of the EM). This is correlated to the different control strategy used in the two cases. From the plant side, the main action to be done is to insert the right vehicle principal characteristics in the longitudinal dynamic block as well as in the propeller and driveline side. After this initial set-up procedure, the simulation is ready to be launched and studied.

### 5.1.1 Validation on experimental results

This section is dedicated to the analysis and comparison between the numerical data obtained using the virtual vehicle model in Simulink and the experimental one extracted from the real vehicle in two driving scenarios. As stated in the proper chapter the main aim of the validation process is the one of having the highest fidelity and close match between the virtual and real simulation to be able to assess that the corresponding numerical model is well representative of the vehicle behavior. At this regard, the discussion is divided in two parts, one related to the WLTC and one to the RDE, since the operating conditions and vehicle requirements are completely different.

**WLTC simulation**

The beginning of the validation process starts with the verification of the actual speed profile, in order to be sure to have a fair comparison between experimental and numerical value. This can be associated to a sort of hypothetical mental scheme that follows the same order of block present in the plant and controller side. Going back to the actual vehicle speed, there is a range of acceptance of vehicle speed, represented by two dynamic thresholds that reproduce the reference speed values but multiplied by a certain gain (that are larger and lower than one). In particular, these values correspond to the 5% more and less of the homologation driving cycle speed, thus the gain are 1.05 for the upper value and 0.95 for the lower one. Another crucial aspect is that the driver model present in the controller side has been tuned in order to be more compliant with the driving cycle characteristics. In practice, the proportional and integrative part have been decreased with respect to the standard initial values, so that the driver has been relaxed to meet more the WLTC main features.

| WLTC driver model parameters | |
|---|---|
| Proportional | 0.35 |
| Integrative | 0.3 |

Table 5.1: WLTC driver model

As can be seen from the Figure 5.1, there is a perfect match between the experimental and numerical vales, thus it is possible to proceed with the analysis. Now the focus can be put on the requested torque, that for the current powertrain configuration, is completely satisfied by the internal combustion engine. Starting from this variable it is possible to see
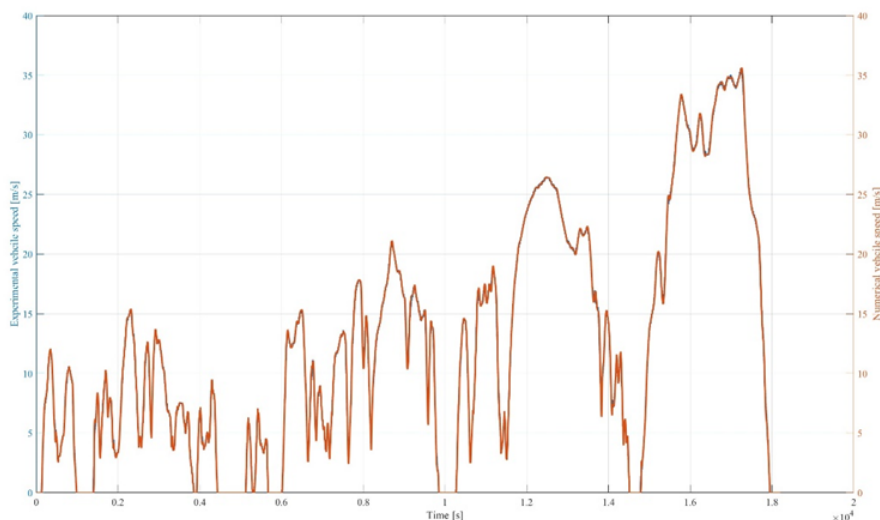
Figure 5.1: WLTC vehicle speed

the first small mismatches between the two types of data. Before analyzing the remaining parameters, it is worth noting highlighting the possible reasons of the not perfect match:

- Assumptions and simplifications: numerical simulations often rely on assumptions and simplifications in order to simplify complex physical phenomena. These simplifications can lead to inaccuracies in the simulation results, especially if the underlying assumptions are not well-validated or do not accurately represent the real-world conditions.

- Modeling errors: numerical simulations rely on mathematical models to represent physical phenomena. Modeling errors could arise if the models used are not accurate, or if they are not appropriately calibrated or validated.

- Input data: numerical simulations rely on input data to provide the necessary parameters for the simulation. If the input data is inaccurate or incomplete, it can lead to differences in the simulation results.

- Experimental errors: experimental measurements can also be subject to errors and uncertainties, especially if the experimental setup is not well-controlled or calibrated. These errors can propagate into the numerical validation process and lead to mismatches between the experimental and numerical values.

- Sensitivity analysis: it is also possible that the numerical simulation results are sensitive to certain input parameters or modeling assumptions. In this case, the mismatch between the experimental and numerical values may be due to the sensitivity of the simulation results to specific factors.

Taking a step back to the ICE requested torque the figure below graphically represents the previously described differences.

77
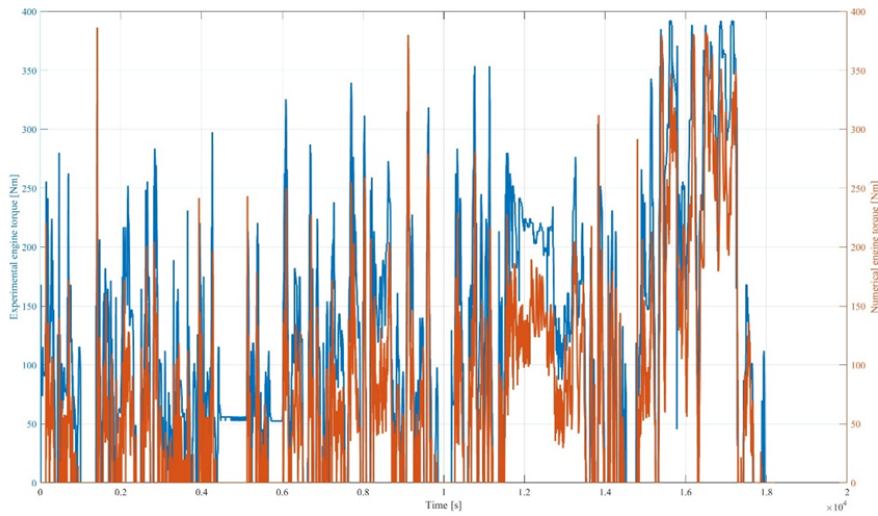
Figure 5.2: Experimental and numerical engine torque comparison

Strictly related to the engine torque, directly produced from the throttle signal, the internal combustion engine revolution speed can be analyzed and studied. The latter is child of the upstream torque request, so that the ICE working points are adjusted in order to meet the above descried demand. Going more in detail, the simulated numerical vehicle model seems to be less aggressive than the real system and this can be observed by the several spikes present in the experimental data. More in general, the numerical values tend to be always below the other one.
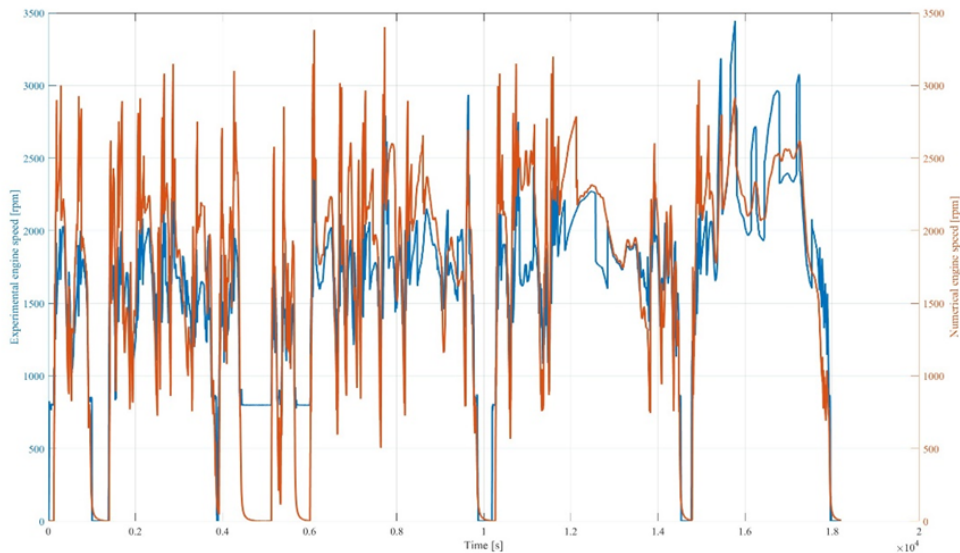


Figure 5.3: WLTC engine revolution speed

78

Having said that, as introduced in the previous chapter a huge importance is covered by the gear shifting strategy used. As a matter of fact, it influences the main vehicle variables and could be also the reason of the mismatches. This was the reason why part of this thesis work was dedicated just to understand and extrapolate the logic present in the real vehicle so that it can be implemented in both the two driving cycles. As can be seen from the figure beneath, the small differences presence, especially in the last part of the cycle (the highway section), are responsible for the not perfect match in terms of ICE revolution speed and torque. Nevertheless, it has been decided to avoid reproducing the frequent upshift and downshift present in the experimental data in the last part of the cycle because this would cause some modifications in the medium-high speed region in the numerical model. Another reason is represented by the fact that the same logic has to be implemented in two completely different scenarios, where vehicle requests (in terms of aggressivity) are completely different.
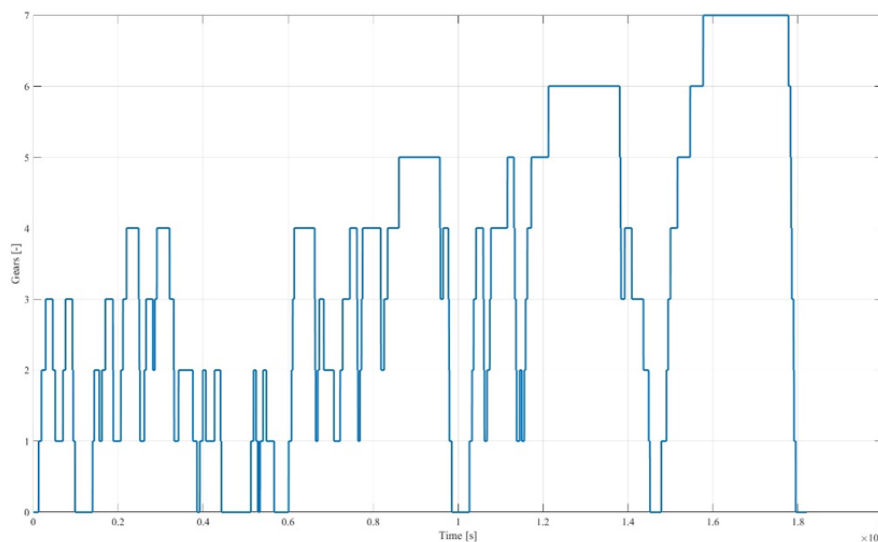


Figure 5.4: WLTC gears

Moving the attention towards the consumption and emissions side it is possible to state that for what concerns the former the discussion can be split in two parts: without the TCF and with the TCF. In fact, just considering the model as it is the level of mismatch between experimental and numerical model is larger and in the range of 13.92%, so considerably high. This gap can be seen in the following graph.

| Experimental fuel consumption [l] | Numerical fuel consumption [l] |
|---|---|
| 2.793 | 2.404 |

Table 5.2: Experimental and numerical fuel consumption comparison

However, if the transient correction factor is considered the gap decrease in a relevant way, going down to 6.16%. This is representative of the increased accuracy in the
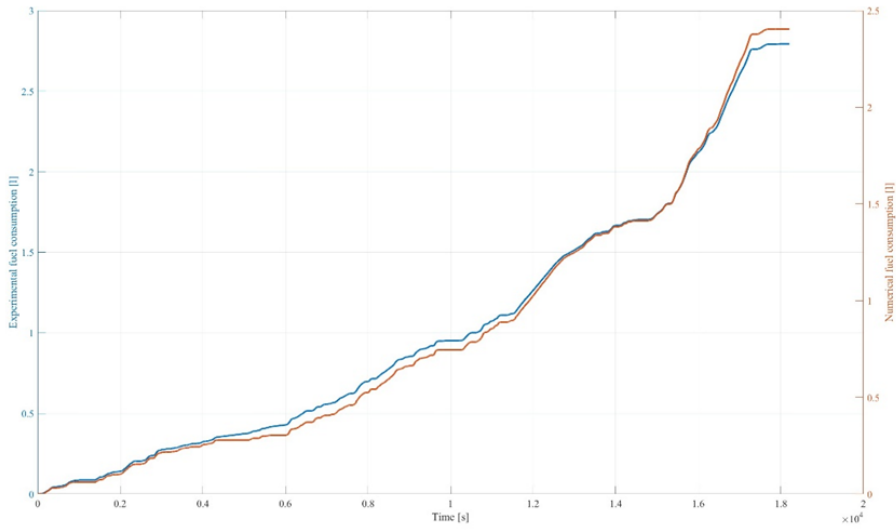
Figure 5.5: Experimental and numerical fuel consumption comparison
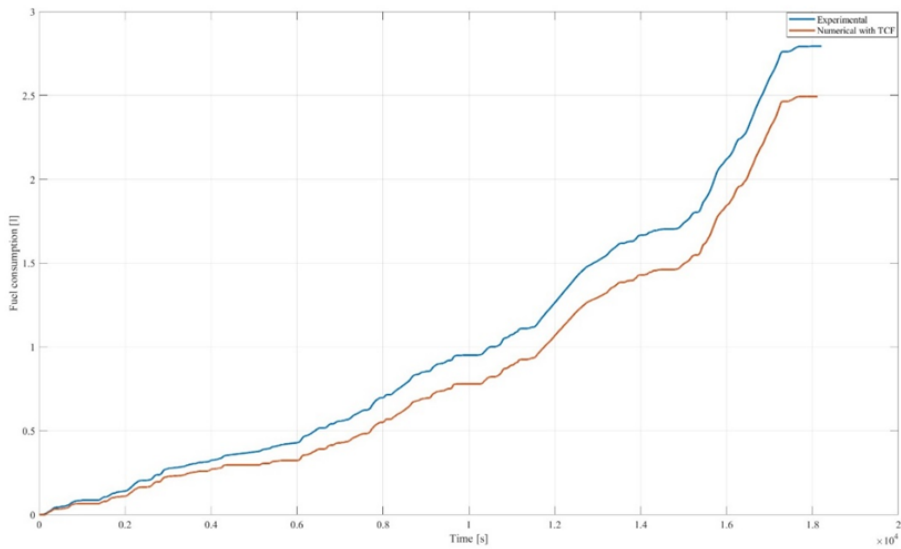


Figure 5.6: Experimental and numerical with TCF fuel consumption comparison

modelling phase of the internal combustion engine.

Another way in which it is possible to assess the improvement in reproducing the vehicle behaviour is by looking at the fuel consumption rate emissions, that, as shown in Figure 5.7, depicts very little discrepancies. The same discussion holds for the $CO_2$ emissions without and with the correction related to the transient phases of the engine. In fact, at the beginning the difference between the two types of data is in the range of 9.33%, thus still high to be considered an acceptable result.

80

| Experimental fuel consumption [l] | Numerical fuel consumption [l] |
|:---:|:---:|
| 2.793 | 2.563 |

Table 5.3: Experimental and numerical with TCF fuel consumption comparison
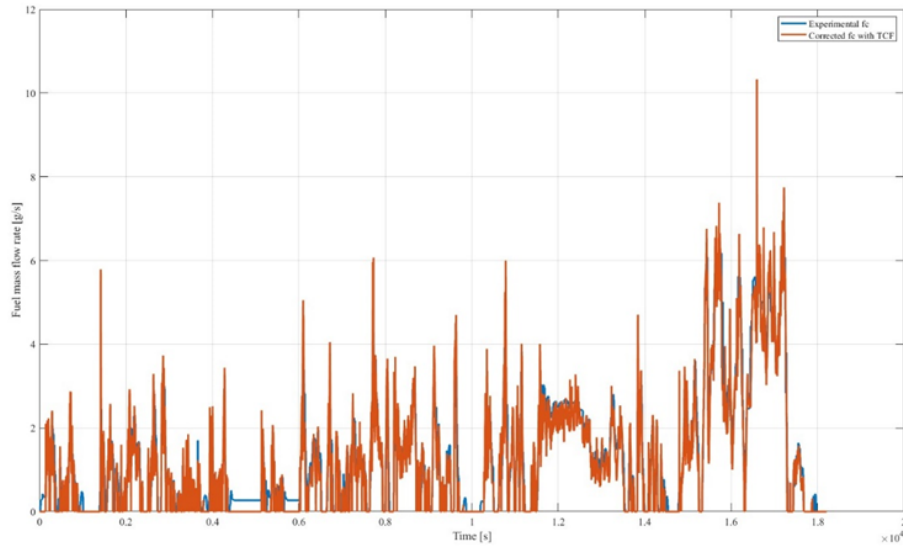


Figure 5.7: Experimental and numerical fuel rate comparison
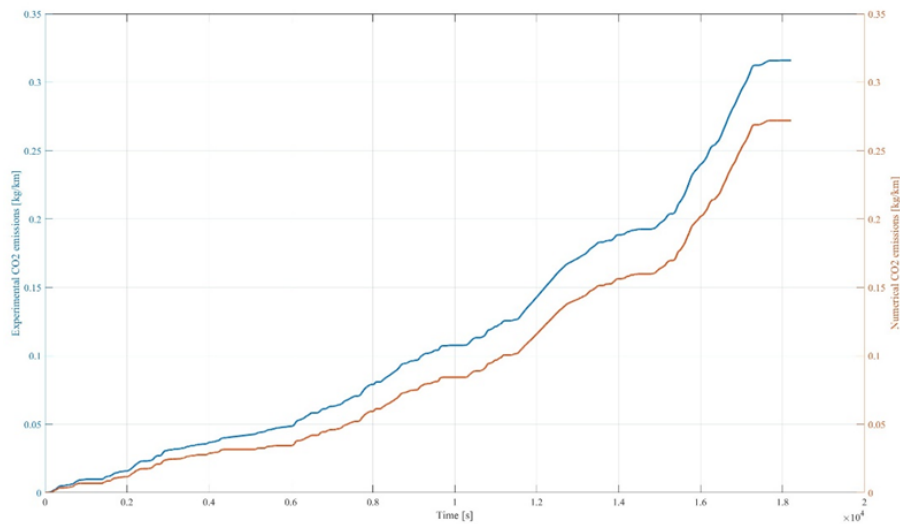


Figure 5.8: Experimental and numerical CO2 emissions comparison

After the implementation of the correction factor the newer difference is of 1.45%, leading to much better measurement and model fidelity. The improvements can also be

| Experimental CO2 emissions [kg/km] | Numerical CO2 emissions [kg/km] |
|:---:|:---:|
| 300 | 272 |

Table 5.4: Experimental and numerical CO2 emissions comparison

seen graphically from the graph and table beneath.
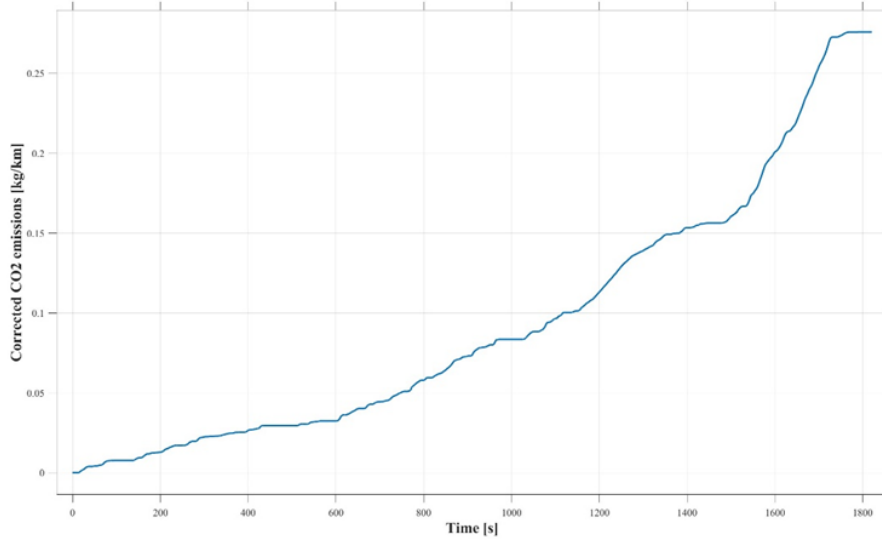


Figure 5.9: WLTC CO2 emissions with TCF

**Coast down test**

Another field of the validation process, not strictly related to the homologation driving cycle, is the previously described Coast Down method. In particular, the aim of this analysis is to evaluate and compare the power delivered at 100 km/h using the experimental and numerical data. In particular, the vehicle mass value used for this test is no longer 2610 kg (value used for the two simulations over the driving cycles) but 3283 kg. This increment is due to the addition of weight to simulate the full load condition, where are considered the occupants, of 70 kg each and the luggage weight of 10kg.

| Vehicle characteristics | |
|:---:|:---:|
| Mass [Kg] | 3283 |
| Frontal area $[m^2]$ | 5.657 |
| Drag coefficient [-] | 0.361 |
| Rolling resistance coefficient [-] | 0.0107 |

Table 5.5: Vehicle characteristics

Concerning this work, the procedure adopted to reproduce this maneuver consists of repeated vehicle acceleration from standstill up to always increasing speed values. More

in detail, in Simulink environment a ramp signal it is adopted for this purpose where the final speed value goes from 0 km/h up to 140 km/h with a step of 10 km/h for each simulation, in order to obtain the resistive forces and as a consequence, the corresponding power values. Furthermore, for what concerns the experimental initial values, they are related to the three terms constituting the corresponding resistive force expression, as show below:

| Experimental data | |
|---|---|
| F0 [N] | 345 |
| F1 $[N/(km/h)]$ | 0 |
| F2 $[N/(km/h)^2]$ | 0.1007 |

Table 5.6: Experimental input values

With the knowledge of the previously computed numerical forces, it has been possible to obtain the three coefficients, that show a good match with the experimental ones, as demonstrated in the following table:

| Numerical data | |
|---|---|
| F0 [N] | 347 |
| F1 $[N/(km/h)]$ | 0 |
| F2 $[N/(km/h)^2]$ | 0.1005 |

Table 5.7: Numerical input values
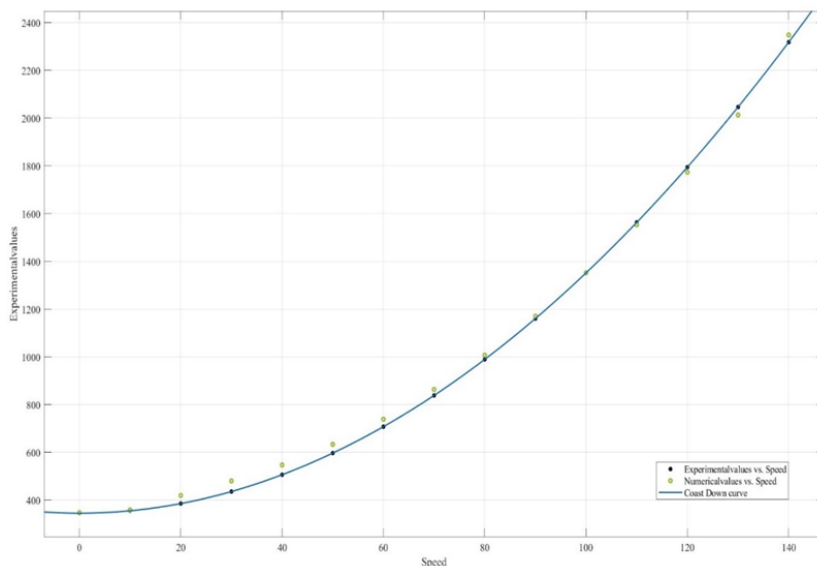


Figure 5.10: Experimental and numerical coast down curve

| Experimental values | | |
|:---:|:---:|:---:|
| Speed [km/h] | Power [kW] | Force [N] |
| 0 | 0.00 | 345.0 |
| 10 | 0.99 | 355.1 |
| 20 | 2.14 | 385.3 |
| 30 | 3.63 | 435.6 |
| 40 | 5.62 | 506.1 |
| 50 | 8.29 | 596.8 |
| 60 | 11.79 | 707.5 |
| 70 | 16.30 | 838.4 |
| 80 | 21.99 | 989.5 |
| 90 | 29.02 | 1160.7 |
| 100 | 37.56 | 1352.0 |
| 110 | 47.77 | 1563.5 |
| 120 | 59.84 | 1795.1 |
| 130 | 73.91 | 2046.8 |
| 140 | 90.17 | 2318.7 |

Table 5.8: Experimental coast down values

| Numerical values | | |
|:---:|:---:|:---:|
| Speed [km/h] | Power [kW] | Force [N] |
| 0 | 0.00 | 345 |
| 10 | 1.00 | 358.20 |
| 20 | 2.328 | 419.04 |
| 30 | 3.999 | 479.87 |
| 40 | 6.078 | 547.01 |
| 50 | 8.796 | 633.33 |
| 60 | 12.313 | 738.80 |
| 70 | 16.789 | 863.45 |
| 80 | 22.383 | 1007.24 |
| 90 | 29.255 | 1170.22 |
| 100 | 37.565 | 1352.35 |
| 110 | 47.472 | 1553.63 |
| 120 | 59.136 | 1774.08 |
| 130 | 72.717 | 2013.69 |
| 140 | 91.354 | 2349.10 |

Table 5.9: Numerical coast down values

Moreover, in order to obtain the power values corresponding to the resistive forces it is simply necessary to multiplied the latter to the vehicle speed value at which the ramp simulation is performed. The results are shown in the previous tables. Finally, using the corresponding three coefficient obtained the numerical model and using the experimental

data it is performed a linear regression using a dedicated function of Matlab, thanks to which the two coast down curves are obtained. The correctness and high fidelity of the numerical model is shown by the almost perfect match between the two curves, as depicted in Figure 5.10.

**RDE simulation**

Related to the real driving emissions simulation, the discussion about the validation process is slightly different because the only experimental data available, always with respect to the pure thermal configurations, related to:

- Actual vehicle speed,

- Fuel consumption,

- CO2 emissions.

Due to the lower number of experimental data, at the beginning, the description of this paragraph is related to the three above written variables and then is extended to all the others. Concerning the first bullet point, the driver model has to been tuned according to the new scenario characteristics, thus it is chosen a more aggressive and responsive driver model. In fact, the newer proportional and integrative values are:

| RDE driver model parameters | |
|---|---|
| Proportional | 0.98 |
| Integrative | 0.11 |

Table 5.10: RDE driver model parameters

After this initial modification, the simulation procedure remains exactly the same of the previous driving cycle, so that the comparison between reference experimental and numerical speed can be conducted.

As can be seen, due to the more demanding scenario the numerical vehicle model has some difficulties in reproducing with perfection the last part of the cycle, where the vehicle speed is very high. Having said that, in the urban part, so in the repeated TFL, the velocity trend is respected with high fidelity. Going one with the second experimental variable, the fuel consumption, there is a good level of match between the two data types. In fact the difference is just in the order of 4.69%.

| Experimental fuel consumption [l] | Numerical fuel consumption [l] |
|---|---|
| 11.5 | 10.96 |

Table 5.11: Experimental and numerical fuel consumption comparison

In a similar way, the comparison between experimental and numerical values obtained for the CO2 emissions are in accordance with the good level of match found for the previous variable. As a result of this, the mismatch is just of 4.17%.
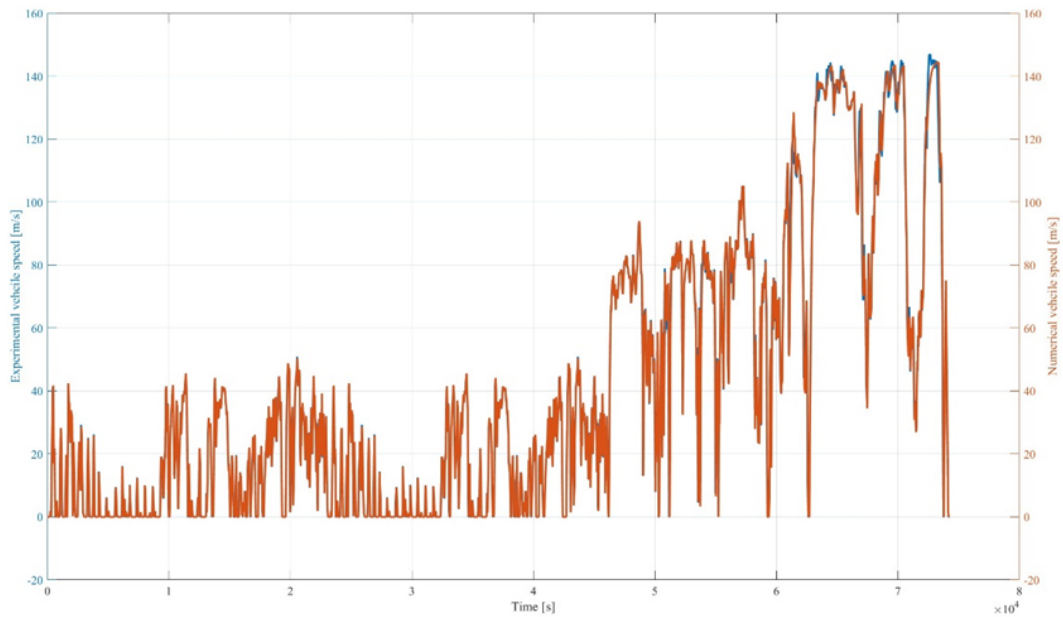
Figure 5.11: RDE vehicle speed
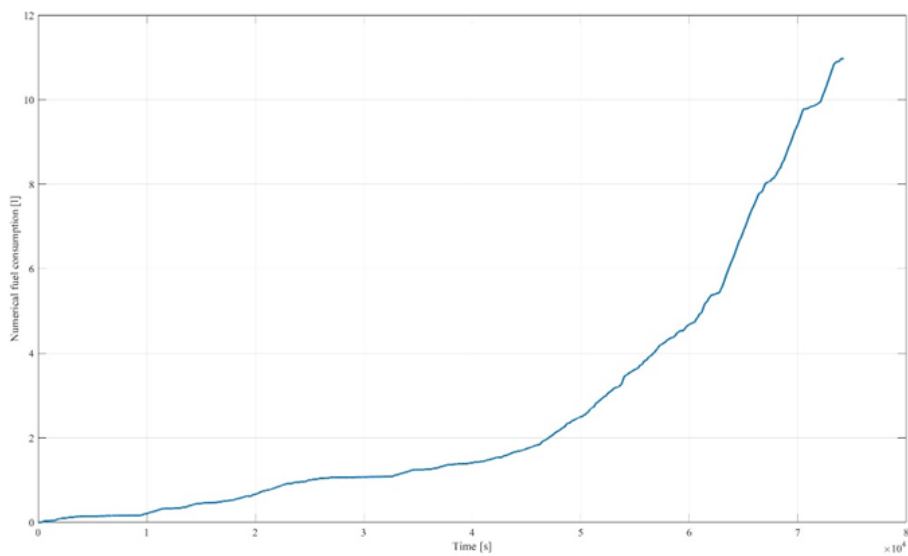


Figure 5.12: RDE fuel consumption

Now that the experimental data are finished, the analysis is extended to the variables descried also for the WLTC case. The considerations can start with the internal combustion engine revolution speed, where from the figure below, it is possible to state from the repeated spikes, that the ICE is more stressed. This is due to the frequent acceleration and decelerations phases that characterize the initial part of the driving cycle. Moreover,
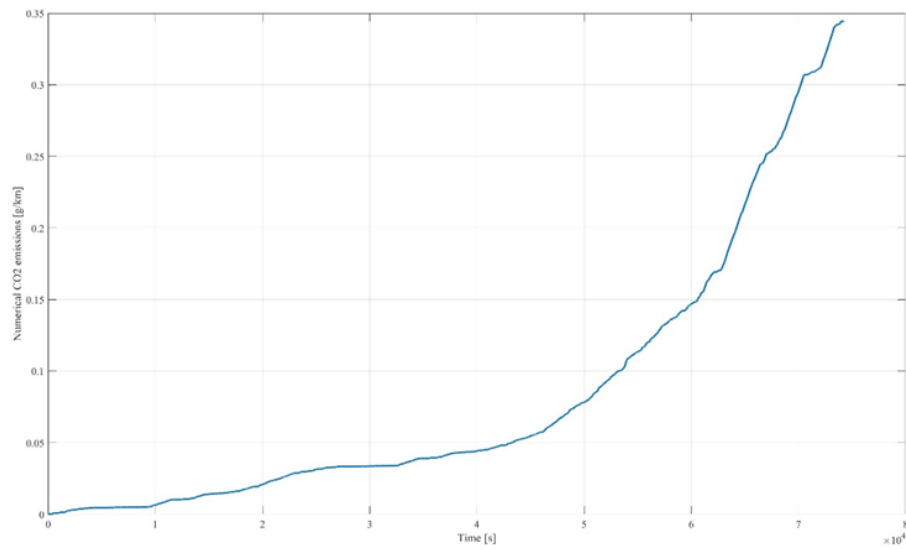
Figure 5.13: RDE CO2 emissions

with respect to the previous driving cycle, the ICE works almost every time at speed close to the upper limit of 4000 rpm.
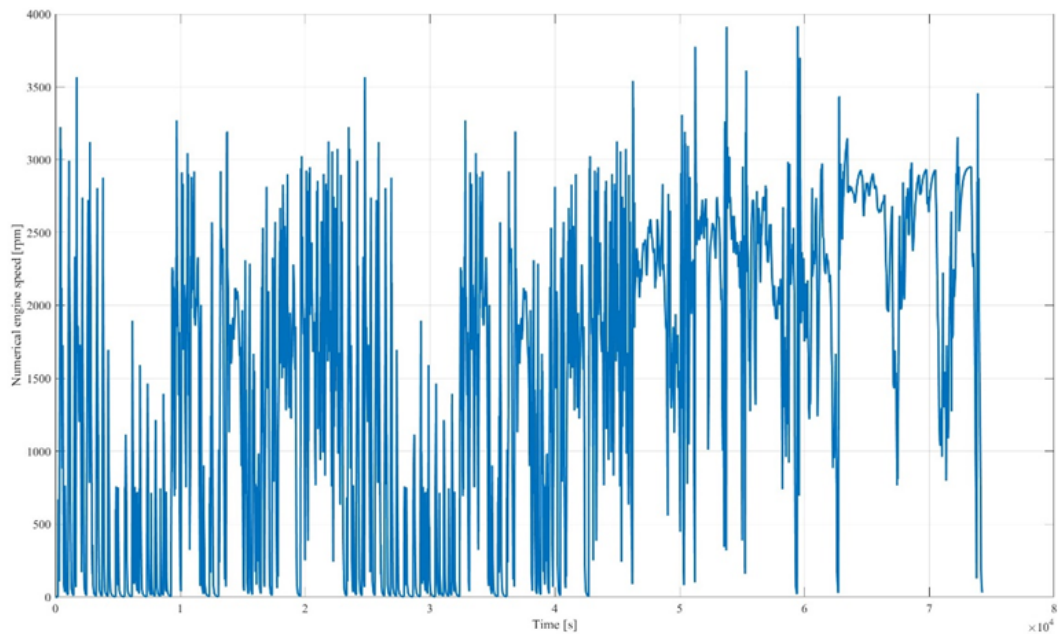


Figure 5.14: RDE engine revolution speed

It is worth noting recalling the fact that the gear shifting logic implemented in the RDE case is the same as the one used for the laboratory cycle. So based on the ICE

87

revolution speeds introduced in section 2.4.2 the gears are upshifted and downshifted.
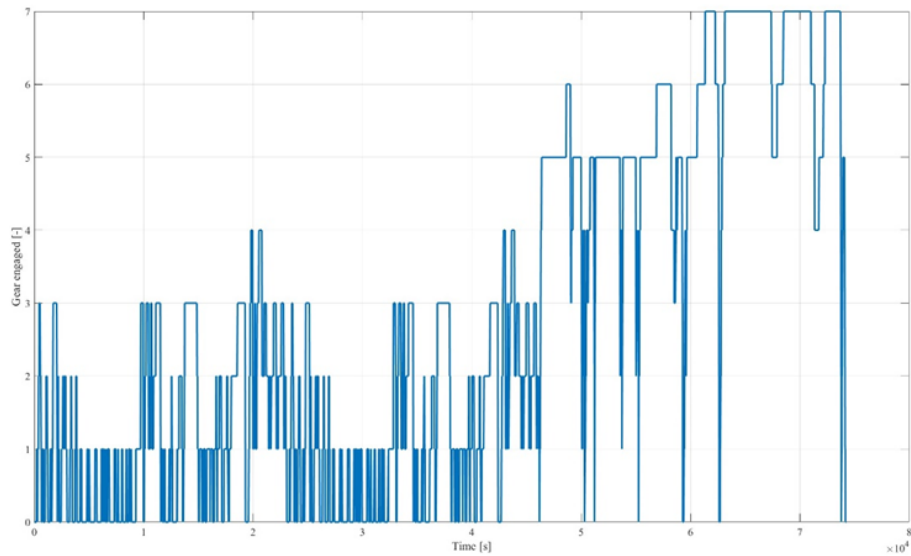


Figure 5.15: RDE gears

To conclude the chapter related to the RDE simulation and more in general to the pure thermal configuration, the requested torque is depicted. As it could be expected the values, especially in the latest part, are close to the maximum torque the ICE can provide, thus this represent how aggressive and demanding is this cycle.
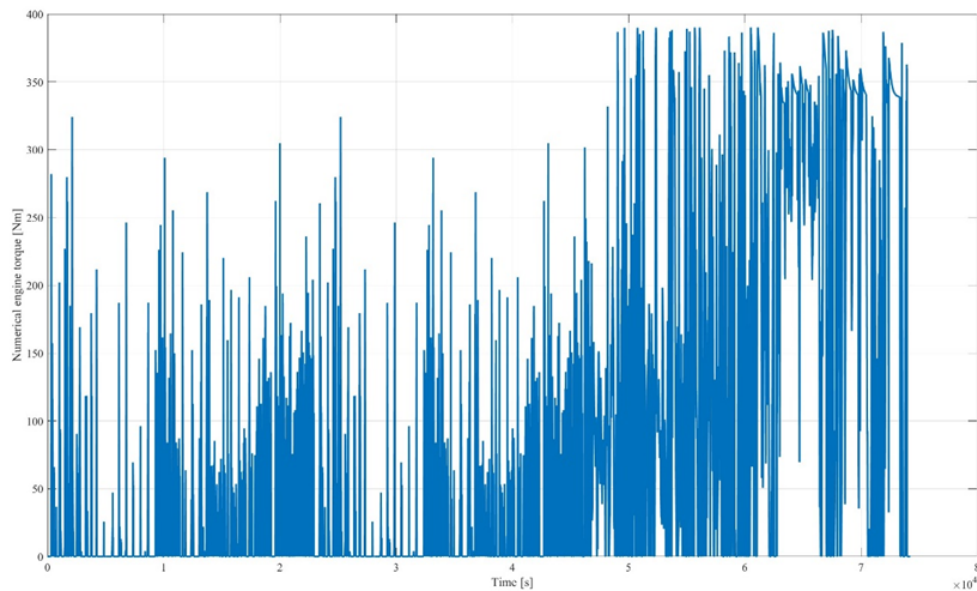


Figure 5.16: RDE engine torque

## 5.2  Simulation of P1 hybrid configuration

This section is related to the simulations analysis of the hybrid architecture used to perform the already described driving cycles. It is clear that the discussion will be widened since new vehicle components are present, that allow to enhance vehicle performance. In fact, a crucial step is the assessment of the improvement that this new powertrain configuration brings, in terms of reduced fuel consumption and CO2 emissions. As done for the previous section, the analysis is divided between the WLTC and RDE driving scenarios.

**Hybrid WLTC simulation**

In order to make a fair comparison and be able to clearly assess the benefits related to the hybrid architecture, the same variables of section 5.1.1 are analyzed except for the vehicle speed since it is not altered. In addition to the latter, neither the internal combustion engine speed and as a consequence the engaged gears undergo radical changes. Having said that, what is really changing and causing a fuel consumption and CO2 reduction is the different way in which the requested torque is satisfied. In fact, by looking at Figure 5.17 it is clearly visible the intervention of the electric machine that helps and reduce the burden to the ICE. The main operations of the P1 electric motor are mainly during the braking phases (negative EM torque values), but also during the most challenging parts of the cycle. At the same time whenever the torque request is very high or the SOC of the battery has reached the lower threshold value, the hybrid control strategy, so the ECMS, let just the ICE fulfil the corresponding torque values and this is visible when the orange line (P1 torque is null).
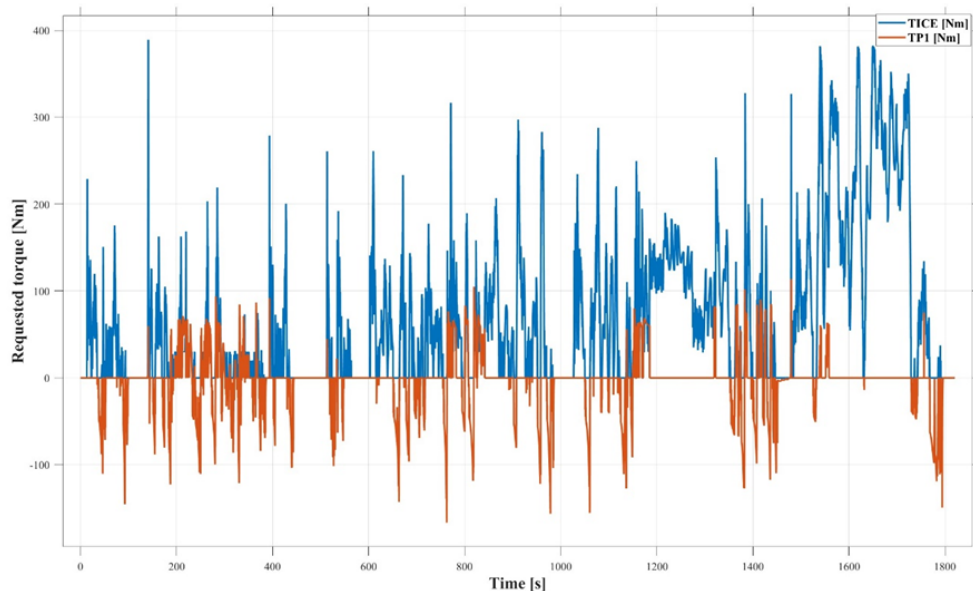


Figure 5.17: Hybrid WLTC requested torque

For what concerns the improvements that the presence of the electric motor brings,

the most relevant one are for sure the fuel consumption and the CO2 emissions. Related to the former the reduction that it is possible to achieve over the driving cycle is in the order of 4.65% and this can be addressed to two aspects: during the acceleration phases the EM helps the ICE in satisfying the requested torque and during the deceleration phases the braking torque is just provided by the electric motor, thus reducing the ICE burden.
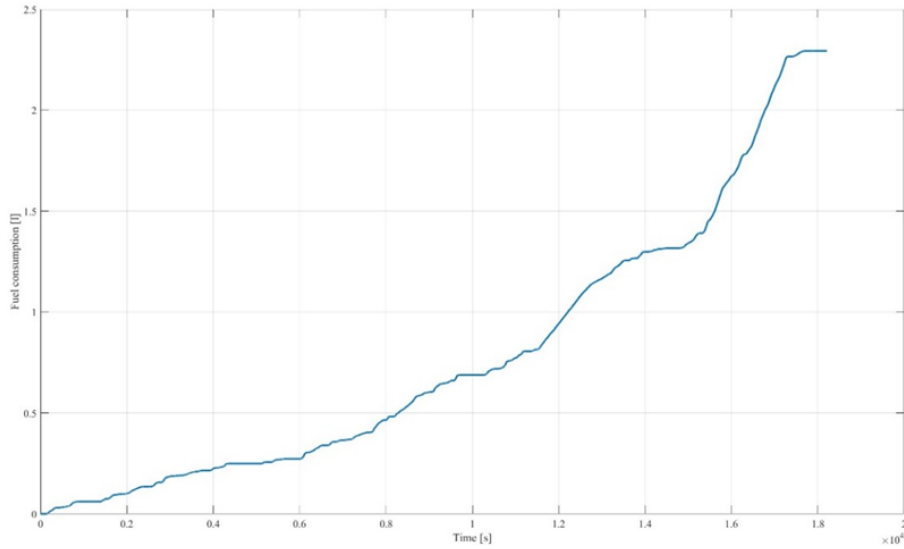


Figure 5.18: Hybrid WLTC fuel consumption

| Hybrid fuel consumption [l] | Reduction percentage [%] |
|:---:|:---:|
| 2.293 | 4.65 |

Table 5.12: Hybrid WLTC fuel consumption reduction

The other field of inspection for improvements are the CO2 pollutant emissions, that follows the same decreasing trend of the fuel consumption. As a matter of fact, the obtained reduction is in the same order of the previous variable, thus leading to a 4.65% improvement.

Finally, it is necessary to give the right attention to a fundamental parameter when dealing with hybrid architecture that is the state of charge (SOC) of the battery. As a matter of fact, the importance of this factor includes two aspects: the correct functioning of the battery pack in terms of charge sustaining strategy and the homologation purpose. Related to the former it is possible to state that the charge sustaining strategy is a technique used to maintain the state of charge (SOC) of a battery pack while it is being used in an electric or hybrid vehicle. This strategy is designed to ensure that the battery pack is able to provide consistent performance over the course of a driving cycle, which is important for both vehicle performance and safety. During a driving cycle, the battery pack may be subjected to a variety of different loads and operating conditions, which can
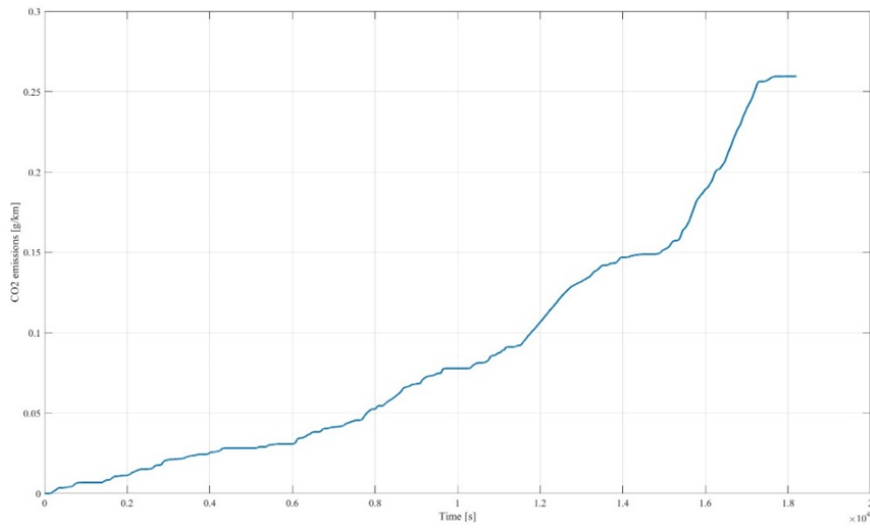
Figure 5.19: Hybrid WLTC CO2 emissions

| Hybrid CO2 emissions [kg/km] | Reduction percentage [%] |
|:---:|:---:|
| 259.4 | 4.65 |

Table 5.13: Hybrid WLTC CO2 emissions reduction

cause the SOC to fluctuate. If the SOC drops too low, the battery may not be able to provide the necessary power to the vehicle, which can result in decreased performance and even safety issues.
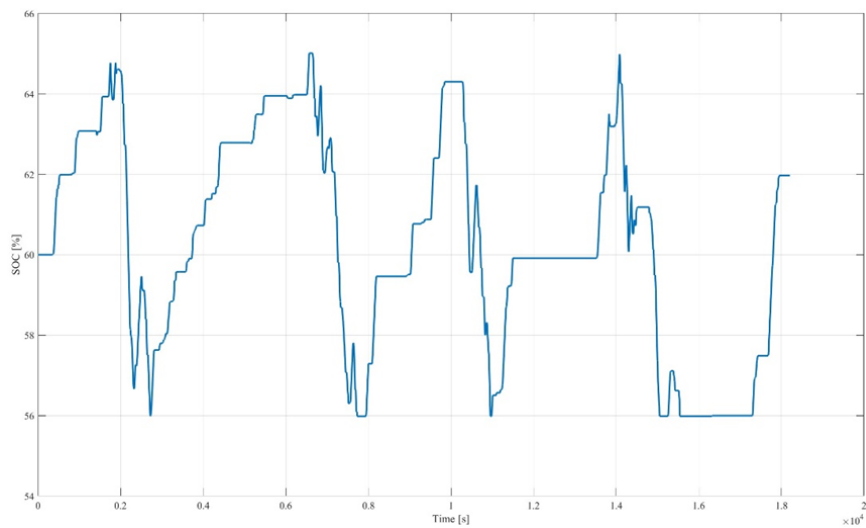


Figure 5.20: SOC hybrid WLTC

91

Conversely, if the SOC is too high, it can lead to overcharging, which can cause damage to the battery and reduce its overall lifespan. To address these issues, charge sustaining strategies use a combination of battery management techniques, such as regenerative braking and engine power management, to maintain the SoC within a safe and optimal range. This can help to ensure that the battery pack is able to provide consistent performance over the course of a driving cycle, which is important for both vehicle performance and safety. Whereas related to the homologation purpose it is necessary to ensure that the final state of charge value is the same as the initial one. The reason behind this is that the energy that the electric source is providing must be equal to the one that is regenerated during the braking phases to have a fair estimation of the fuel consumption and most importantly of the pollutant emissions. In a more practical way, inside the ECMS function it is necessary to choose the right working window of the battery to have the desired result. For what concerns the numerical vehicle model, the SOC obtained within the entire WLTC driving cycle is respecting the previously mentioned constraint and it is shown below.

**Hybrid RDE simulation**

The last section of this chapter is related to the RDE simulation using the hybrid P1 architecture. Due to the more demanding and aggressive driving cycle the advantages in terms of reduced fuel consumption and CO2 emissions are lower. The reason behind this statement in addition to what just written is the longer cycle duration, in particular in terms of highway part. Following the same order of the previous section, the analysis does not consider the actual vehicle speed, the internal combustion engine and the corresponding engaged gears, since they are not affected by the presence of the electric machine can start by looking at the internal combustion engine revolution speed.
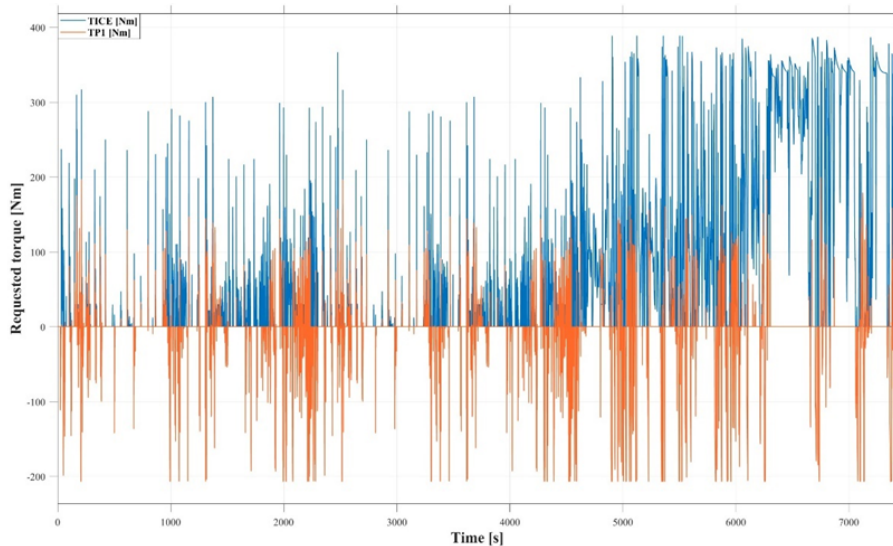


Figure 5.21: Hybrid RDE requested torque

92

Having said that, the requested torque is a clear example of the obtained reduction in fuel consumption and emissions as depicted in Figure 5.22. As a matter of fact, all the braking phases are managed by the P1 electric machine that acts as a generator, thus regenerates the kinetic energy that otherwise would be dissipated. These are not the only situations in which the EM enters in action, in fact, due to the higher aggressivity of the cycle, also during the traction phases there is a certain amount of aid coming from the electric propeller.

In terms of vehicle improved performance, the reduction of fuel consumption over the entire cycle is of 4.2%, thus still a remarkable enhancement.
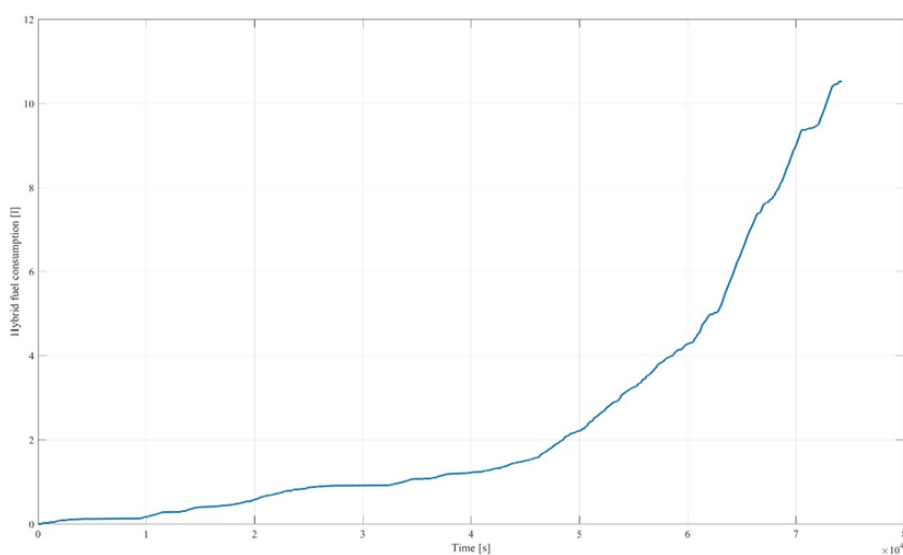


Figure 5.22: Hybrid RDE fuel consumption

| Hybrid fuel consumption [l] | Reduction percentage [%] |
|:---:|:---:|
| 10.5 | 4.2 |

Table 5.14: Hybrid RDE fuel consumption reduction

For what concerns the pollutant emissions, the discussion traces the fuel consumption reduction, thus leading to the same percentage of improvement.

Also for the RDE scenario it is necessary to put attention on the SOC trend, especially due to the aggressiveness of the cycle. As a result of this, the oscillations of this variable are frequent and quite deep, going from the upper to lower threshold values. This for sure, in a prolonged and repeated scenario could negatively affect the battery health and overall electric powertrain performance.
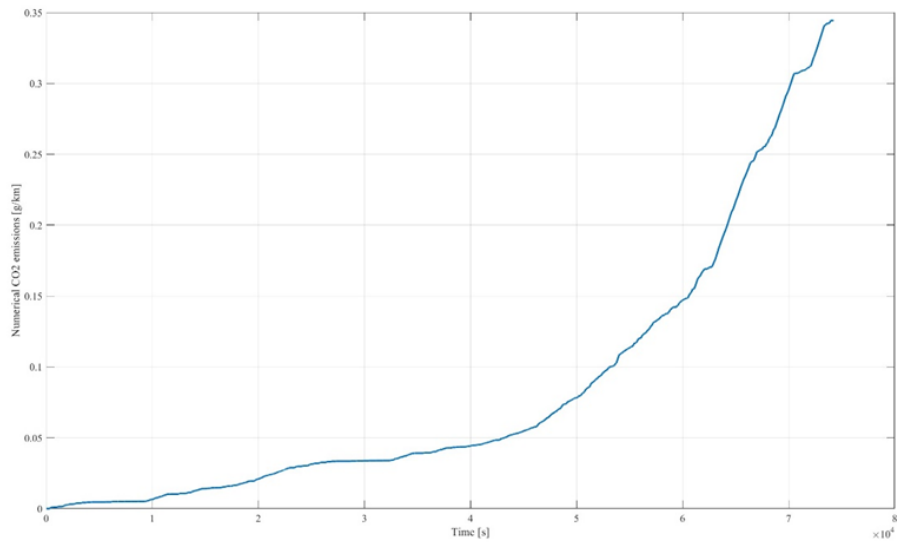
Figure 5.23: Hybrid RDE CO2 emissions

| Hybrid CO2 emissions [kg/km] | Reduction percentage [%] |
| --- | --- |
| 259.4 | 4.65 |

Table 5.15: Hybrid RDE CO2 emissions reduction
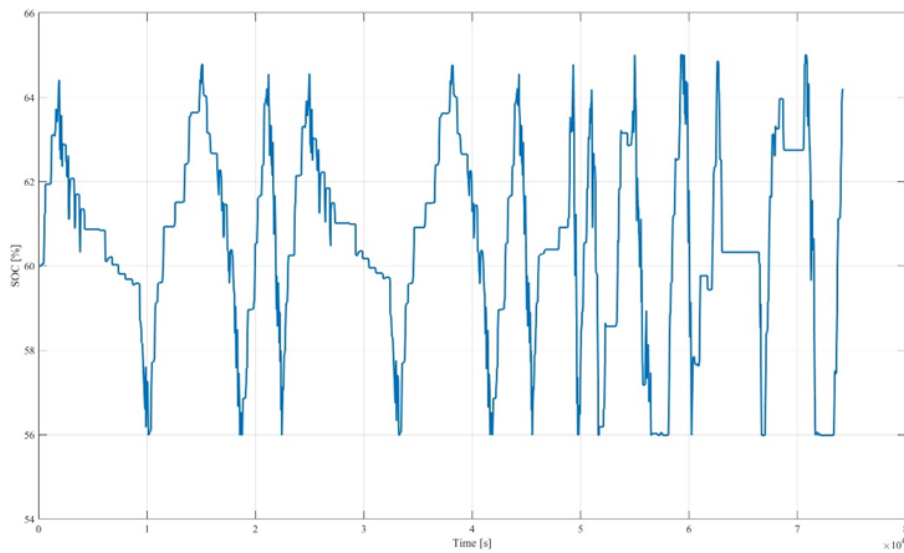


Figure 5.24: SOC for hybrid RDE simulation

94

## 5.3   Fine model tuning based on chassis dynamometer tests

This last section is dedicated to some improvements performed to the numerical vehicle model level after the tests conducted at the chassis dynamometer. Before proceeding with the enhancements, it is worth noting highlighting the importance of these type of test in correlation with virtual modelling. As a matter of fact, there main benefits are:

- Real-world simulation: a chassis dynamometer allows for testing in a real-world environment, which can provide more accurate data than simulated environments. This data can then be used to refine virtual models and simulations to make them more accurate.

- Reproducibility: chassis dynamometer tests are highly repeatable, which allows for precise comparisons between different vehicles and components. This level of reproducibility is difficult to achieve in virtual simulations.

- Data collection: chassis dynamometers can collect a wide range of data, including engine performance, emissions, and vehicle dynamics. This data can be used to validate virtual models and simulations, and to identify areas where improvements can be made.

- Safety: chassis dynamometers allow for controlled testing in a safe environment. This can reduce the risk of accidents and injuries during testing, which can be a concern when testing in real-world environments.

- Cost savings: by using a chassis dynamometer to refine virtual models and simulations, manufacturers can reduce the need for expensive physical prototypes and real-world testing. This can result in significant cost savings over the long term.

Overall, the use of a real vehicle chassis dynamometer for testing can provide valuable data that can be used to refine virtual models and simulations, resulting in more accurate and efficient vehicle components.

**Torque converter**

An example of what just written concerns the torque converter modelling phase. In fact, after several test performed on the chassis-dynamometer it was found that the torque converter speed ratio and torque ratio were not the standard one present inside the Simscape block. As can be seen from Figure 5.25, especially for low speed ratio values, there is a remarkable difference between the two lines. This will inevitably cause a worsening in variables measurement and as a consequence a reduction in the model accuracy.
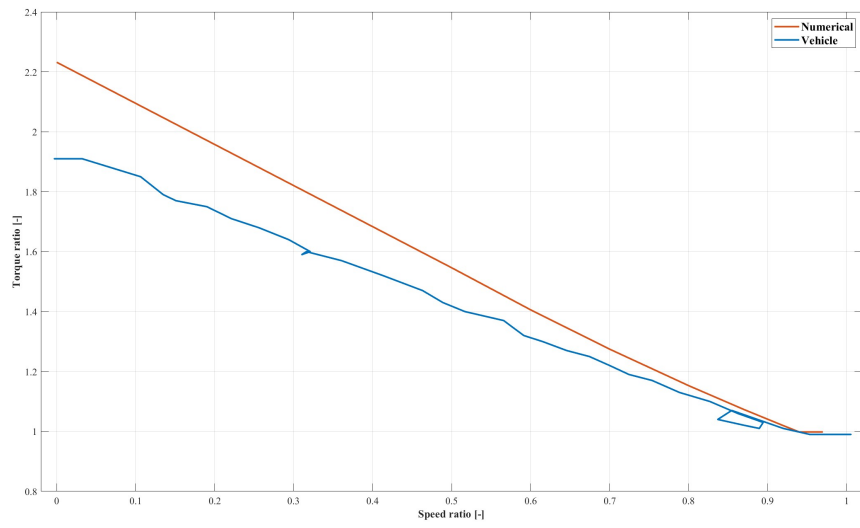
Figure 5.25: Torque converter graph comparison

# Chapter 6

# Conclusion

Nowadays the attention and care of environment is increased in an exponential way with respect to previous years and in the automotive sector this is translated into always more stringent rules to reduce pollutant emissions. To achieve this goal car companies are investing their time and money in hybrid and full electric vehicles, in which the presence of the thermal power source is foreseen to be decrease more and more as time goes by. At the same time, it is necessary to reproduce with high fidelity possible the vehicle and in particular the powertrain behavior, to have a reliable estimation of fuel consumption and as a consequence of greenhouse emissions. As a matter of fact, this thesis tries to be representative of the changes that the automotive industry is phasing and attempts at providing answers to the current worldwide situation. In particular, the focus is put on an vehicle sector where the evolution seems to not keeping up with the rest of the automotive field: the light-duty vehicles.

In fact, one of the aims of this thesis work is to provide, based on experimental data, a validation of a numerical vehicle model that reproduces the overall system performance. Actually, is of fundamental importance to have a robust baseline from which is then possible to perform some improvement in order to meet the current regulations. At this regard, always to achieve a decarbonization in the transport sector, a second step along this thesis, is the hybridization of the vehicle under study, through an electric motor in position P1. The latter is able to reduce the fuel consumption and CO2 of remarkable percentages with respect to the pure thermal configuration. As a result, during the WLTC driving cycle there is a 4.65% of reduction and for what concerns the RDE scenario the improvement is in order of 4.2%. These enhancements are addressed to the presence, in one hand of the electric machine, that reduces the effort of the internal combustion engine and let it works in a more efficient region and on the other of a hybrid control strategy, ECMS, that allows to have an optimal split between the two propellers. In addition to this control policy, other improvements are performed in order to increase the performance of the hybrid architecture and to further reduce the emissions, like using an optimal gear shifting logic. Another crucial step, after the hybrid configuration was properly set, is the usage of the validated vehicle model to verify and demonstrate that the ADAS sensors can lead to fuel consumption and pollutant emission reduction in addition to increased driving comfort and safety. More in detail, after the employment of

the necessary hardware and software required by the adaptive cruise control (ACC), the constant time gap (CTG) policy is implemented in order to keep a constant safe distance between the lead and ego vehicle. In particular, in order to assess any improvements, it is performed a dynamic parameter tuning phase based on the driving cycle time related to the time gap and default spacing. This implementation has made possible to obtain 9.10 % reduction of fuel consumption compared to the baseline WLTC configuration. Finally, the last thesis activities are addressed at validating the experimental data related to the two driving cycles no more using the virtual vehicle model, but with the real vehicle installed in a dynamometer test bench. This phase was also functional at understanding and verifying whether the principal vehicle components were properly modelled in Simulink environment.

# Bibliography

[1] Creutzig F., R. Muhlhoff, and J. Romer. "Decarbonizing urban transport in European cities: four cases show possibly high co-benefits". (2012) Environmental Research Letters 7, 044042. 2. doi: 10.1088/1748-9326/7/4/044042, ISSN: 1748-9326. (cit. on page 1)

[2] Corbett J., H. Wang, âJ. Winebrake. "The effectiveness and costs of speed reductions on emissions from international shipping".(2009) Transportation Research Part D: Transport and Environment 14, 593-598. doi: 10.1016/j.trd.2009.08.005, ISSN: 1361-9209. (cit. on page 2)

[3] Yedla S., R. Shrestha, and G. Anandarajah. "Environmentally sustainable urban transportation comparative analysis of local emission mitigation strategies vis-a-vis GHG mitigation strategies". (2005) Transport policy 12, 245-254 (cit. on page 4)

[4] L. Guzzella, A. Sciarretta. "Vehicle Propulsion Systems: Introduction to Modelling and Optimization" (Springer, Berlin, 2013) (cit. on page 7)

[5] H.B. Pacejka. "Tire and Vehicle Dynamics" (Butterworth-Heinemann, Oxford, 2012) (cit. on page 15)

[6] Cho, D. and Hedrick, J.K. "Automotive Powertrain Modelling for Control" ASME Journal of Dynamic Systems, Measurement and Control, Vol. 11 1, pp. 568-576 (cit. on page 15)

[7] Hucho WH. "Aerodynamics of road vehicles", (1998) SAE Publishing, Warrendale, PA (cit. on page 16)

[8] Wong, J.Y. "Theory of Ground Vehicles", Wiley-Interscience, ISBN 0-471-35461-9, Third Edition, (2001). (cit. on page 18)

[9] Guzzella L, Onder C. "Introduction to modelling and control of internal combustion engine systems" (2010), 2nd edn. Springer, Berlin (cit. on page 19)

[10] A.J. Kotwicki. "Dynamic models for torque converter equipped vehicles". SAE Technical Paper No. 820393 (1982) (cit. on page 22)

[11] G. Genta, L. Morello. "The automotive chassis â Components design", (2009) Vol. 1 pp. 506-510 (cit. on page 23)

[12] O. Balci. "Verification validation and accreditation of simulation models". In D. H. Withers, B. L. Nelson, S. Andradottir, and K. J. Healy, editors, Proc. of the 29th WSC, pages 135-141, (1997). (cit. on page 25)

[13] IEEE std 1012. "2004 IEEE standard for software verification and validation". IEEE Std 1012-2004 (Revision of IEEE Std 1012-1998), pages 1, 110, (2005). (cit. on page 25)

[14] "ISO 9001 quality management systems - requirements". pages 1, 30, (2008). (cit. on page 26)

[15] B. Zeigler, H. Praehofer, and T. G. Kim. "Theory of Modeling and Simulation". Academic Press, London, (2000). (cit. on page 26)

[16] G. J. Myers. "The Art of Software Testing". John Wiley Sons, Inc., 1979. (cit. on page 30)

[17] European Commission. "Commission regulation (EU) 2017/2400". Official Journal of the European Union, 60(L 349) (2017). URL https://eur-lex.europa.eu/ legal-content/EN/TXT/?uri=OJ:L:2017:349:TOC. (cit. on page 31)

[18] B. Giechaskiel. "Real Driving Emissions (RDE)", Joint Research Centre (2018) (JRC), ISSN 1831-9424 doi:10.2760/553725 (cit. on page 36)

[19] TNO Innovation for Life. "Road Load Determination of Passenger Cars". (November 2017). Available at: https://www.tno.nl/media/1971/roadload/determination /passengercarstnor10237/pdf (cit. on page 36)

[20] UNECE. "World Forum for the Harmonization of Vehicle Regulation (WP.29)" Available at: https://www.unece.org/trans/main/welcwp29.html. (cit. on page 36)

[21] Cheli, F. Gobbi, M. Holjevac. "Vehicle subsystemsâ energy losses and model-based approach for fuel efficiency estimation towards an integrated optimization". Int. J. Veh. Des. (2018), 76, 46, 81. (cit. on page 36)

[22] Yakhshilikova, G.; Ruzimov, S.; Ezemobi, E.; Tonoli, A.; Amati, N. "Development of Optimization Based Control Strategy for P2 Hybrid Electric Vehicle including Transient Characteristics of Engine". Appl. Sci. (2022). https://doi.org/ 10.3390/app12062852 (cit. on page 41)

[23] W. Liu. "Introduction to Hybrid Vehicle System Modeling and Control" (Wiley, Hoboken, 2013) (cit. on page 44)

[24] C.C. Chan. "The state of the art of electric and hybrid vehicles". Proc. IEEE 90(2), 245â275 (2002) (cit. on page 45)

[25] L. Serrao, C. Hubert, G. Rizzoni. "Dynamic modeling of heavy-duty hybrid electric vehicles", in Proceedings of the 2007 ASME International Mechanical Engineering Congress and Exposition (2007) (cit. on page 48)

[26] S. Lee, J. F. McDonald, J. Cherry. "Modelling and Validation of 48V Mild Hybrid Lithium-Ion Battery Pack", SAE International Journal of Alternative Powertrains (2018) (cit. on page 48)

[27] D. Bianchi, L. Rolando, L. Serrao, S. Onori, G. Rizzoni, N. Al-Khayat, T.M. Hsieh, P. Kang. "Layered control strategies for hybrid electric vehicles based on optimal control". (2011) Int. J. Electr. Hybrid Veh. 3(2), 191-217 (cit. on page 48)

[28] B. Zhou, J. B. Burl, A. Rezaei. "Equivalent Consumption Minimization Strategy With Consideration of Battery Aging for Parallel Hybrid Electric Vehicles" (2020). (cit. on page 49)

[29] A. Rezaei, J. B. Burl, and B. Zhou. "Estimation of the ECMS equivalent factor bounds for hybrid electric vehicles", IEEE Trans. Control Syst. Technol., vol. 26, no. 6, pp. 2198-2205, (2018), doi:10.1109/TCST.2017.2740836. (cit. on page 52)

[30] Lee, B., Lee, S., Cherry, J., Neam, A. et al. "Development of Advanced Light-Duty Powertrain and Hybrid Analysis Tool (ALPHA)", SAE Technical Paper 2013-01-0808, (2013), doi:10.4271/2013-01-0808. (cit. on page 54)

[31] S. Onori, L. Serrao, G. Rizzoni. "Hybrid Electric Vehicles, Energy Management Strategies", (Springer, New York, 2016), pp. 45-47 (cit. on page 55)

[32] "SAE Levels of Driving Automation Refined for Clarity and International Audience", (May 2021), available at https://www.sae.org/blog/sae-j3016-update (cit. on page 63)

[33] L. Yu, R. Wang. "Researches on Adaptive Cruise Control system: A state of the art review", Volume 236, Issue 2-3, https://doi.org/10.1177/09544070211019254 (cit. on page 65)